UNIVERSITY OF MINNESOTA

This is to certify that I have examined this bound copy of a master's thesis by

Thomas Gerard Muhich

and have found that it is complete and satisfactory in all respects, and that any and all revisions required by the final examining committee have been made.

Penelope Morton

Name of Faculty Adviser

[redacted]

Signature of Faculty Adviser

Aug 16, 1993

Date

GRADUATE SCHOOL

Movement of titanium across the Duluth Complex - Biwabik Iron Formation Contact at Dunka Pit, Mesabi Iron Range,northeastern Minnesota.

A Thesis Submitted to
The Faculty of the Graduate School of
The University of Minnesota

In Partial Fulfillment of the Requirements
for the Degree of Master's of Science

by Thomas G. Muhich

August, 1993

ABSTRACT

In the north half of the Dunka open pit iron ore mine (T60N-T61N, R12W) of northeastern Minnesota, the Biwabik Iron Formation (BIF) is in direct contact with the South Kawishiwi Intrusion (SKI) of the Duluth Complex. Progressive contact metamorphism of the BIF originally was thought to be isochemical (Bonnichsen, 1968), however this study presents evidence that titanium was introduced into the BIF from the SKI.

Field and petrographic observations show that within 25 feet of the SKI the BIF has been highly altered. Textures include: (1) ilmenite intergrown in magnetite layers of the BIF, (2) layers of plagioclase, clinopyroxene, orthopyroxene and other commonly magmatic minerals in the BIF, and (3) symplectite of plagioclase-orthopyroxene and orthopyroxene-Fe-Ti oxide. Ilmenite forms partial pseudomorphs after magnetite in the altered BIF, as well as lamellae and rims around magnetite. Layers of magmatic minerals which are not found elsewhere in the iron formation in any abundance appear to be intergrown in magmatic textures.

Within 25 feet of the iron formation, the SKI is also considered altered on the basis of: (1) increased amounts of magnetite, clinopyroxene, orthopyroxene, and amphibole, (2)

loss of olivine, and (3) increased amounts of symplectite of plagioclase-orthopyroxene and orthopyroxene-Fe-Ti oxide. Magnetite in the altered SKI occurs in similar textures to the most altered BIF, with ilmenite partially forming pseudomorphs after magnetite. Loss of olivine and gain of pyroxene may be explained by the assimilation of quartz, which reacted with the olivine in the SKI magma to form pyroxene. Symplectites of orthopyroxene-plagioclase and orthopyroxene-Fe-Ti oxide are also present in the unaltered SKI, but in the altered SKI their abundance is much greater.

Magnetite from altered BIF is higher in TiO_2 (3.15 wt.% on average) than that in unaltered BIF (0.29 wt.% on average). Composition of titaniferous magnetite and ilmenite from both the altered BIF and SKI were used to calculate values of temperature of metamorphism/intrusion and fO_2 using the QUILF PASCAL program (Andersen, Lindsley and Davidson, 1992). Values on a log fO_2 - temperature plot appear above the fayalite-magnetite-quartz buffer curve, in the range of 550°C to 689°C and -15.2 to -18.8 log fO_2 for both the most altered SKI and BIF.

Whole rock analyses of altered BIF show gains of TiO_2, V, Al_2O_3, CaO, Na_2O, K_2O, Ba, Rb, Sr, MgO, Cu, Ni, and H_2O content, and loss of SiO_2 and P_2O_5 compared to altered BIF. Present elevated amounts of ilmenite, plagioclase, sulfides, and actinolite correlate with these gains. Loss of SiO_2 from the altered BIF correlates with the loss of quartz from the

most altered BIF via assimilation into the SKI. Chemical components gained to the altered SKI include K_2O, Rb, S, Fe_2O_3, and H_2O. Gains in K_2O, Rb and H_2O correlate with increased biotite and amphibole content in the most altered SKI, especially hornblende, which is hydrous and contains some potassium. Ferric iron gained to the most altered SKI represents a change in oxidation state of the magma due in part to assimilation of some of the magnetite in the iron formation. Loss of TiO_2 and MnO appear to be related to the formation of ilmenite in the most altered BIF.

Oxygen isotope studies show that the altered BIF contains quartz which is lower in $\delta^{18}O$ ($\delta^{18}O$ = 10.82 parts per thousand) than quartz in altered BIF ($\delta^{18}O$ = 15.21 parts per thousand, Perry and Bonnichsen, 1966). The altered SKI shows greater $\delta^{18}O$ (7.00 to 9.40 parts per thousand) than the altered SKI (5.94 to 6.57 parts per thousand).

Fingers of SKI magma assimilated quartz from the BIF, enriching the altered SKI in ^{18}O, K_2O, Fe_2O_3, and LOI, whereas depleting the BIF of SiO_2. Layers of magnetite in the altered BIF have been enriched in Ti, while preserving the original layering, indicating some diffusion or infiltration of titanium into the magnetite has occurred. Combination of infiltration of "fingers" of SKI magma into the BIF, and enrichment of BIF magnetite in titanium occurs only where the SKI is in direct contact with the BIF. None of the above textures, changes in mineralogy, or titanium enrichment occur

where the Virginia Formation lies between the Duluth Complex and the Biwabik Iron Formation. Thus, textures, changes in mineralogy, and titanium enrichment in the most altered BIF must be caused by direct contact with the SKI of the Duluth Complex.

TABLE OF CONTENTS

LIST OF FIGURES

LIST OF TABLES

ACKNOWLEDGEMENTS

The writer acknowledges the advice and guidance of Penelope Morton who suggested the problem on which this thesis is based and provided instruction in the use of the electron microprobe. Ron Graber and Cliffs Mining Services Co. allowed access to the Dunka Pit Mine, provided a topographic sheet of the mine area, and provided access to crushed drill core and driller's logs. Mark Severson, Steven Hauck, and Linda Lindberg of the Natural Resources Research Institute (NRRI) are thanked for assistance in operating the electron microprobe, advice on various geochemical problems, and assistance in operation of thin section polishing machinery. Rick Ruhanen and Al Dzuck of the Department of Natural Resources allowed access to drillcore repository in Hibbing, MN for sampling. James Grant instructed the writer in the use of the isocon method. Edward Ripley is thanked for analyzing samples for oxygen isotopic compositions, and for assistance in interpretation of the results. Whole rock major element geochemistry was provided by XRAL Laboratories, and trace element geochemistry was provided free of charge by Coleraine Research Laboratory. Also my fellow graduate students at the University of Minnesota-Duluth are thanked for advice and assistance in AutoCAD mapping, photomicrography, thin section work, proofreading abstracts

for publication and production of slides for presentation. Finally, I would like to thank my wife, Brandy, for providing undying support throughout the duration of this thesis work.

I. INTRODUCTION

Dunka Pit iron ore mine is located on the eastern end of the Mesabi Iron Range, at T60N - T61N, R12W, in St.Louis County of northeastern Minnesota. Formerly owned and operated by Erie Mining Co., the iron ore (taconite) mine is now owned by LTV Steel Co. and managed by Cleveland Cliffs Co. The Biwabik Iron Formation has been mined from Dunka Pit for its magnetite, which is interlayered with slate and quartzite, and shipped for processing to make taconite pellets. Having been in production for over 25 years, the bulk of the iron formation in the area has been removed. This thesis deals with the northern portion of this iron mine where the Biwabik Iron Formation is in contact with the Duluth Complex, a gabbroic intrusion (figure 1-1).

This thesis work examines the petrologic, mineralogic and geochemical changes resulting from the introduction of titanium into the Biwabik Iron Formation in the Dunka Pit area. Significant titanium in the iron formation exists along the contact with the Duluth Complex and was first noticed when the iron ore extracted near the contact was found to have titanium levels unacceptable for blast furnace separation. Assays of the concentrated ore showed values of TiO_2 of 1 to 6%; this amount of titania was affecting the percentage of extractable total iron (Erie Mining/Cleveland

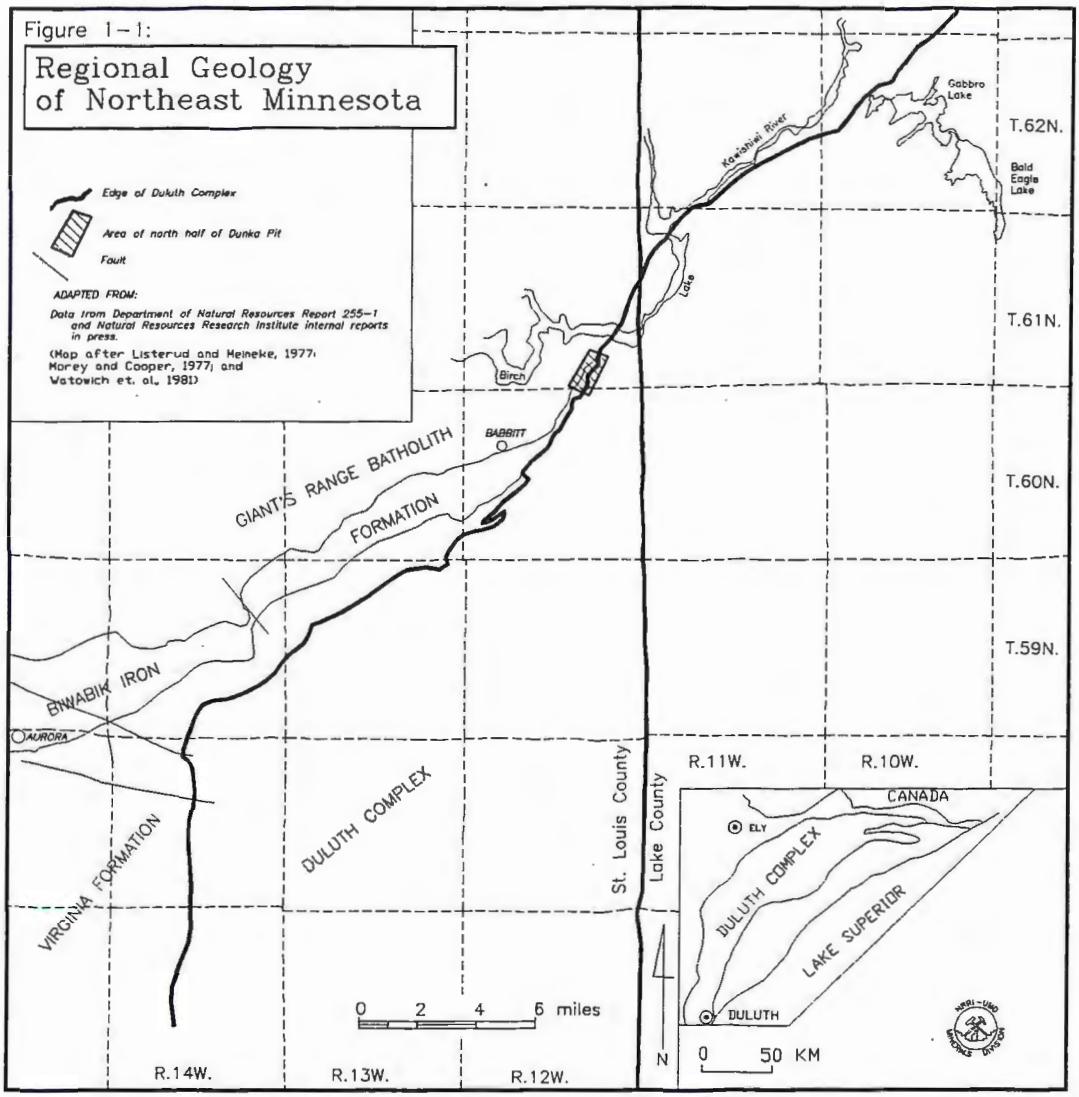
Figure 1-1:
Regional Geology of Northeast Minnesota
Edge of Duluth Complex
Area of north half of Dunka Pit
Fault
ADAPTED FROM:
Data from Department of Natural Resources Report 255-1 and Natural Resources Research Institute internal reports in press.
(Map after Listerud and Meineke, 1977; Morey and Cooper, 1977; and Watowich et. al, 1981)
Gabbro Lake
Kawishiwi River
Bald Eagle Lake
Birch Lake
BABBITT
GIANT'S RANGE BATHOLITH
FORMATION
BIWABIK IRON
AURORA
VIRGINIA FORMATION
DULUTH COMPLEX
St. Louis County
Lake County
T.62N.
T.61N.
T.60N.
T.59N.
R.14W.
R.13W.
R.12W.
R.11W.
R.10W.
0 2 4 6 miles
CANADA
ELY
DULUTH COMPLEX
LAKE SUPERIOR
DULUTH
N
0 50 KM

Cliffs drillcore logs; Ron Graber, personal communication). The magnetite in the iron formation was affected by the introduction of titanium, producing titanomagnetite and ilmenite. This process has also introduced Ca, Al and Na. The significance of the transfer of titanium is important because it is normally considered to be immobile. Also the iron ore in the northern end of Dunka Pit is of much lower, uneconomic grade where affected by chemical change.

This thesis incorporates field mapping of the pit area; petrography, for mineral and textural analysis of the altered rocks; electron microprobe analysis of minerals; whole rock geochemical analysis by x-ray fluorescence spectrometry (XRF); trace element analysis by induced coupled plasma spectrometry (ICP); the study of oxygen isotopic compositions of the altered vs. unaltered rocks; and relies also on data from previous authors (Lepp, 1966, 1972; Morey, 1992; Severson, in progress) to outline the extent and significance of the exchange of titanium across the Duluth Complex - Biwabik Iron Formation contact in the Dunka Pit area.

The early Proterozoic Biwabik Iron Formation underwent progressive contact metamorphism caused by the intrusion of the mid-Proterozoic Duluth Complex (French, 1968). The highest grade metamorphism was reached near the contact with the Duluth Complex in the Dunka Pit area. Some retrograde metamorphism occurred, as evident in the formation of hydrous phases such as amphibole. The metamorphism was thought to be

isochemical except for the original loss of H_2O and CO_2 (French, 1968; Bonnichsen, 1968). The contact between the Duluth Complex and the Biwabik Iron Formation dips at a low angle to the south and is intersected by faults, one of which is subparallel it.

Exposure of bedrock in the area was originally widespread, but today most of the iron formation has been removed, and the surrounding outcrop has been covered with extensive waste rock piles. Previous investigations by various authors (Bonnichsen, 1968; Severson, in progress) have provided the author with geologic maps which were utilized in field mapping. A topographic base map was provided by Cliffs Mining Services Co. Field mapping at a scale of 1:4800 was done to update previous information and provide a basis for this study. Extensive diamond drilling has provided previous authors with a wealth of information. However, almost all drill core owned by LTV Steel Co. has been crushed, removed for sampling and/or discarded. This has limited the amount of information available in large part to crushed core and driller's logs provided by Cliffs Mining Services Co. Diamond drilling of the Duluth Complex in the area done by Newmont Exploration Co. for copper and nickel sulfide exploration has provided whole saved drill core from the gabbroic intrusion near the contact with the iron formation.

Existence of the Biwabik Iron Formation has been known

since 1871, but the first detailed work on the extent and geologic nature of the iron formation was conducted by Grout and Broderick (1919). Gunderson and Schwartz (1962) studied the mineralogy and stratigraphy of the proposed site of the Peter Mitchell Mine which is now adjacent to Dunka Pit. French (1964) researched the mineralogy associated with the progressive metamorphism of the Biwabik Iron Formation. Investigations in the Dunka Pit area include a master's thesis on the petrology and metamorphism of the Biwabik Iron Formation (Bonnichsen, 1968). Bonnichsen also produced other publications on the metamorphic pyroxenes and amphiboles of the area (1969) and a summary of the geology of the southern Duluth Complex (1972). Holst et al. (1986) worked on the relationship between the structural geology and economic mineralization of the Duluth Complex citing specifically the Dunka Pit area. An ongoing investigation by Mark Severson of the Natural Resources Research Institute on the geology of the Duluth Complex along its basal contact has provided considerable information on the subsurface structural geology of the area. Compositional data on the eastern Biwabik Iron Formation is included in a recent publication (Morey, 1992).

II. REGIONAL GEOLOGY

Precambrian rocks of northeastern Minnesota can be divided into the Archean metavolcanic metasedimentary and granitic rocks, early Proterozoic metamorphosed Animikie sedimentary rocks, and mid-Proterozoic volcanic rocks and intrusions (Table 2-1).

Archean rocks constitute the shield terrane which extends from the northeastern Minnesota (Vermilion district) into Canada's Abitibi province. The earliest of these Archean rocks are the metabasalt and metasedimentary rock of the Ely Greenstone (older than 2.7 Ga), which along with the Soudan Iron Formation constitute the Keewatin Group. The greenstones are mainly pillowed metabasalt at the base of the formation overlain by metabasalt flows, banded iron formation of the Soudan Iron Formation, laminated tuff and interbedded volcanogenic agglomerate which have been regionally metamorphosed to the greenschist facies. The Ely Greenstone forms a thick unit totalling approximately 10,000 feet (Morey et al., 1970, p.12). Accompanying these subaqueous basalts are sedimentary rocks which were derived from the volcanic rocks. These include metagreywacke, quartzite, conglomerate, and lesser interbedded tuff and lava of the Lake Vermilion Formation and the Knife Lake Group. Both units are generally similar in lithology and correlative in age, but are not in contact with each other. The Vermilion Formation has also

Table 2-1: Stratigraphic succession of Precambrian Rocks of northeastern Minnesota (modified from Goldich, 1968; Bonnichsen, 1968)

AGE (Ma)	EON	ERA	MAJOR SEQUENCE	FORMATION / INTRUSIONS
570	PROTEROZOIC	LATE		
900		MIDDLE	KEWEENAWAN	Hinkley Sandstone
				Fond du Lac Sandstone
1100			Unconformity North Shore Volcanic Gp.	Duluth Complex and related intrusions
				Puckwunge Sandstone
1600		EARLY	Unconformity	Virginia/Rove/ Thomson Fms.
			Animikie Group	Biwabik/Gunflint Iron Fms.
				Pokegama Quartzite
2500	ARCHEAN	LATE	Unconformity	Algoman Intrusions
2600			Knife Lake Group	Undivided: incl. Vermilion Fm.
2700			Unconformity	Laurentian Intrusions
			Keewatin Group	Ely Greenstone & Soudan Iron Fm.
3000				

been considered to be a member of the Knife Lake Group (Goldich, 1968). These metagreywackes and metabasalts are intruded by the large granitic Giants Range, Vermilion and Saganaga Batholiths of the Algoman orogeny (2.4 - 2.7 Ga). The granitic intrusions are approximately 50 to 100 million years younger than the greenstone they intrude. Granite, granodiorite, adamellite, and lesser syenite and more mafic gneissic rock constitute the rock types of the large batholiths of the Algoman orogeny (Sims and Viswanathan, 1972).

Proterozoic rocks of northeastern Minnesota include early Proterozoic sediments of the Animikie Group (1.7 Ga) which are overlain unconformably by mid Proterozoic (1.1 Ga) basalts and minor rhyolites of the North Shore Volcanic Group. Animikian sedimentary rocks of the area can be divided into the Pokegama Quartzite, Biwabik and Gunflint Iron Formations, and greywackes of the Virginia, Rove and Thomson Formations. The Animikian sedimentary rocks lie unconformably on the Archean granite and greenstone. The Pokegama Quartzite is the oldest of the Animikie Group and was originally a quartz sandstone with minor muddy beds. This unit is discontinuous and does not completely underly the Biwabik Iron Formation on its eastern end. The Biwabik Iron Formation and Gunflint Iron Formation, which conformably lie on top of the Pokegama Quartzite, are chemical sedimentary rocks and consist of layers of magnetite and

hematite alternating with either cherty or slaty layers to form taconite. Hematite is more abundant in the upper weathered zones of the iron formation on the western end of the Mesabi Range (Gruner, 1924; Gruner, 1946; Bonnichsen, 1968). Iron silicate, especially phyllosilicate, and iron carbonate are present in lesser amounts. The Virginia, Rove and Thomson Formations, which lie conformably upon the iron formations, dominantly consist of argillite and greywacke. These 3 units are all considered to be correlatable, if not continuations of the same unit (Goldich, 1968). Directly overlying the Biwabik Iron Formation, the Virginia formation consists of a succession of argillite at least 2000 feet thick (White, 1954).

The much younger North Shore Volcanic Group which overlies the Animikie Group is a composite of mainly basaltic lava flows with lesser rhyolite, icelandite, pyroclastic rocks, granophyre and granodiorite dikes and sills, diabase sills, and interflow sedimentary rocks. These tholeiitic lava flows occurred as a result of the mid-Continent rifting (1.1 Ga) in the Lake Superior basin. The petrology of these flows has been extensively studied by Green (e.g. 1968, 1971, 1993).

Intruding these volcanic rocks and also a result of the mid-Continent rifting is the Duluth Complex. The Duluth Complex is a troctolitic to anorthositic intrusion which covers a large arc-shaped area from Duluth to the Canadian

border and lies between the overlying North Shore Volcanics and the underlying Animikie sediments and Archean granite-greenstone terrane. The Duluth Complex consists of a series of intrusions of Keweenawan age (1.12 ± .15 Ga) and are nearly contemporaneous with the North Shore Volcanic Group lava flows which they intrude (Silver and Green, 1963; Paces and Miller, in press). The intrusions range from layered (Partridge River Troctolite intrusion) to unlayered heterogeneous bodies (South Kawishiwi, and undivided anorthosites) that vary in grain size from fine to coarse, with minor pegmatites (Weiblen and Morey, 1980). At the base of the Duluth Complex, near the contact with the Animikie sediments are several magmatic sulfide deposits of subeconomic value. The base of the Duluth Complex has been the subject of continuing research (Mainwaring and Naldrett, 1977; Foose and Weiblen, 1986; Ripley and Alawi, 1986; Ripley and Al-Jassar, 1987; Severson and Hauck, 1990; Severson, in prep.) because of the presence of these Cu-Ni sulfide bodies and also because of the presence of iron-titanium oxide deposits to the south known as the Longnose and Longear. The Longnose and Longear are oxide-rich ultramafic intrusions in the Duluth Complex which contain sub-economic amounts of the titanium ore mineral ilmenite (Bill Ulland, personal communication).

The Precambrian bedrock of northeastern Minnesota is overlain by Quaternary glacial deposits. These local glacial

deposits consist mainly of a continuous blanket of variably thick unconsolidated tills and moraines which effectively cover the majority of the bedrock (Ojakangas and Matsch, 1982).

The area of concern for this thesis investigation is the intersection of the Archean granite - greenstone terrane, the early Proterozoic Animikie sediments, and the mid-Proterozoic Duluth Complex igneous intrusion (Figure 2-1, map in pocket in back cover). At this point the Biwabik Iron Formation overlies the Giants Range granitic batholith and has been intruded by the South Kawishiwi troctolitic intrusion (Foose and Weiblen, 1986). The Biwabik Iron Formation has been metamorphosed progressively to the pyroxene hornfels facies. In this thesis investigation it is proposed that in the area of the Dunka Pit iron mine, the iron formation has been altered by injection of magma from the Duluth Complex, and titanium has been introduced metasomatically into the layers of magnetite in the iron formation from these "fingers" of magma.

Figure 2-1:

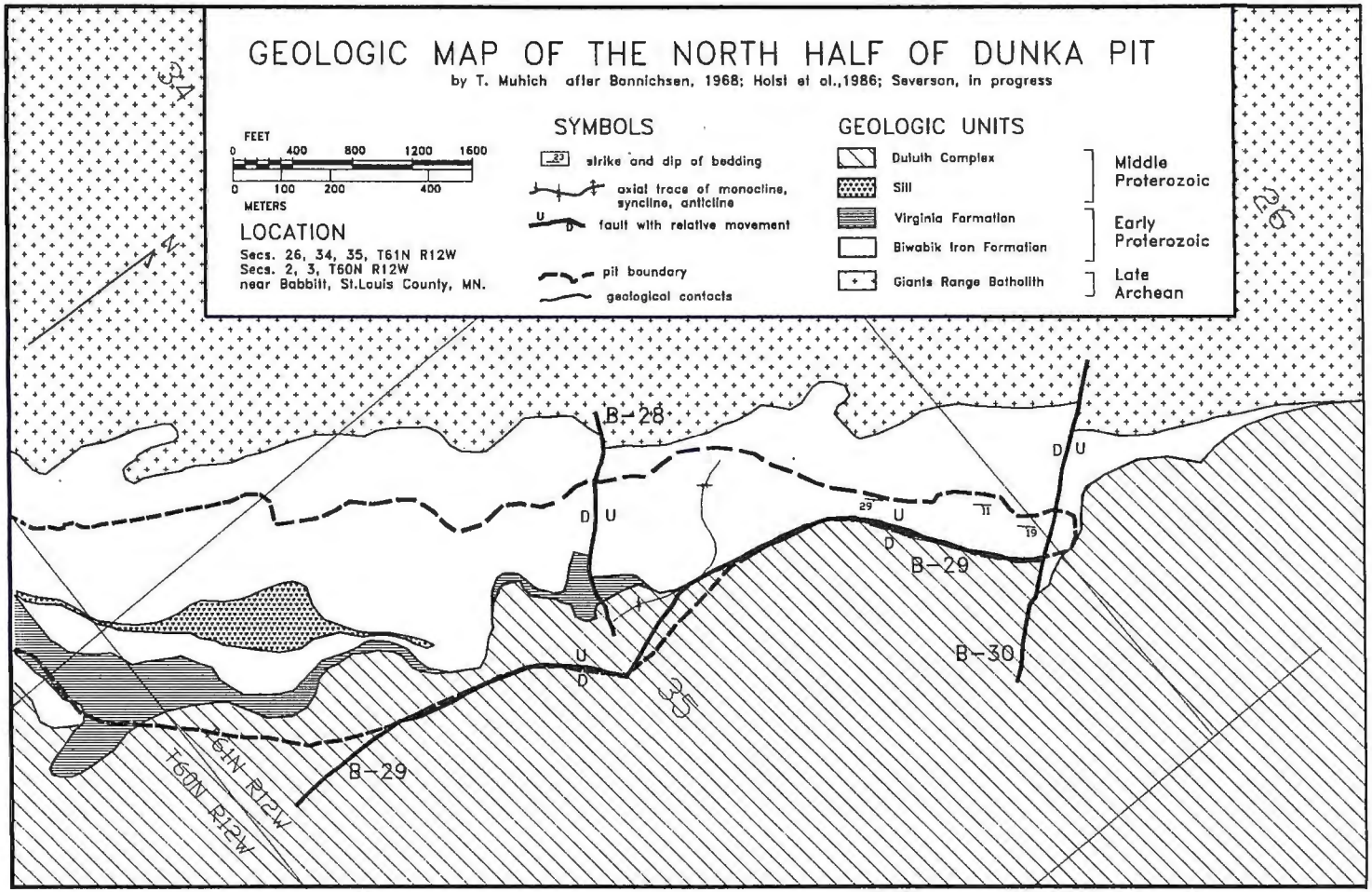
GEOLOGIC MAP OF THE NORTH HALF OF DUNKA PIT
by T. Muhich after Bonnichsen, 1968; Holst et al.,1986; Severson, in progress
FEET
0 400 800 1200 1600
0 100 200 400
METERS
LOCATION
Secs. 26, 34, 35, T61N R12W
Secs. 2, 3, T60N R12W
near Babbitt, St.Louis County, MN.
SYMBOLS
strike and dip of bedding
axial trace of monocline, syncline, anticline
fault with relative movement
pit boundary
geological contacts
GEOLOGIC UNITS
Duluth Complex
Sill
Virginia Formation
Biwabik Iron Formation
Giants Range Batholith
Middle Proterozoic
Early Proterozoic
Late Archean
34
N
26
B-28
B-29
B-30
B-29
35
T61N R12W
T60N R12W
D U

III. LITHOLOGY

Principal lithologic units in the Dunka Pit area are the Giants Range Batholith, Biwabik Iron Formation, Virginia Formation, Duluth Complex and a diabase sill. Granitic rocks of the Archean Giants Range Batholith in the area of this study are overlain unconformably by the early Proterozoic sedimentary rocks of the Biwabik Iron Formation and Virginia Formation, which are intruded by the mid Proterozoic gabbroic rocks of the Duluth Complex and a diabase sill. The lithology of these rocks has been studied in outcrop, drillcore and also utilizes the work of previous investigators (Gunderson, 1958; Bonnichsen, 1968; Severson, in progress).

Giants Range Batholith

A ridge of granitic rock exists adjacent to the Biwabik Iron Formation on its north side. This ridge is Giants Ridge, and the Giants Range Batholith takes its name from it as it forms the core of this ridge. Initial work done on the batholith (Allison, 1925) describes this 100 mile long granitic body as being a complex succession of intrusive rocks ranging from diabasic gabbro, hornblendite and shonkinite (potassium rich mafic syenite) through monzonite and granite, with mafic rocks constituting the smaller

portion of the total succession. Later work concentrates on petrology and describes the batholith as being composed dominantly of hornblende adamellite to granodiorite (Sims and Viswanathan, 1972). Northeast of Dunka Pit the Giants Range Batholith is intruded by the Duluth Complex, and shows evidence of contact metamorphism in its sugary, recrystallized texture and poikilitic augite-granite composition near the contact with the Duluth Complex. The poikilitic augite near the contact contain fine rods and needles of "a black metallic mineral which is probably ilmenite" due to slight addition of titanium and iron from the Duluth Complex (Allison, 1925). No outcrop of the Giants Range Batholith was observed for this thesis, but in drillcore and thin section examination, medium- to coarse-grained porphyritic biotite-hornblende diorite and coarse-grained porphyritic biotite granite were observed. The batholith has been dated at 2670 ± 65 m.y. by Rb-Sr isochron dating (Prince and Hanson, 1972), and 2705 ± 25 m.y. by $^{207}Pb/^{206}Pb$ dating of titanite (Catanzaro and Hanson, 1971). Granitic rocks of the Vermilion and Giants Range Batholiths are considered to be part of the Algoman orogeny 2400-2700 m.y. (Goldich, 1968).

Biwabik Iron Formation

The Biwabik Iron Formation (BIF) has been extensively

studied since the early 1900's (Grout and Broderick, 1919), and much information exists on its stratigraphy and structure (White, 1954; Gunderson and Schwartz, 1962), its composition (Gruner, 1946; Lepp, 1966, 1968, 1972; and Morey,1992), its isotopic geochemistry (Perry and Bonnichsen, 1966; Perry et al., 1973; and Abrajano et al., 1991), and its metamorphism (Gunderson and Schwartz, 1962; French, 1968; Bonnichsen, 1968, 1969; Morey et al.,1972) to name only a few contributors in a few fields.

Stratigraphically, the Biwabik Iron Formation has been divided into four members, the Upper Slaty, Upper Cherty, Lower Slaty, and Lower Cherty (Gruner, 1946) on the basis of texture and composition with 22 submembers, A - V on the basis of mineralogy and bedding characteristics (Gunderson, 1958) (Fig 3-1). All of these units exist at the Dunka Pit area, but the upper slaty and upper cherty are the main concentration of this thesis as these units are thickest of the four members and well exposed in the walls of Dunka Pit, allowing for examination of the these units, especially near the contact with the Duluth Complex.

Structurally, the Biwabik Iron Formation strikes approximately northeast and dips 5 to 15 degrees southeast (White, 1954). Numerous northwest trending faults intersect the iron formation with displacements of less than 200 feet, and minor folds have axes normal to the strike of the iron

Figure 3-1: Generalized columnar section of the Biwabik Iron Formation (after Gundersen and Schwartz, 1962)

Member -Main Mesabi	Member -East Mesabi	Sub-Member -East	Description of Submembers -East Mesabi
UPPER SLATY	Aub_6	A (5)*	Calcite marble
		B (16)	layered chert diopside tac
	Aub_5	C (42)	laminated qtz-opx-mt tac
		D (7)	laminated actin-mt-qtz tac
		E (6)	granule qtz tac
		F (20)	bedded qtz-cumm-mt tac
		G (25)	qtz tac
UPPER CHERTY	Aub_4	H (10)	layered qtz-actin-mt tac
		I (5)	algal qtz-mt tac
		J (16)	granule qtz-mt tac
		K (35)	layered qtz-actin-opx-mt tac
		L (30)	layered opx-qtz-mt-hbd tac
		M (20)	layered fay-qtz-mt tac
		N (4)	fay-qtz tac
		O (17)	bedded granule qtz-fay-mt tac
LOWER SLATY	Aub_3	P (60)	shaly qtz-fay tac
	Aub_2	Q (26)	argillaceous gph-opx-qtz tac
LOWER CHERTY	Aub_1	R (11)	layered fay-qtz-mt tac
		S (8)	layered qtz-mt tac
		T (5)	granule qtz-mt tac
		U (10)	layer/granule cumm-qtz-mt tac
		V (3)	qtz tac

* ( ) = approximate thickness in feet
abbreviations: mt=magnetite; qtz=quartz; tac=taconite
opx=orthopyroxene; actin=actinolite; cumm=cummingtonite
hbd=hornblende; fay=fayalite; gph=graphite

formation (White, 1954). Of the faults in the Dunka Pit area, one exists subparallel to the contact with the Duluth Complex (Fig 2-1).

Included in the iron formation are recrystallized chert, iron oxide, iron silicate, carbonate and many minor minerals which make up the rock known as taconite. Taconite is defined as a quartz-rich (cherty) rock which contains significant amounts of iron silicate, carbonate, oxide, and hydroxide which may be sedimentary or metamorphic, but which are not highly oxidized (Gunderson and Schwartz, 1962). The most recent work done on compiling a statistically valid average composition for the whole rock composition of the eastern Biwabik Iron Formation yielded in weight percent: 43.61 SiO_2, 1.24 Al_2O_3, 0.12 TiO_2, 16.74 Fe_2O_3, 19.28 FeO, 0.88 MnO, 3.04 MgO, 2.71 CaO, 0.07 Na_2O, 0.19 K_2O, 0.09 P_2O_5, 0.05 S, 10.42 CO_2, 1.74 H_2O (Morey, 1992).

Progressive contact metamorphism of the Biwabik Iron Formation by the Duluth Complex ranges from pyroxene hornfels facies near the contact with the Duluth Complex to unmetamorphosed taconite in the western half of the iron formation. French (1968) divided the eastern Biwabik Iron Formation into 4 zones based on textural relations and mineralogy. According to French, the Dunka Pit area is in zone 4, the most highly metamorphosed taconite. Mineralogy of the taconite in this area is dominated by quartz, magnetite, fayalite, ferrohypersthene, hedenbergite,

hornblende, actinolite, and cummingtonite; some minerals are a product of the pyroxene hornfels facies metamorphism and some due to retrograde metamorphism (Gunderson and Schwartz, 1962).

Virginia Formation

Most of the Virginia Formation consists of fine-grained, thin-bedded grey and black argillite dominated by a matrix of clay minerals, chlorite and graphite with few clastic grains of quartz and feldspar (White, 1954). Total thickness of the Virginia Formation is at least 2000 feet, however in the Dunka Pit area thicknesses range from 0 to 50 feet. Where the Virginia Formation pinches out the Duluth Complex is directly in contact with the Biwabik Iron Formation, and this is where the iron formation is enriched in titanium. Alteration effects of the Duluth Complex on the Virginia Formation are not within the scope of this thesis, although it is noted that rims of silica exist around hornfels inclusions in the Duluth Complex, suggesting the transfer of silica from the Virginia Formation into the Duluth Complex (Severson, 1992, personal communication). In the Dunka Pit area, the Virginia Formation is metamorphosed to a cordierite-biotite-plagioclase+/-orthopyroxene+/-quartz hornfels which locally has abundant thin beds of pyrrhotite. A subeconomic magmatic sulfide deposit exists to the south of

Dunka Pit known as the Babbit Cu-Ni deposit which contains numerous inclusions of Virginia Formation (Weiblen and Morey, 1976; Mainwaring and Naldrett, 1977; Tyson, 1979; Ripley and Alawi, 1986).

Diabase sill

A diabase sill, approximately 1 to 5 feet thick, exists as an intrusion in the Upper Slaty member of the Biwabik Iron Formation in Dunka Pit. The sill has a fine-grained chill zone at its contacts with the iron formation. Well formed columnar jointing exists perpendicular to its contacts. Similar diabase sills and dikes in the adjacent Peter Mitchell mine pit have been considered to be older than the Duluth Complex as they show evidence of having been contact metamorphosed by the Duluth Complex in their corroded, partly resorbed plagioclase laths, and slightly recrystallized augites (Gunderson and Schwartz, 1962). The sill in the Dunka Pit area shows similar evidence of metamorphism, although no detailed study of it was undertaken.

Duluth Complex

This large arc-shaped mafic intrusion consists of several separate intrusions, of which the South Kawishiwi Intrusion (SKI) is the magmatic body intruding the Virginia

Formation and Biwabik Iron Formation in the Dunka Pit area. The South Kawishiwi Intrusion is a heterogeneous pluton composed of troctolite, anorthosite, gabbro, norite, oxide-rich ultramafic rock, and numerous inclusions of cordierite-rich hornfels, and large "rafts" of iron formation (Foose and Weiblen, 1986; Severson, personal communication). Of drill core and outcrop, the most common lithology in the Dunka Pit area is medium- to coarse-grained gabbro to anorthositic gabbro with lesser troctolite and norite. The Basal Heterogenous unit described by Severson outcrops adjacent to the Biwabik Iron Formation at Dunka Pit and constitutes a large portion of the Duluth Complex intrusion at depth adjacent to the Dunka Pit (Severson, in progress). Near the contact with the Biwabik Iron Formation, the South Kawishiwi Intrusion contains sheets of biotite granite pegmatite.

IV. STRUCTURE

In the north half of the Dunka Pit area the Biwabik Iron Formation (BIF) and Virginia Formation unconformably overlie the older Archean Giants Range Batholith. Striking N40°E to N45°E, the Biwabik Iron Formation and overlying Virginia Formation dip at 15-30°SE. These Animikian sedimentary rocks are gently folded and intruded first by sills and then by the Proterozoic South Kawishiwi Intrusion (SKI) of the Duluth Complex. All of these rock units are in turn faulted. Folds in the Animikie sedimentary rocks are generally small scale (Fig 4-1, cross section A-A'). A series of NW trending faults intersect the Animikie Sedimentary rocks perpendicular to their strike, and a major fault exists subparallel to the contact between the Biwabik Iron Formation and the South Kawishiwi Intrusion trending NE (Bonnichsen, 1968). Faults in the north half of Dunka Pit are B-28, B-29, and B-30 (nomenclature after Holst et al., 1986). B-28 and B-30 belong to the NW trending group which have movement of the southern block down relative to the northern block (Fig 2-1) with displacements of tens of feet (Bonnichsen, 1968). B-29 trends north to northeast subparallel to the intrusive contact of the South Kawishiwi Intrusion. Movement along B-29 consists of the south block moving down 150 to 200 feet relative to the north block (Fig 4-1). Field observations of intrusive contacts in outcrop and drillcore indicate that the

Figure 4–1: Cross Sections in Dunka Pit area
See Fig 4–2 for location of cross sections

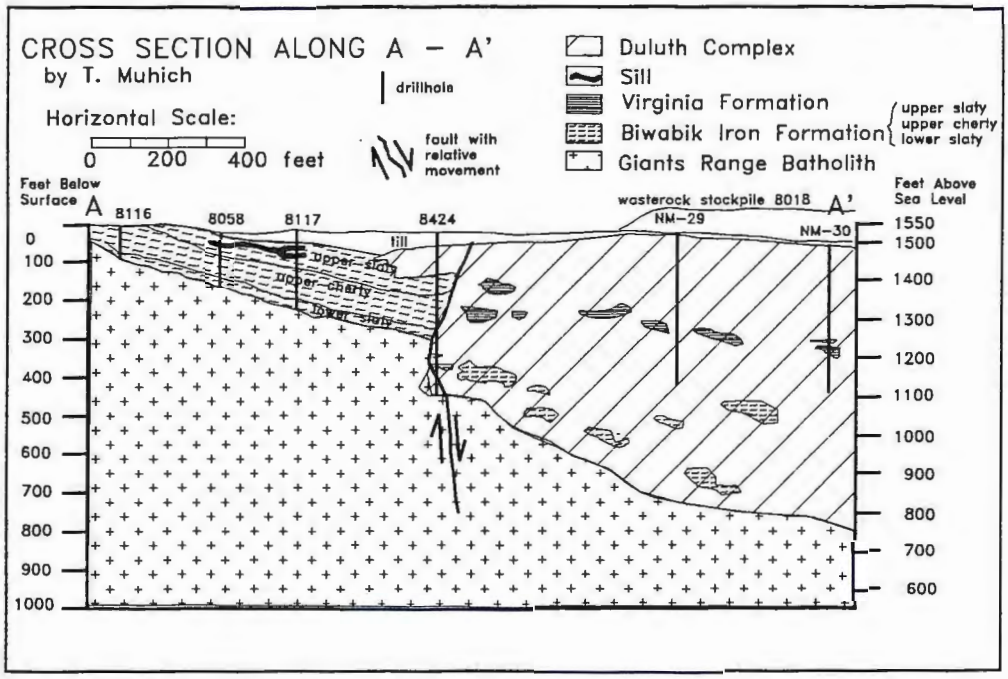

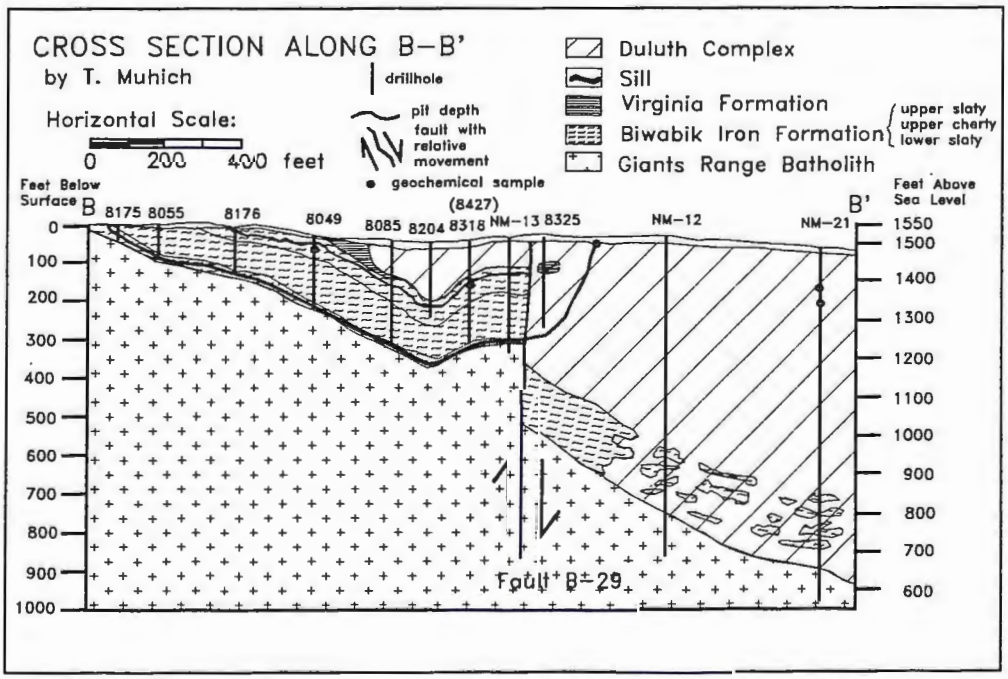

Figure 4–1 cont'd.

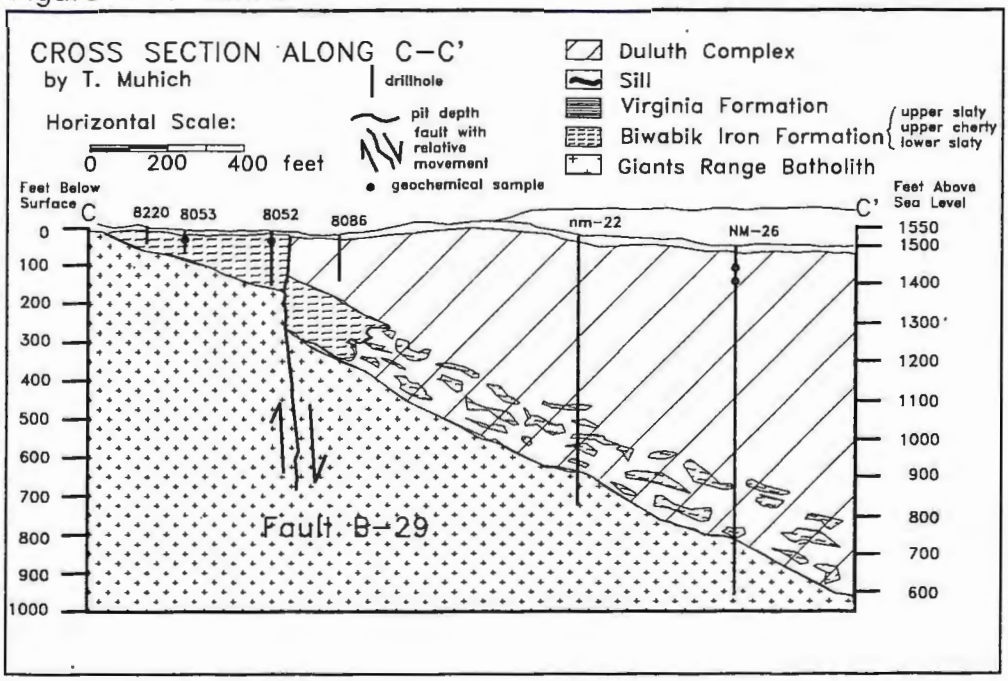

Figure 4-2:

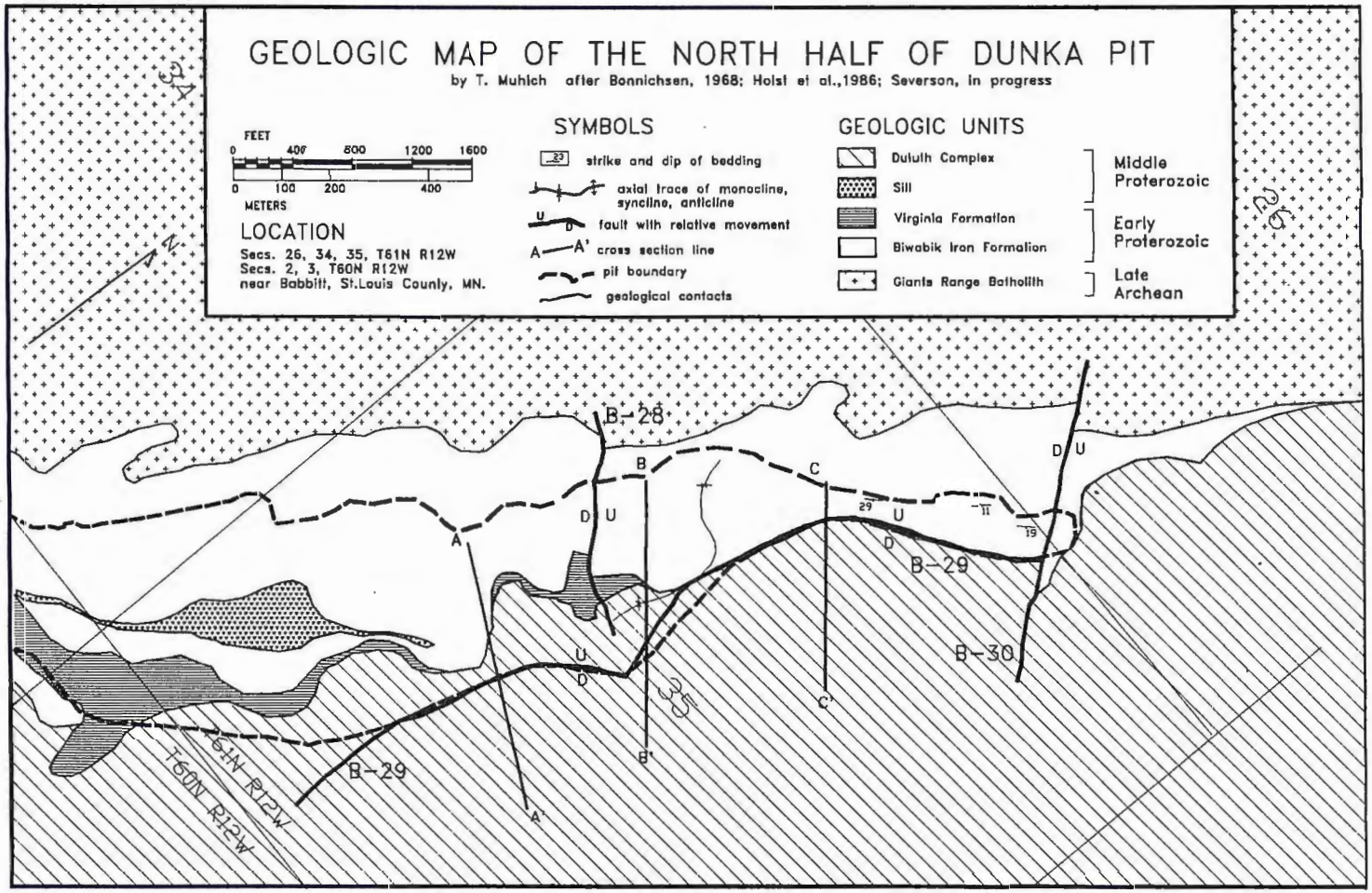
GEOLOGIC MAP OF THE NORTH HALF OF DUNKA PIT
by T. Muhich after Bonnichsen, 1968; Holst et al.,1986; Severson, in progress
FEET
0 400 800 1200 1600
0 100 200 400
METERS
LOCATION
Secs. 26, 34, 35, T61N R12W
Secs. 2, 3, T60N R12W
near Babbitt, St.Louis County, MN.
SYMBOLS
strike and dip of bedding
axial trace of monocline, syncline, anticline
fault with relative movement
A—A' cross section line
pit boundary
geological contacts
GEOLOGIC UNITS
Duluth Complex
Sill
Virginia Formation
Biwabik Iron Formation
Giants Range Batholith
Middle Proterozoic
Early Proterozoic
Late Archean
B-28
B-29
B-30
B-29
35
T61N R12W
T60N R12W

South Kawishiwi Intrusion intruded along a rampart formed by the Fault B-29 and other faults, although later movement along B-29 probably occurred.

Numerous inclusions of both Virginia Formation and Biwabik Iron Formation can be seen in the South Kawishiwi Intrusion. Large "rafts", or nearly intact pieces of Biwabik Iron Formation are evident in drillcore. These sections of iron formation show evidence of alteration. For example, fayalitic olivine-rich layers of the Biwabik Iron Formation can be observed at the same depth within the SKI as olivine-rich, oxide-rich ultramafic intrusives (Severson, personal communication). However, these rafts of BIF are not included in the scope of this thesis. Rather, the section of the Biwabik Iron Formation outcropping in Dunka Pit which shows evidence of alteration is the focus.

V. PETROGRAPHY

Introduction:

Mineralogical changes caused by direct contact of the South Kawishiwi Intrusion (SKI) with the Biwabik Iron Formation (BIF) are documented using petrographical methods, specifically, to examine (a) the change in percentage of existing minerals in the BIF and/or the SKI, (b) new minerals created in BIF or SKI, (c) textural relations among all minerals, and (d) to find evidence for the origin of these minerals/textures, especially ilmenite.

77 polished thin sections and 12 polished sections were described and classified into one of five categories:

(I) least altered BIF
(II) most altered BIF
(III) least altered SKI
(IV) most altered SKI
(V) other

Classification into these five categories is based on the proximity to the BIF/SKI contact and the mineralogical/textural relations observed in thin section. Specifically, those rocks near the contact with the SKI (within 25 feet) which show relict layering or are dominated by "normal" iron formation minerals, but have significant amounts of minerals not found in "normal" iron formation are

classified as most altered BIF. It should be noted that in samples of the BIF which are not in contact with the SKI, that is, samples from locations where any thickness of Virginia Formation lies between the BIF and SKI, no abnormal textures or minerals exist. These samples, which are from BIF which was "buffered" by the Virginia Formation, are not considered to be most altered BIF, due to the lack of abnormal textures or minerals. Two of the most strikingly abnormal minerals in the most altered BIF are plagioclase and ilmenite. Those samples hundreds of feet away from the BIF/SKI contact with no signs of abnormal mineralogy or textures are considered least altered BIF.

Rocks near the contact with the BIF (within 25 feet) displaying abnormal textural features, and abnormal mineralogy are considered to be most altered SKI. Increased amounts of magnetite, hydrous minerals, abundant orthopyroxene/plagioclase symplectite (>10% of plagioclase is symplectite), or abundant oxide/silicate symplectite are among the petrographic criteria for classification of a rock as most altered SKI. Lack of these minerals and textures, and distance from the contact of 100 feet or greater qualify the rock as least altered SKI. Those samples in the "other" category were mainly those showing intermediate textures, and are not discussed in this section in order to concentrate on overall changes. Four thin sections were point counted from each group to check the accuracy of volume percent modal

estimates of minerals present in Appendix A.

I. Least Altered BIF:

All samples of least altered BIF taken from outcrop were made into polished thin sections whereas those taken from crushed drillcore were made into polished sections and thin sections of grain mounts. All samples, six in total, were taken from similar layers of the Upper Slaty member, mainly layers C - G (Gunderson, 1958). The overall lithology of the upper slaty BIF is fine- to medium-grained, dark grey, granoblastic to hypidiomorphic magnetite-orthopyroxene-quartz-olivine meta-iron formation with lesser clinopyroxene, apatite, biotite, sulfide, and iron phyllosilicate with 1mm-1cm layering.

Magnetite: avg 20.3%, range (7-53%); size (0.01-2.0 mm)

Typically subhedral, magnetite ranges from anhedral poikiloblasts to euhedral octahedra, and is seen enclosing small inclusions of quartz, olivine and amphibole. Magnetite, like most major minerals of the BIF, can be observed concentrated in layers, or bands. Some thin sections show granoblastic magnetite textures, whereas in others < 1.0 mm euhedral magnetite is rimmed by acicular amphibole, probably cummingtonite/grunerite (Fig 5-1). Weathering of magnetite along fractures is seen to yield iron oxide and hydroxide. Lamellae of hercynite spinel exsolved

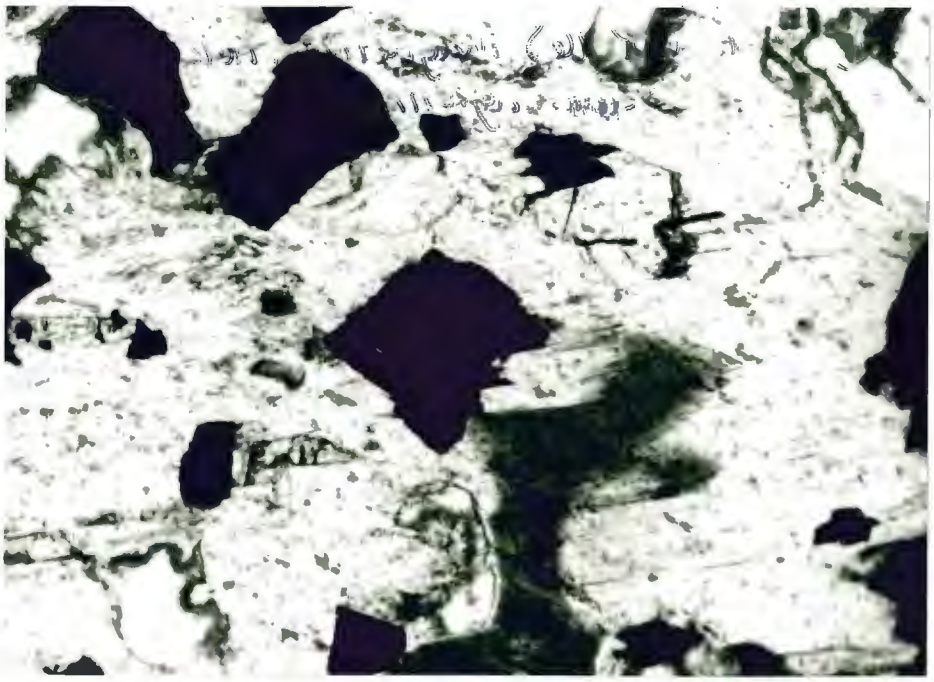

Fig 5-1 : (DP-46) Crossed-polars, transmitted light; subhedral magnetite grains enclosed by cummingtonite/grunerite in least altered fayalite-grunerite-quartz BIF. Width of view is 2.6 mm.

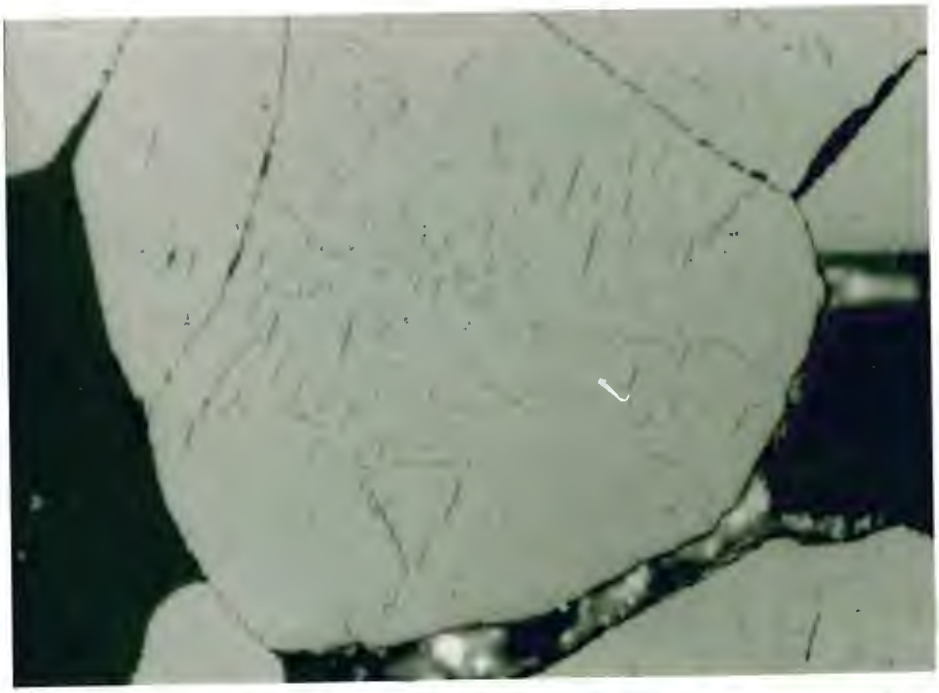

Fig 5-2 : (DP-8049) Plane, reflected light; magnetite with hercynite lamellae along (111) planes in least altered orthopyroxene-quartz-magnetite BIF. Width of view is 0.3 mm.

along (111) planes is seen in most sections to varying degrees (Fig 5-2). Hercynite lamellae are typically very fine, on the order of <0.01mm in width, and 0.05mm in length. These hercynite lamellae are distinguished from the surrounding magnetite by darker color in plane reflected light.

Orthopyroxene: 21.8% (0-45%); (0.05-3.0 mm)

In thin section orthopyroxene, mostly ferrohypersthene (Bonnichsen, 1968) exists as subhedral poikiloblasts enclosing magnetite or as euhedral grains with few inclusions. Typical pale green and pale rose pleochroism is common. Rims of orthopyroxene around olivine (fayalite), especially between olivine and quartz exist commonly in all thin sections containing olivine (Fig 5-3). Replacement of orthopyroxene by amphibole along cleavages and crystallographic planes is observed in all thin sections. These amphiboles may be retrograde replacement of orthopyroxene as Bonnichsen suggests (Bonnichsen, 1968).

Quartz: 28.5% (23-40%); (0.05-3.0 mm)

Quartz is present in all thin sections as anhedral grains commonly with numerous fluid inclusions and lesser inclusions of magnetite and fayalitic olivine. Rims of cummingtonite/grunerite or more commonly orthopyroxene enclose quartz grains. Cummingtonite/grunerite needles

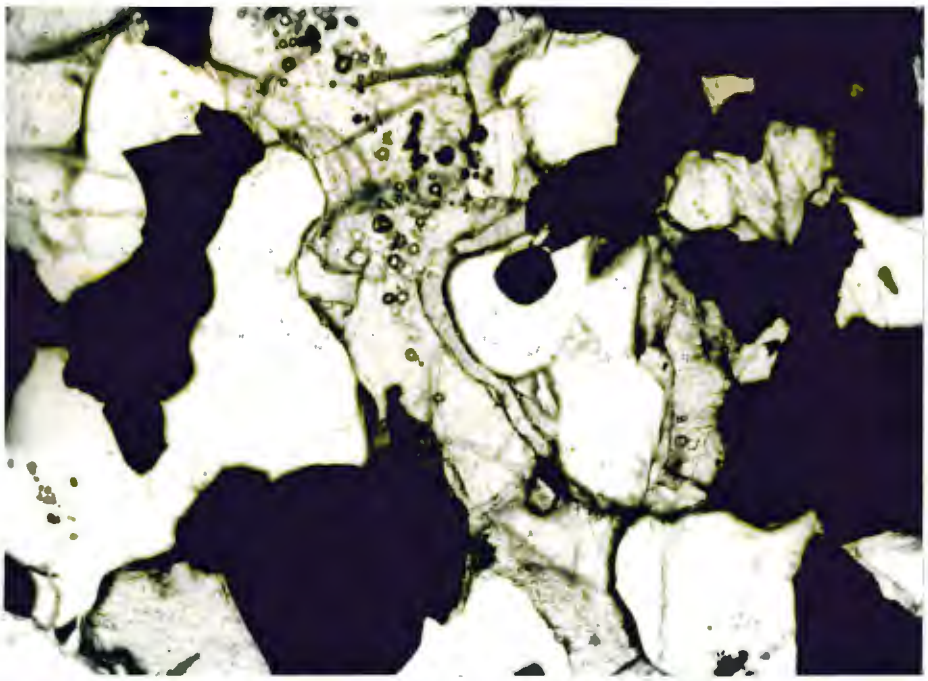

Fig 5-3 : (DP-57) Plane, transmitted light; orthopyroxene rims between inclusion-rich olivine and quartz in least altered magnetite-quartz-fayalite BIF. Width of view is 1.3 mm.

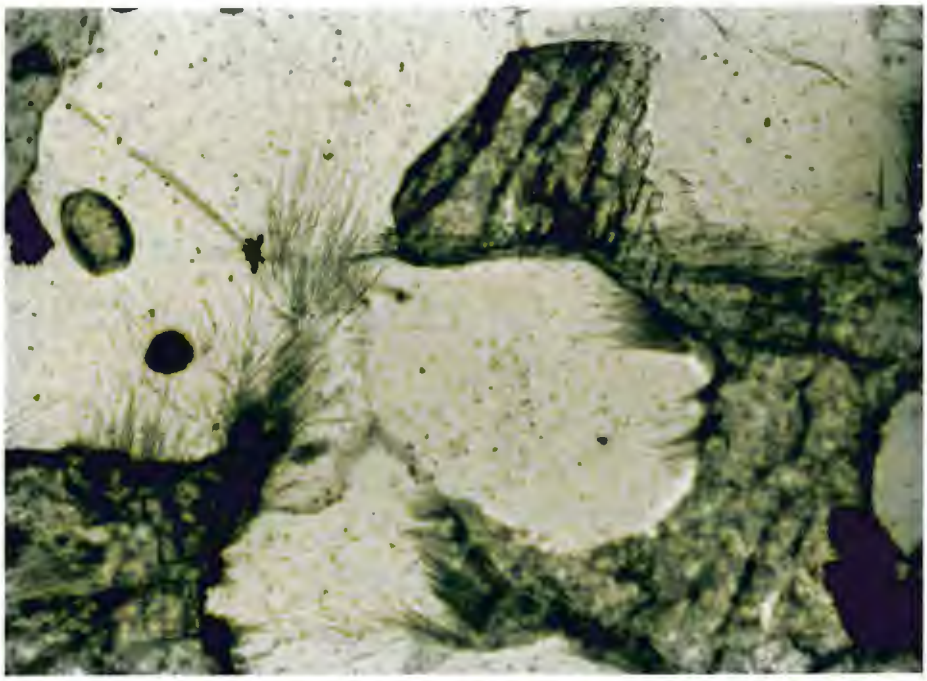

Fig 5-4 : (DP-8053) Plane, transmitted light; cummingtonite needles in quartz in least altered orthopyroxene-quartz-magnetite BIF. Width of view is 0.6 mm.

radiating from adjacent magnetite into quartz possibly indicate a metamorphic reaction between the quartz and magnetite. The reaction of $Fe_3O_4 + 3SiO_2 = 3FeSiO_3 + 0.5O_2$ is suggested by the rims of orthopyroxene between magnetite and quartz.

Cummingtonite/Grunerite: 8.2% (3-17%); (0.05-2.0 mm)

Acicular to granoblastic grains of green pleochroic cummingtonite/grunerite are occasionally seen enclosing quartz and magnetite as poikiloblasts with typical polysynthetic twins. However, most grains occur as acicular needles along cleavage/crystal planes of orthopyroxene or olivine, or sprays of needles radiating from a magnetite grain into quartz (Fig 5-4).

Olivine: 13.3% (2-46%); (0.1-2.0 mm)

Anhedral, granoblastic, pale green pleochroic fayalitic olivine grains coexist with quartz and magnetite with lesser orthopyroxene and grunerite. Some layers of nearly monomineralic granoblastic olivine exist, typically on the scale of 1mm to 2cm. Numerous inclusions of spherical quartz, smaller olivine, or fluid are common in olivine when not in monomineralic layers.

Clinopyroxene: 5.3% (0-14%); (0.1-1.5 mm)

Dominantly augite with lesser pigeonite, clinopyroxene

forms subhedral and rarely euhedral grains. Clinopyroxene commonly is observed poikiloblastically enclosing quartz and magnetite. Small anhedral biotite occurs as alteration of clinopyroxene along with rare grunerite. A few clinopyroxene grains show anomalous very pale purple to pale green interference colors, indicating an iron- and aluminum-rich composition (Deer, Howie and Zussman, 1992).

Biotite: 1.3% (0-3%) (0.01-1.0 mm)

Biotite occurs as anhedral grains altered from clinopyroxene, orthopyroxene and less commonly olivine, or as larger isolated subhedral grains. Anhedral biotite is seen formed along fractures. All biotite is titanium rich, distinguished by its very distinct red-orange pleochroism.

Apatite: 0.3% (0-1%); (0.05-0.1 mm)

Apatite occurs as very small subhedral inclusions in quartz. Slightly larger, more euhedral tapered hexagonal prisms occur partly included in magnetite or as isolated grains.

Sulfide: 0.2% (0-1%); (0.01-0.1 mm)

Sulfide in the BIF includes pyrrhotite and chalcopyrite, less commonly pentlandite, cubanite, and rarely covellite. The grains are typically anhedral, infrequently found in or with magnetite. Pyrrhotite shows exsolution blebs and zones

of chalcopyrite, cubanite and pentlandite; whereas covellite occurs as isolated grains.

Stilpnomelane: 0.5% (0-1%); (0.01-0.05)

Small amounts of stilpnomelane, distinguished from biotite by the lack of 'birds-eye' extinction, higher birefringence and the poor second cleavage, is seen as an alteration mineral rarely associated with fayalite and other iron silicates.

Chlorite: 0.4% (0-1%); (0.01-0.2)

Minor amounts of anhedral, pale to dark green pleochroic chlorite occur associated with clinopyroxene, orthopyroxene and olivine. Chlorite is not distinguished from other minerals of the chlorite group having very similar appearance and occurrence.

II. Most Altered BIF:

12 samples were taken from outcrop of BIF within 25 feet of the contact with the SKI and made into polished thin sections. One sample from drillcore was made into a thin section from a grain mount and into a polished section also. Layers C-G of the upper slaty iron formation were sampled to be consistent with the least altered BIF. The lithology is fine- to coarse-grained, dark grey, layered, heterogeneous,

poikilitic, hypidiomorphic to granoblastic magnetite-orthopyroxene-plagioclase-clinopyroxene-amphibole iron formation.

Magnetite: 27.0% (0-55%) (0.05-1.0 mm)

Magnetite occurs in the most altered BIF as anhedral to euhedral crystals found in distinct layers or less distinct masses which are typically poikilitically enclosed by plagioclase, clinopyroxene, orthopyroxene, and less commonly olivine. Ilmenite exists intergrown with magnetite in 80% of samples examined: 15% as lamellae in magnetite (Fig 5-5), 10% as rims around magnetite grains or interstitial blebs (Fig 5-6), 15% as individual isolated grains, and most importantly, 40% as replacements of cores of magnetite grains/layers of grains (Fig 5-7). Equant isometric crystals of magnetite are partially to totally pseudomorphed by ilmenite.

Other textures involving magnetite include: hercynite lamellae oriented along {111} crystallographic planes (Fig 5-8), stilpnomelane rimming or poikilitically enclosing magnetite grains, magnetite associated with sulfide, and symplectites of magnetite and orthopyroxene (Fig 5-9). Hercynite lamellae are found in most of the magnetites from the most altered BIF and have the same appearance and {111} orientation as those from the least altered BIF. Stilpnomelane, which is seen rimming/enclosing magnetite, is probably of retrograde metamorphic origin, as it is a lower

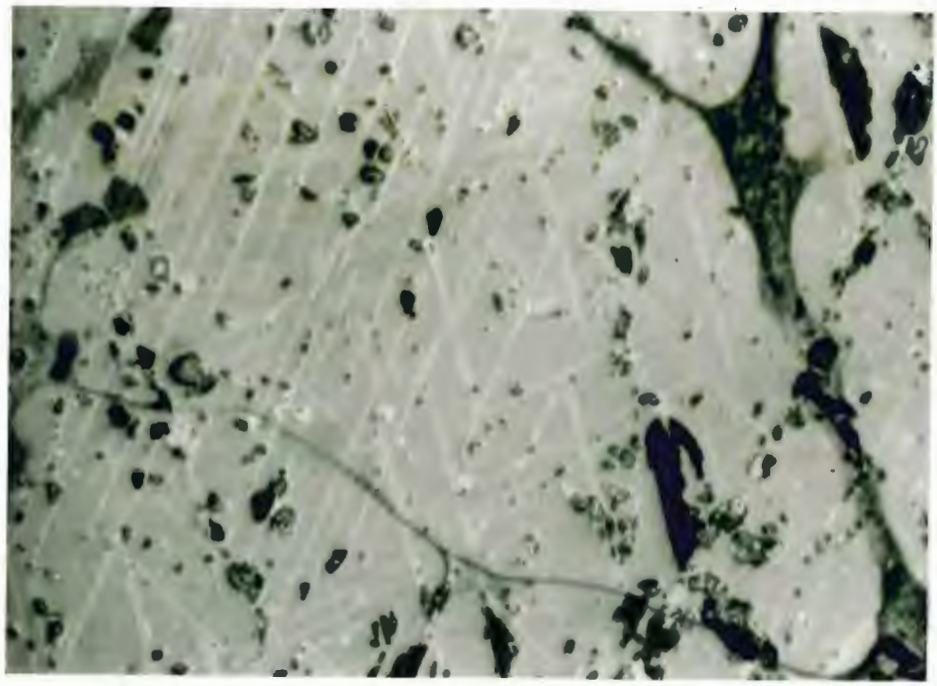

Fig 5-5 : (DP-23A) Plane, reflected light; magnetite (darker grey) with abundant ilmenite lamellae along (111) in most altered plagioclase-amphibole-magnetite BIF. Width of view is 0.6 mm.

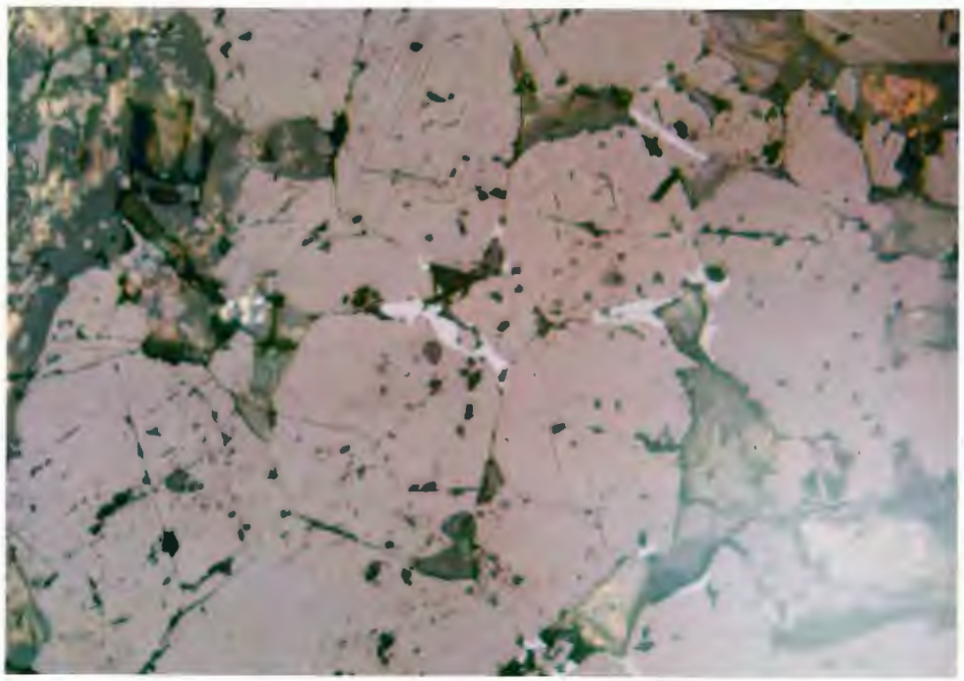

Fig 5-6 : (DP-31) Crossed Polars, reflected light; magnetite (dark grey) with ilmenite rims (light grey) in most altered magnetite-plagioclase-augite BIF. Width of view is 1.3 mm.

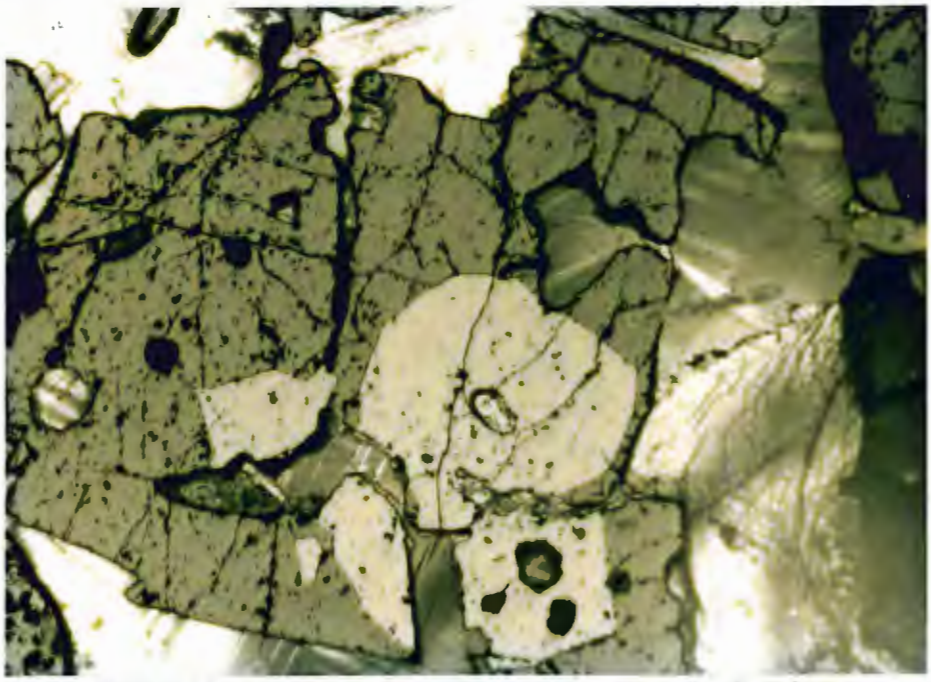

Fig 5-7 : (DP-15A) Crossed polars, reflected light; nearly euhedral ilmenite plates (white, center) partially pseudomorphing magnetite (grey) in most altered plagioclase-pyroxene-magnetite BIF. Width of view is 2.6 mm.

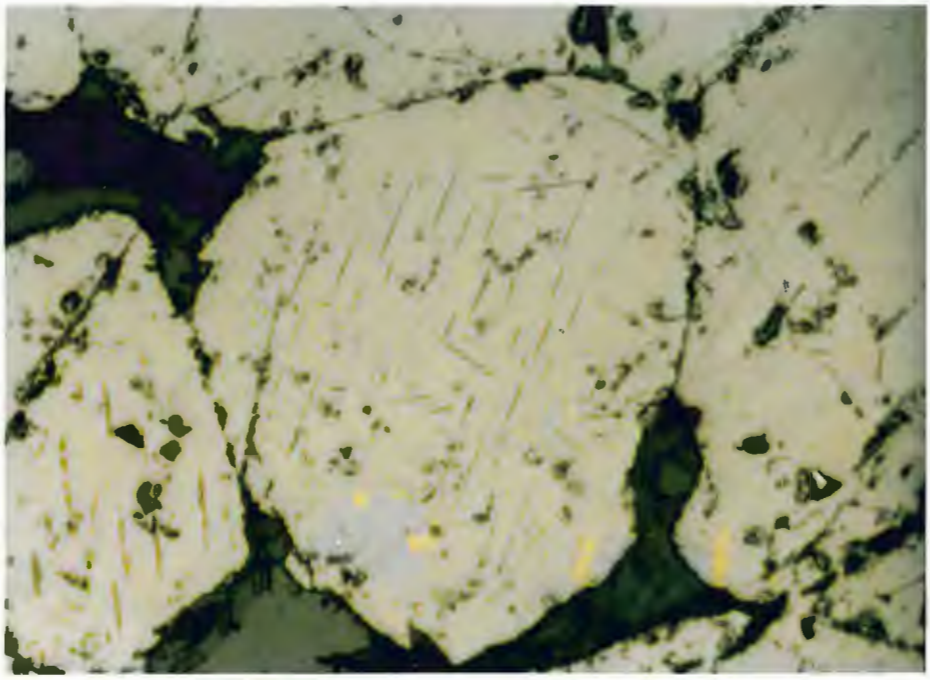

Fig 5-8 : (DP-31) Plane, reflected light; hercynite lamellae along (111) planes in magnetite in most altered magnetite-plagioclase-augite BIF. Width of view is 0.6 mm.

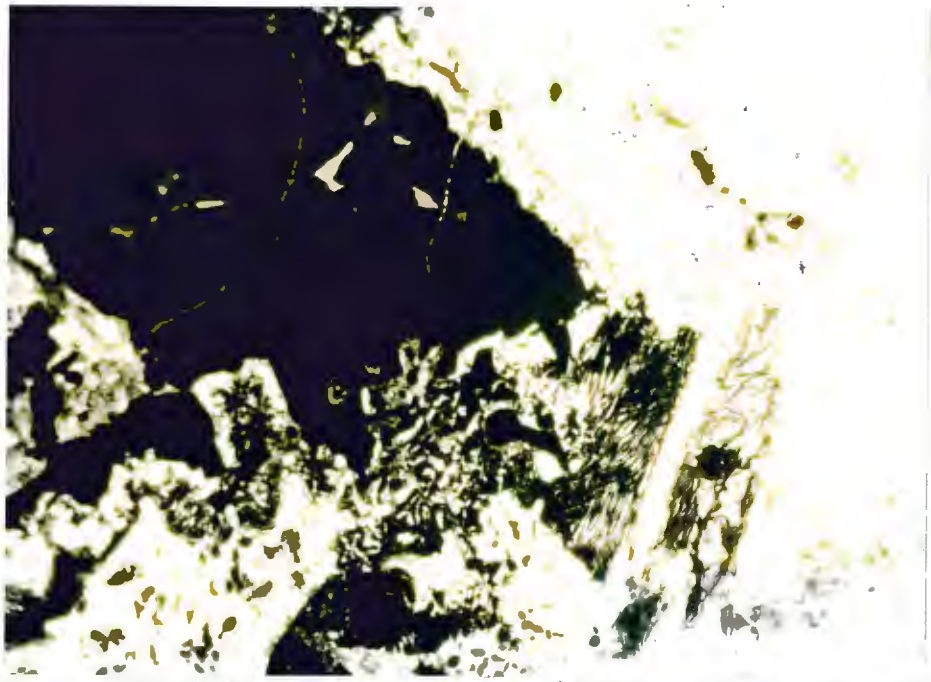

Fig 5-9 : (DP-16B) Plane, transmitted light; magnetite-orthopyroxene symplectite near larger magnetite grain in most altered plagioclase-pyroxene-magnetite BIF. Width of view is 2.6 mm.

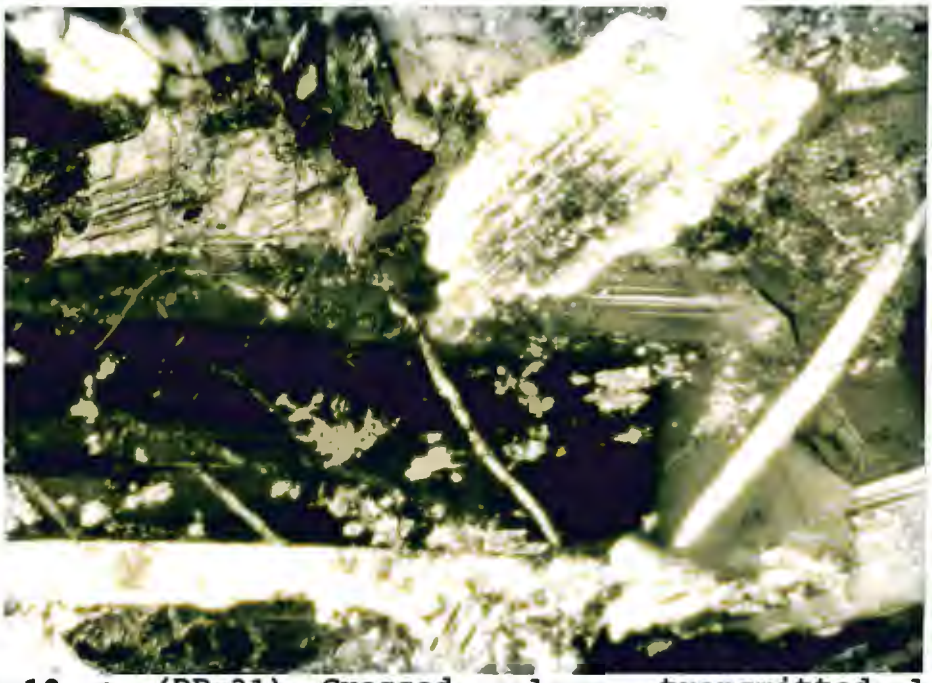

Fig 5-10 : (DP-31) Crossed polars, transmitted light; normally zoned plagioclase (center) slightly altered to saussurite in most altered magnetite-plagioclase-augite BIF. Width of view is 2.6 mm.

temperature hydrous mineral which would not exist under pyroxene hornfels facies conditions. Sulfide intergrown or associated with magnetite occurs in trace amounts as in the least altered BIF, with the exception of a few thin sections exhibiting up to 7% sulfide. Orthopyroxene/magnetite symplectites are common, and could be the result of recrystallization of olivine, which upon cooling resulted in the simultaneous nucleation of orthopyroxene and magnetite from the original olivine composition (Barton and Van Gaas, 1988). These symplectites are found adjacent to magnetite layers, and could also be formed by replacement of magnetite by iron silicate, or the replacement of orthopyroxene by magnetite.

Plagioclase: 17.1% (0-60%); (0.1-6.0 mm)

Subhedral to anhedral plagioclase commonly encloses magnetite layers in the most altered BIF. Plagioclase compositions vary from An_{36} to An_{59} in the altered BIF (Michel-Levy). Most plagioclase exhibits normal zoning, with a larger undulose extinction of plagioclase lamellae in the core of the crystal and a lesser extinction angle at the rim (Fig 5-10). Cores of plagioclase crystals altered to, and in some cases pseudomorphed by, actinolite and saussurite are common. Foliation of plagioclase crystals perpendicular to magnetite layers was observed in a few thin sections, generally for plagioclase crystals 0.1 to 2.0 mm in size.

Numerous very fine spinel inclusions, usually in the form of rods or lamellae, exist in most coarser-grained plagioclase, although some overgrowths of more albitic plagioclase are devoid of spinel inclusions. Elongate, slender apatite prisms commonly are observed as inclusions in plagioclase. Intergrowths of plagioclase with orthopyroxene in symplectite is also commonly observed (Fig 5-10).

Orthopyroxene: 9.4% (0-70%); (0.01-5.0 mm)

Orthopyroxene occurs mainly as subhedral poikiloblastic crystals enclosing magnetite grains and/or layers of magnetite and as anhedral symplectic intergrowths with plagioclase, and less commonly as rims around olivine, rims between magnetite and quartz, or non-poikiloblastic isolated crystals interstitial to plagioclase. Subhedral poikiloblasts which enclose magnetite and less commonly quartz, are typically larger crystals which appear to have grown around relict layers of magnetite (Fig 5-11).

Orthopyroxene-plagioclase symplectites appear to have grown as radiating masses which nucleate on plagioclase or pyroxene crystals (Fig 5-10). The origin of these symplectites is not known, but they do occur throughout the basal unit of the SKI as well.

Rims of orthopyroxene around olivine may simply be the result of the reaction of olivine with silica-rich minerals, or a silica rich fluid/magma. Orthopyroxene rims between

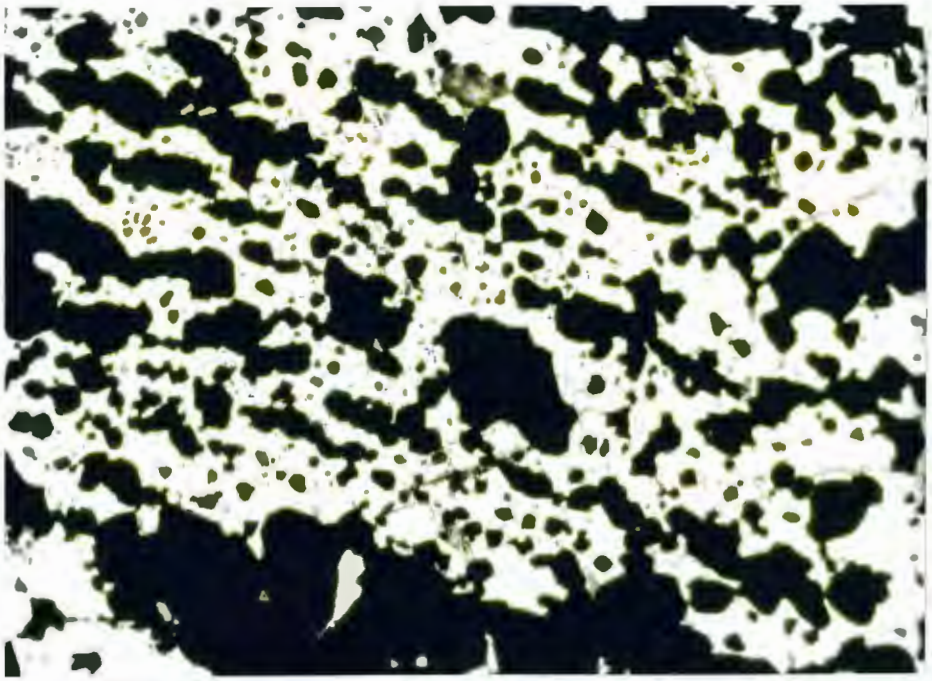

Fig 5-11 : (DP-15A) Plane, transmitted light; orthopyroxene (white) enclosing magnetite layer (black) in most altered plagioclase-pyroxene-magnetite BIF. Width of view is 1.3 mm.

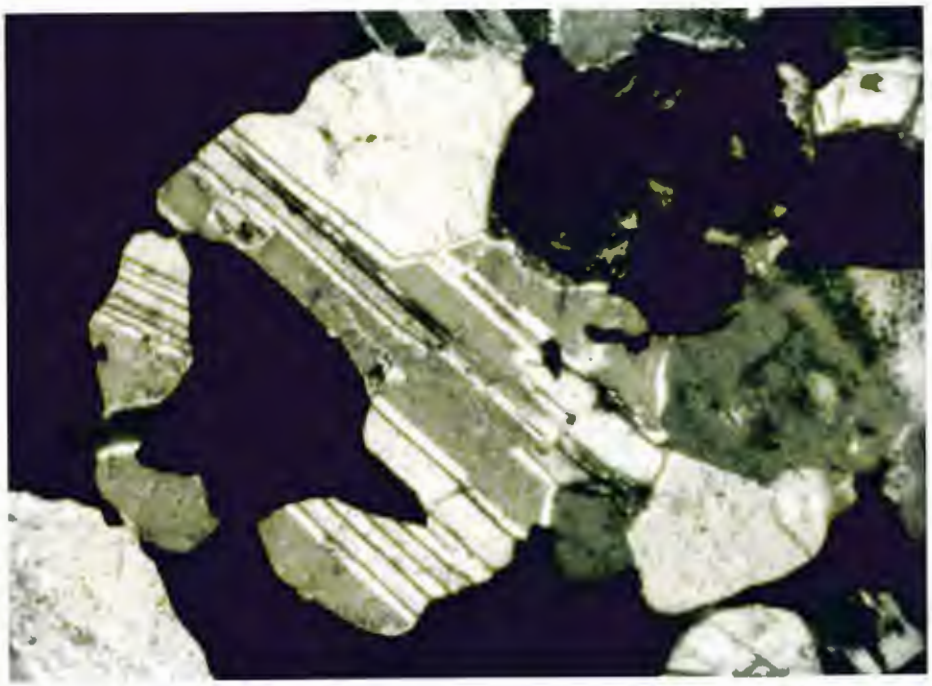

Fig 5-12 : (DP-18C) Crossed polars, transmitted light; cummingtonite/grunerite with abundant twin lamellae surrounded by magnetite (black) in most altered magnetite-amphibole-quartz BIF. Width of view is 1.3 mm.

adjacent magnetite and quartz are probably the result of the reaction of $Fe_3O_4 + 3SiO_2 = 3FeSiO_3 + 0.5O_2$. Isolated orthopyroxene crystals which are not intergrown with magnetite are less common, and typically have opaque rods of what is probably spinel. Alteration of orthopyroxene to bastite is also common.

Clinopyroxene: 12.1% (0-46%); (0.05-6.0 mm)

Subhedral to anhedral augite and less commonly pigeonite occur in the most altered BIF as poikiloblastic crystals enclosing magnetite, as isolated interstitial crystals, or as subhedral to euhedral grains having a cumulate-like texture in rocks rich in clinopyroxene. In many thin sections pigeonite or orthopyroxene is observed to have abundant exsolution lamellae of augite. Similar to orthopyroxene, clinopyroxene commonly has rods or lamellae of some opaque spinel or ilmenite. Clinopyroxene also may be heavily altered to uralite.

Amphibole:

Cummingtonite/Grunerite: 5.8% (0-24%); (0.05-3.5 mm)

Occurring as subhedral to euhedral crystals in magnetite-rich layers, cummingtonite/grunerite is distinguished from other amphiboles by its higher birefringence and abundance of polysynthetic twin lamellae (Fig 5-12). Specific compositions were not measured for

these amphiboles, and a range of colorless crystals to green pleochroic crystals indicates the presence of both cummingtonite and grunerite compositions, as noted by Bonnichsen (1968). Fine, anhedral to subhedral radiating acicular cummingtonite/grunerite occurs radiating from the surface of magnetite grains into quartz grains.

Actinolite: 7.4% (0-40%); (<0.01-1.0 mm)

Masses of acicular actinolite showing lower birefringence and a lack of twinning are present in the most altered BIF as replacement or alteration of clinopyroxene, orthopyroxene or plagioclase. In places actinolite appears to have replaced more than one mineral in the same thin section. This replacement occasionally appears to be along fractures, and because of its hydrous nature appears to be related to the presence of some fluid.

Hornblende: 2.2% (0-12%); (0.05-4.0 mm)

Subhedral to anhedral, shreddy masses of brown-green pleochroic hornblende have also been observed as a common alteration mineral in the most altered BIF. Hornblende replaces orthopyroxene or both orthopyroxene and clinopyroxene in the same thin section.

Quartz: 6.2% (0-50%); (0.05-4.0 mm)

Anhedral quartz grains occur as inclusions in magnetite, or as distinct layers dominantly composed of quartz. Inclusions of quartz in magnetite usually show

cummingtonite/grunerite crystals radiating from the magnetite into the quartz grains similar to Fig 5-4. When concentrated in layers, the quartz grains usually have a granoblastic texture. Rocks containing an abundance of quartz appear to have substantially decreased amounts of plagioclase and pyroxenes, and in some cases elevated amounts of magnetite relative to rocks with only minor amounts of quartz.

Phyllosilicates:

Biotite: 0.7% (0-2%); (<0.01-2.0 mm)

Titanium-rich and iron-rich biotite occurs in the most altered BIF much the same as in least altered BIF: as anhedral to subhedral grains replacing clinopyroxene or orthopyroxene, or as subhedral isolated grains. Occasionally biotite is also found intergrown with hornblende. All Ti-rich biotites have a reddish to pale orange pleochroism.

Stilpnomelane: 1.9% (0-20%); (0.1-1.0 mm)

Stilpnomelane occurs most commonly in the most altered BIF as brownish to greenish pleochroic grains interstitial in magnetite layers or poikiloblastically enclosing magnetite. Stilpnomelane is distinguished from biotite by its browner color, and poor second cleavage. Because both Ti-rich biotite and stilpnomelane have such deep color and pleochroism, their interference colors were masked, and the difference between their interference colors was not used as a diagnostic property. Less commonly, stilpnomelane is

altered to actinolite and clay minerals.

Chlorite: 1.6% (0-7%); (0.1-0.3 mm)

Chlorite commonly occurs as an alteration of orthopyroxene, clinopyroxene or olivine, usually with actinolite and fine-grained magnetite. Chlorite forms in masses, veins or shreddy micaceous form altering from stilpnomelane.

Apatite: 0.7% (0-3%); (<0.05-1.0 mm)

Subhedral to euhedral elongate prisms of apatite occur as small (<0.2mm) inclusions in biotite or amphibole. Apatite included in or intergrown with magnetite, plagioclase or orthopyroxene generally is larger than 0.2 mm. Less common 1.0mm euhedral apatites are seen as isolated crystals not totally enclosed by any specific mineral.

Sulfides: 0.8% (0-7%); (<0.01-1.5 mm)

The sulfides that occur in the most altered BIF include pyrrhotite and chalcopyrite with less common pentlandite and cubanite. Sulfides are generally disseminated throughout the rock or associated with magnetite and ilmenite. Sulfide abundances in the most altered BIF are similar to the least altered BIF, with the exception of a few thin sections containing up to 7% sulfides. These sulfide enriched rocks also have a greater amount of ilmenite, and occur closer to the SKI.

Olivine: 0.1% (0-1%); (0.1-0.7 mm)

Anhedral olivine occurs only rarely in the most altered BIF as part of layers rich in silicates, such as plagioclase and orthopyroxene. The olivine appears to be iron rich, indicated by the distinct greenish pleochroism and 2V of >115°.

SUMMARY OF PETROGRAPHY OF THE BIWABIK IRON FORMATION

The main petrographic differences between the least altered and the most altered BIF are as follows: (1) the presence of new minerals in the most altered BIF, (2) the change in abundance of minerals, (3) and the very different textural relations seen in the most altered BIF.

Minerals occurring in the most altered upper slaty BIF which didn't previously exist in the least altered samples of the upper slaty BIF include: plagioclase, ilmenite and actinolite. The presence of abundant plagioclase, a common igneous mineral, and actinolite, a common igneous alteration mineral, in the most altered BIF are evidence for infiltration of "fingers" of magma into the iron formation. These "fingers" of magma may have intruded into layers of quartz and iron silicates in the BIF and directly crystallized plagioclase and pyroxene. However, the presence of ilmenite cannot be accounted for by direct crystallization from magma, as ilmenite appears within partially pseudomorphed magnetite grains. Ilmenite in the most altered

BIF appears to have been formed by the introduction of titanium into layers of magnetite by some metasomatic mechanism from the "fingers" of magma.

Minerals whose volume percent drastically changed from the least altered to the most altered upper slaty BIF include: quartz, orthopyroxene, olivine, clinopyroxene, magnetite, hornblende, sulfide, stilpnomelane and chlorite (Table 5-1). Overall gains and losses shown in Table 5-1 are strictly differences in the average modal composition of the upper slaty BIF, and great variability of the abundance of certain minerals occurs, especially in the most altered upper slaty BIF. For example, on average the most altered BIF lost 12.4% of its orthopyroxene relative to the least altered, but one sample of most altered BIF contained more orthopyroxene (54%) than any of the least altered BIF samples, which have at most 45% orthopyroxene. The overall amount of olivine decreases, along with the amount of orthopyroxene and quartz. This could be due to the reaction of olivine and quartz to form orthopyroxene, with subsequent alteration of the orthopyroxene to form hydrous minerals. An increase in the amount of hydrous minerals in the form of actinolite and increased amounts of hornblende, chlorite and stilpnomelane would account for the loss of orthopyroxene via hydrous alteration. Bonnichsen (1968) described the metamorphism of the BIF in the Dunka Pit area as involving the loss of some of the H_2O and all of the CO_2 in the BIF. The presence of

Table 5-1: Comparison of Average Modal Composition of Least/Most Altered BIF (standard deviation in [ ])

Mineral	Least Alt. BIF (n = 6)	Most Alt. BIF (n = 12)	Gain/Loss +/-
Magnetite	20.3% [16.5]	27.0% [23.7]	+ 6.7%
Orthopyroxene	21.8% [18.3]	9.4% [14.9]	-12.4%
Quartz	28.5% [6.5]	6.2% [14.4]	-22.3%
Cummingtonite	8.2% [6.6]	5.8% [8.3]	- 2.4%
Olivine	13.3% [16.8]	0.1% [0.3]	-13.2%
Clinopyroxene	5.3% [4.8]	12.1% [14.6]	+ 6.8%
Biotite	1.3% [1.5]	0.7% [0.7]	- 0.6%
Apatite	0.3% [0.0]	0.7% [1.0]	+ 0.4%
Sulfides	0.2% [0.0]	0.8% [2.1]	+ 0.6%
Stilpnomelane	0.5% [0.5]	1.9% [5.7]	+ 1.4%
Chlorite	0.4% [0.5]	1.6% [3.0]	+ 1.2%
Hornblende	0.1% [0.4]	2.2% [3.5]	+ 2.1%
Ilmenite	0.0%	5.5% [7.3]	+ 5.5%
Plagioclase	0.0%	17.1% [21.1]	+17.1%
Actinolite	0.0%	7.4% [11.3]	+ 7.4%

H_2O as a fluid would aid in the transfer of other components, as well as produce hydrous minerals from retrograde anhydrous pyroxene. An overall increase in the amount of clinopyroxene could be explained by the increase of CaO in the altered BIF, and also may account for the loss of some of the orthopyroxene.

An increase in the amount of magnetite can be explained by the variability of magnetite content inherently in the iron formation; some layers sampled in the least altered upper slaty happened to be less magnetite-rich by chance than those from the most altered upper slaty. Other possible explanations, such as the formation of magnetite from the dissociation of iron silicates, or the introduction of iron metasomatically into the iron formation lack textural evidence and are less likely. The increased sulfide content may be from an increase in overall sulfur in the most altered BIF in the "fingers" of magma, as little sulfide is found in the least altered BIF. Sulfide minerals are found in modal abundances of up to 7% in the most altered BIF.

Textural relations in the least altered and most altered upper slaty BIF include several textures common to both as well as strikingly different textures. Both least and most altered BIF commonly show rims of orthopyroxene between fayalitic olivine and quartz, and alteration of orthopyroxene to cummingtonite/grunerite, chlorite, hornblende, and other hydrous minerals. However, alteration of orthopyroxene and

other Fe-silicates is more prevalent in the most altered BIF. Also, replacement of many minerals by actinolite is unique to the most altered BIF.

Hercynite lamellae are found along {111} planes in magnetite from both the least altered and most altered BIF. The hercynite lamellae appear to be an exsolution texture, however the origin of the aluminum in the magnetite is not fully understood. Magnetite could have gained alumina from surrounding aluminous minerals. Unmetamorphosed upper slaty iron formation to the west contains many minerals which have aluminum in their structure: hornblende, stilpnomelane, biotite, minnesotaite and chamosite (Gunderson and Schwartz, 1962). However, the total amount of Al_2O_3 in the upper slaty is under 2.0 wt.% from whole rock analysis (Lepp, 1966; Morey, 1992).

Textures found exclusively in the most altered BIF include: various symplectites of orthopyroxene, plagioclase, and Fe-Ti oxides; large poikilitic silicates enclosing layers of magnetite; and intergrowths of ilmenite with magnetite. Symplectites of Fe-Ti oxides with Opx are common in the most altered BIF, and can be attributed to one of several origins. Oxide/orthopyroxene symplectite may have formed as a result of overall re-equilibration of originally magmatic minerals in the "fingers" of magma during retrograde metamorphism (Barton and van Gaas, 1988). Another explanation may be the exsolution of iron oxide from a more iron rich silicate

during/after peak metamorphism (Garrison and Taylor, 1981). Both of these possibilities are described for igneous rocks, and involve igneous mechanisms (Barton and van Gaas, 1988; Garrison and Taylor, 1981; Van Lamoen, 1979).

The presence of silicates such as plagioclase, clinopyroxene, and orthopyroxene poikilitically enclosing layers of magnetite are similar to igneous minerals found in the SKI, and are interpreted to be part of "fingers" of magma injected into and partially assimilating the BIF. All of these large (up to 5mm) poikilitic silicates appear to be interconnected with other concentrations of magmatic minerals forming finger-like projections into the BIF.

The various intergrowths of ilmenite with magnetite include: lamellae of ilmenite in magnetite, ilmenite rimming and filling interstices between magnetite grains, and magnetite grains being replaced by ilmenite. These textures appear to be a product of exsolution of ulvöspinel which later oxidized to ilmenite (Ramdohr, 1980). A metasomatic source of the titanium in the magnetite is most strongly argued for in the replacement of magnetite layers and grains by ilmenite. Titanium which exists within an individual magnetite grain could not have been emplaced there via some magmatic mechanism, but must have diffused or infiltrated into the magnetite metasomatically from surrounding "fingers" of magma.

In summary, arguments can be made for the magmatic

origin of certain silicates, such as plagioclase and pyroxenes, as "fingers" of magma seeping in between layers of magnetite in the BIF, but the origin of ilmenite grains within individual magnetites and layers of magnetite must be of metasomatic origin. This metasomatism involved the introduction of Ti into the BIF as evident in the presence of ilmenite partial pseudomorphs of magnetite layers. The presence of H_2O indicates the presence of a fluid, expelled from the BIF during metamorphism, which may have aided the movement of Ti from the "fingers" of SKI into the BIF.

III. Least Altered SKI:

All rocks were sampled from the basal unit of the SKI, which is the intrusive unit in contact with the BIF at Dunka Pit. 11 samples were taken from both outcrop and drillcore and made into polished thin sections. An overall description of the basal SKI is: fine- to coarse-grained generally gabbroic rock varying from gabbro to norite to troctolite with generally ubiquitous ilmenite, biotite, and apatite, with a variety of textures from poikilitic to ophitic to symplectic.

Plagioclase: 59.0% (50-66%); (0.1-12.0 mm)

Generally subhedral and commonly ophitic, plagioclase is

the most common mineral in the basal unit of the South Kiwishiwi intrusion of the Duluth Complex. Plagioclase varies in composition from An_{58} to An_{63} as measured using the Michel-Levy method. Orthopyroxene and clinopyroxene >3mm in size typically enclose plagioclase ophitically. Plagioclase also is, in a few instances, partially enclosed by olivine. Less commonly, foliated plagioclase is present, usually when laths are smaller in size, possibly a product of flow foliation. A few thin sections show a mesocumulate texture, with subhedral plagioclase and olivine surrounded by interstitial anhedral pyroxene, oxide, sulfide, and other minor minerals. Another interesting texture found in the plagioclase of every thin section of least altered SKI is the presence of inclusions of rod-shaped opaque minerals. These rods are typically too fine to be analyzed by an electron microprobe, but do not appear to be anisotropic in reflected light. This would rule out ilmenite, and lead one to believe the rods are probably a spinel. Plagioclase-orthopyroxene symplectite commonly exists at grain boundaries with other minerals, although only less than 5% of the plagioclase is intergrown with orthopyroxene as symplectite.

Augite: 14.0% (5-28%); (0.1-10.0 mm)

Anhedral to subhedral augite grains are commonly altered to biotite and exhibit intergrowths with pigeonite and/or orthopyroxene. These intergrowths consist of pigeonite

exsolving augite, orthopyroxene exsolving augite, orthopyroxene exsolving pigeonite, and combinations of these suggestive of cooling textures with exsolution of more calcic pyroxenes from less calcic pyroxene hosts. Also commonly augite is seen as having very small rods and lamellae of some opaque isotropic mineral, probably ilmenite, which appear to be related to either exsolution and/or oxidation of ferric iron by reaction of the magnetite with deuteric fluids. Augite ophitically encloses plagioclase in many thin sections, and forms rims around olivine (Fig 5-13) in nearly as many, possibly suggesting the reaction of olivine + calcic, silica-enriched liquid = augite.

Olivine: 15.9% (7-25%); (0.2-8.0 mm)

Anhedral olivine occurs partially rimmed by orthopyroxene or clinopyroxene in all thin sections (Fig 5-14), partially altered to magnetite and biotite (20% of the thin sections), poikilitically enclosing plagioclase (5%), as cumulate grains (10%), or as a symplectite with magnetite (1%). Rims of pyroxene around olivine are indicative of the reaction of olivine + liquid = pyroxene. Olivine-magnetite symplectite is rare, and its origin is not fully understood.

Orthopyroxene: 3.9% (trace - 10%); (<0.01-6.0 mm)

Commonly, large (> 3mm) subhedral to anhedral orthopyroxene ophitically enclose plagioclase. Similar rod-

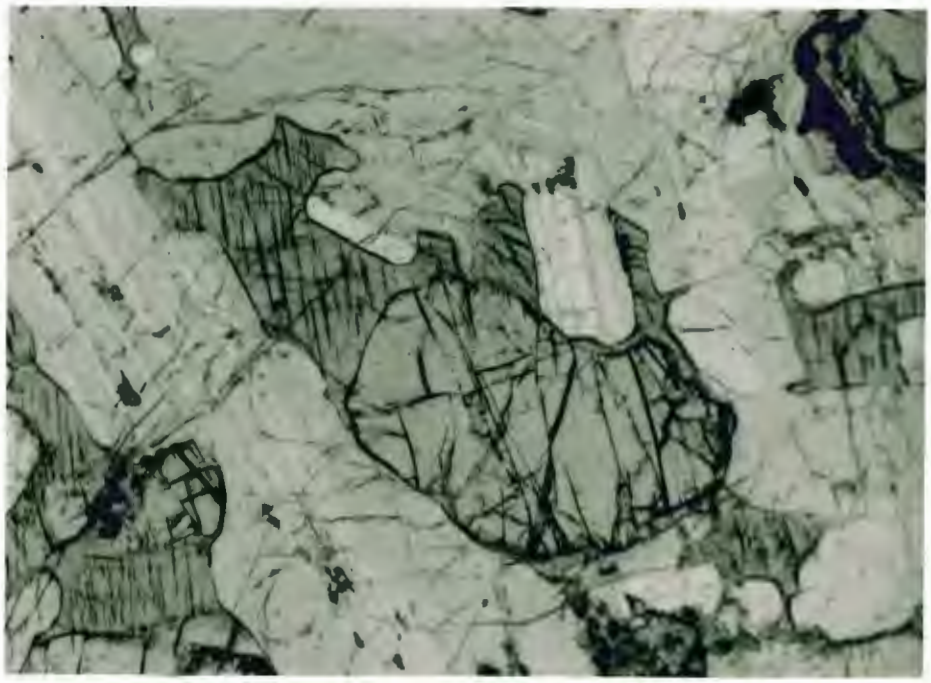

Fig 5-13 : (NM-26A) Plane, transmitted light; rim of augite on olivine in least altered SKI troctolite. Width of view is 2.6 mm.

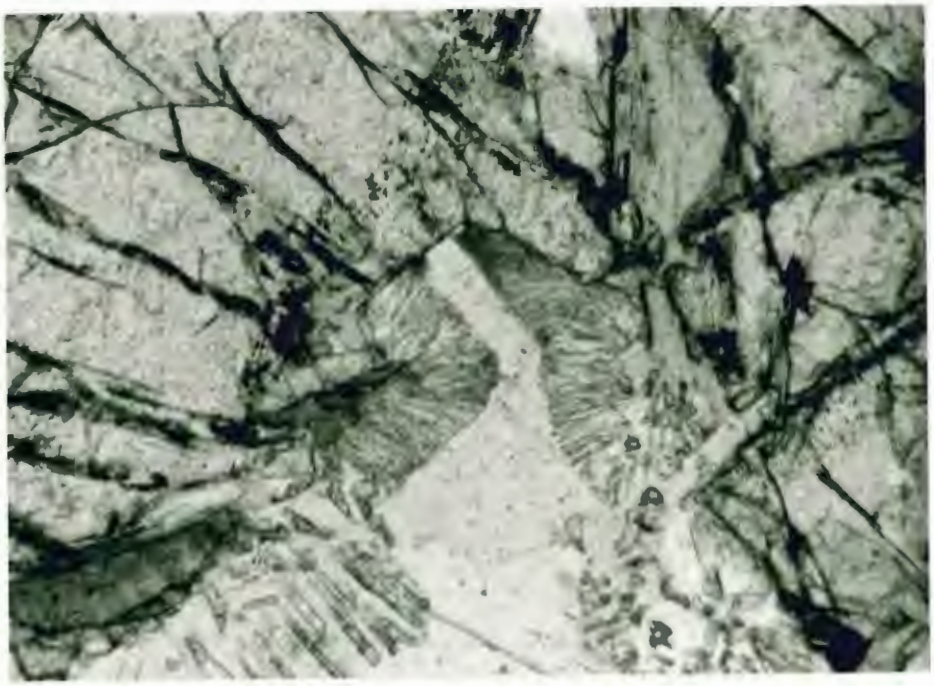

Fig 5-14 : (DP-62) Plane, transmitted light; orthopyroxene-plagioclase symplectite radiating from olivine (upper right and left) in least altered SKI olivine gabbro. Width of view is 1.3 mm.

shaped oxides which occur in plagioclase occur in orthopyroxene, both as ilmenite and spinel. Plagioclase and orthopyroxene show symplectic growth, appearing as an interstitial intergrowth of 50% plagioclase and 50% orthopyroxene radiating from a grain boundary of a larger subhedral mineral (Fig 5-14), usually a plagioclase or pyroxene. Commonly orthopyroxene rims olivine. Alteration to bastite, biotite and magnetite is common in orthopyroxene.

Ilmenite: 3.1% (1-5%); (0.01-5.0 mm)

In every thin section of the basal unit of the SKI ilmenite is at least partially rimmed by iron-rich biotite (Fig 5-16). The origin of this texture may simply be the tendency of biotite to nucleate on oxide, and ilmenite is by far the predominant oxide in the unaltered SKI. Typically, ilmenite has a subhedral platy shape and may be associated with sulfides, if any are present in the rock. Ilmenite and magnetite intergrowths are rarely observed in the least altered SKI, usually occurring as distinct subhedral-anhedral grains with mutual grain boundaries.

Magnetite: 0.5% (0-trace); (0.01-1.0 mm)

A few anhedral isolated magnetite grains have been observed, but more commonly magnetite exists as symplectite with olivine. Also magnetite may be the oxide that exists in plagioclase and the pyroxenes, although the rods are too fine

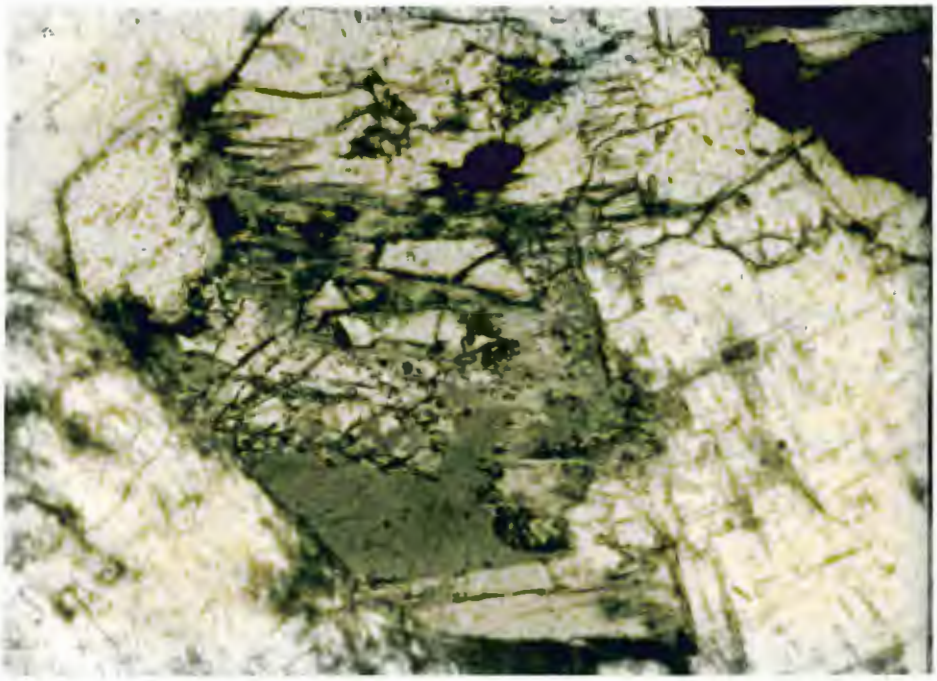

Fig 5-15 : (DP-62) Plane, transmitted light; clinopyroxene (colorless, right) altering to hornblende (grey, center) in least altered SKI olivine gabbro. Width of view is 1.3 mm.

Fig 5-16 : (DP-55) Plane, transmitted light; ilmenite (black) rimmed by biotite (grey) in least altered SKI troctolite. Width of view is 2.6 mm.

for microprobe analyses.

Biotite: 2.5% (trace-5%); (0.01-4.0 mm)

Anhedral to subhedral grains of biotite are most commonly present in the SKI as rims on ilmenite (Fig 5-16). The biotite is Ti-rich, as distinguished by its deep red to pale orange pleochroism. Biotite is also common as inclusions in pyroxene, possibly a product of deuteric alteration.

Apatite: 0.7% (0-1%); (0.05-3.0 mm)

Apatite occurs as subhedral to euhedral hexagonal crystals. Commonly, apatite is associated with plagioclase if the apatite exceeds 0.5mm in size as observed in 25% of the thin sections. However, numerous smaller euhedral inclusions of apatite also occur in biotite in all thin sections examined.

Sulfide: 0.7% (0-1%); (<0.01-1.5 mm)

Pyrrhotite and chalcopyrite occur as the most common sulfides in the SKI in the area of Dunka Pit. These are commonly anhedral and associated with oxide and olivine. Sulfide minerals are disseminated throughout the rock interstitial to silicates, and only rarely exceed 0.2mm in size.

Amphibole: Actinolite & Hornblende: 0.6% (0-2%); (<0.01-0.5mm)

Actinolite occurs mainly as small acicular masses associated with saussuritization of plagioclase, whereas hornblende occurs intergrown with clinopyroxene, in places as partial pseudomorphs. The origin of the hornblende is believed to be deuteric alteration via the reaction: clinopyroxene + fluid = hornblende (Fig 5-15). Hornblende is distinguished from actinolite on the basis of brownish to greenish pleochroism, and normally occurs as larger grains (>0.5 mm).

Chlorite: 0.1% (0-1%); (<0.01-0.1 mm)

Shreddy, anhedral green pleochroic chlorite occurs as an alteration product of olivine and less commonly from alteration of other mafic minerals, such as augite. Chlorite occurring as an alteration product of augite often may be associated with hornblende.

Calcite: 0.1% (0-1%); (<0.01-0.05 mm)

Calcite occurs almost exclusively as anhedral masses associated with saussuritization, but a few rare rhombic crystals are noted, one of which occurs as a vein filling in a small fracture.

Quartz: <0.1% (0-trace %); (0.1-0.2 mm)

Very rare interstitial quartz occurs in the least altered SKI, commonly associated with plagioclase.

IV. Most Altered SKI

Twenty samples collected from the most altered SKI consist solely of outcrop samples, which were made into polished thin sections. The most altered SKI can be described as follows: fine- to coarse-grained gabbro to troctolite containing abundant orthopyroxene-plagioclase symplectite (>10.0% of all plagioclase is in symplectite) and/or Fe-Ti oxide-orthopyroxene symplectite, or elevated abundances of hydrous alteration minerals.

Plagioclase: 56.2% (18-67%); (0.05-7.0 mm)

Plagioclase (An_{55} to An_{65}) is subhedral, and is either normally zoned or has no apparent zonation (Fig 5-17). This composition range shows a certain amount of overlap with least altered SKI (An_{58} to An_{63}), but the zonation of the crystals and the textures of the most altered SKI prove it to be different from the least altered SKI. Ophitic intergrowths of either orthopyroxene or clinopyroxene with plagioclase exist in many of the thin sections studied. Also, commonly plagioclase has abundant rods an isotropic opaque mineral, similar to the least altered SKI (Fig 5-18). Plagioclase intergrown with orthopyroxene in a symplectic texture is ubiquitous throughout the most altered SKI. Less frequent intergrowths of plagioclase include: plagioclase

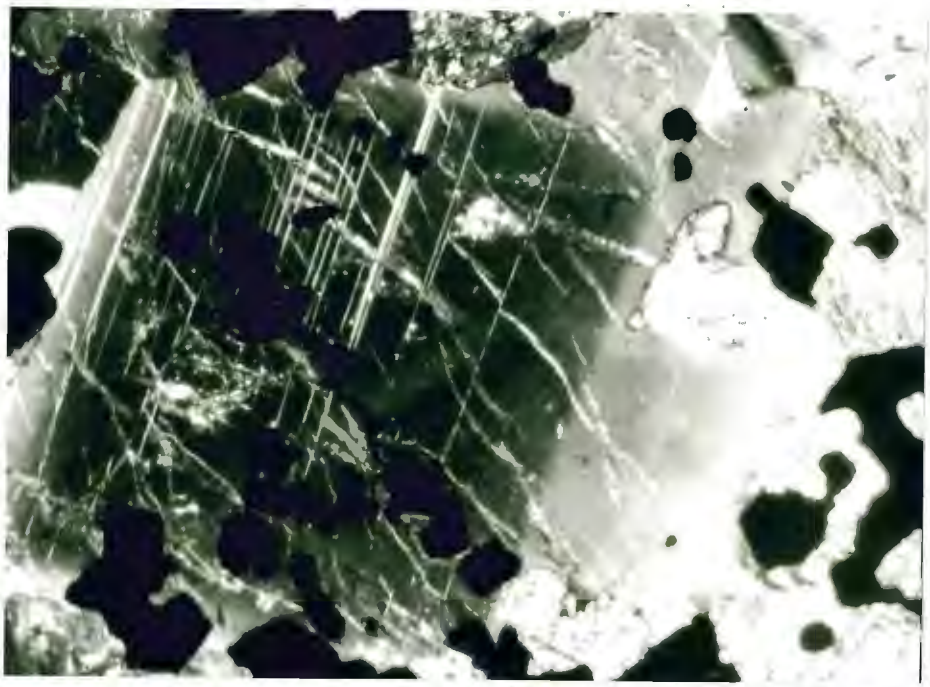

Fig 5-17 : (DP-7) Crossed polars, transmitted light; normally zoned plagioclase crystal with magnetite inclusions (black) in most altered SKI magnetite-ilmenite gabbro. Width of view is 2.6 mm.

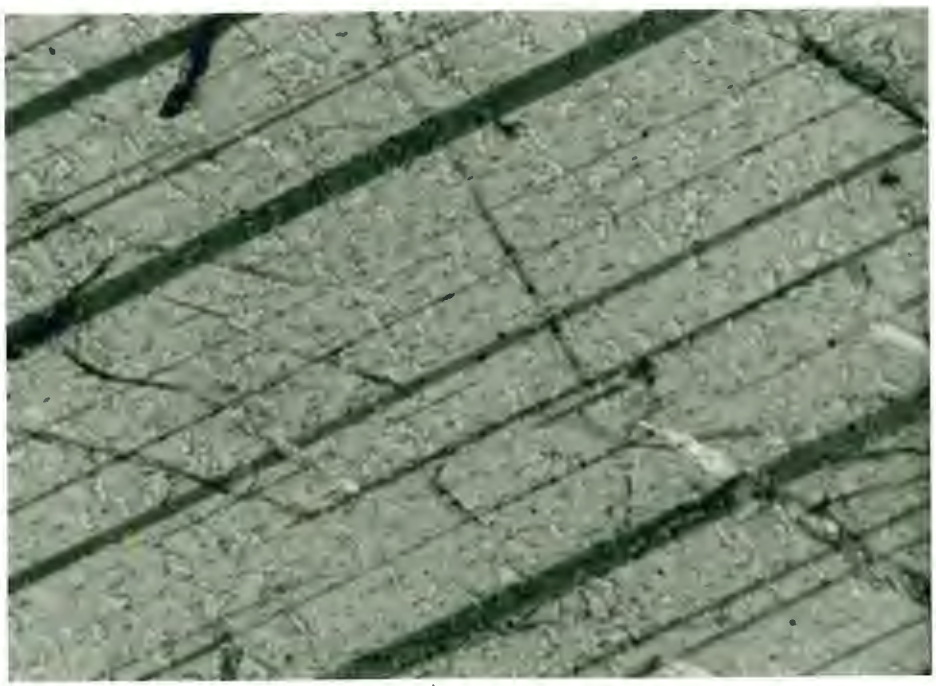

Fig 5-18 : (DP-11A) Crossed polars, transmitted light; plagioclase with oxide rods in most altered SKI biotite-augite troctolite. Width of view is 0.6 mm.

with abundant large magnetite and ilmenite inclusions; cumulate plagioclase (large, subhedral grains) with intercumulus clinopyroxene, orthopyroxene, oxide and sulfide (smaller, anhedral grains interstitial to plagioclase); porphyritic plagioclase; and plagioclase intergrown in olivine grains. Very abundant alteration to saussurite, especially actinolite, indicates an increase in the amount of H_2O in the rock.

Augite: 17.2% (7-30%); (0.05-8.0 mm)

Subhedral augite occurs as isolated or ophitic grains with abundant blebs or short lamellae of magnetite (Fig 5-19). In some cases augite can be seen as lamellae or patches within orthopyroxene or pigeonite as a more calcic exsolution product from less calcic pyroxene hosts. It is inferred that these pyroxene exsolution textures are normal cooling features, due to their abundance also in the least altered SKI. Other textures include less common augite rims on olivine, alteration of augite to biotite and abundant uralite. Pigeonite is less abundant than augite in the most altered SKI rocks, and due to its common intergrowth with augite is included in the percentage of augite listed above.

Orthopyroxene: 5.6% (0-22%); (<0.05-4.0 mm)

Exsolution of clinopyroxene from orthopyroxene in irregular patches or lamellae is a common texture in the most

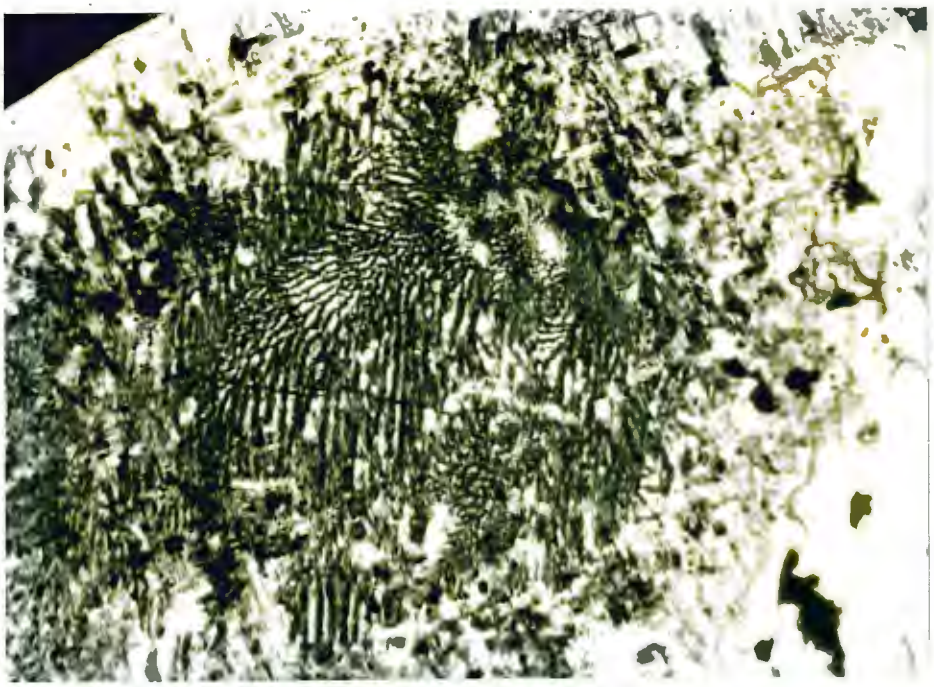

Fig 5-19 : (DP-14) Plane, transmitted light; magnetite blebs and symplectite (black) in augite in most altered SKI saussuritized gabbro. Width of view is 2.6 mm.

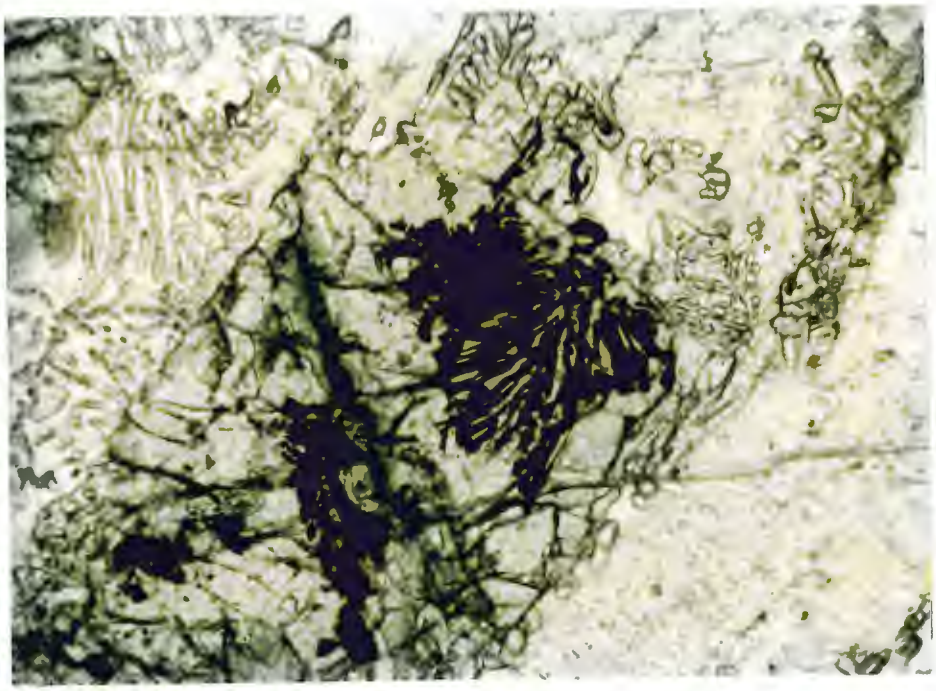

Fig 5-20 : (DP-18B) Plane, transmitted light; larger orthopyroxene enclosing ilmenite symplectite (black) in most altered SKI magnetite gabbro. Width of view is 1.3 mm.

altered SKI rocks, as discussed above. Orthopyroxene rims on olivine exist as indicators of the reaction of olivine + SiO_2-enriched liquid = orthopyroxene. The common association of plagioclase and orthopyroxene in symplectite, as mentioned above, is of uncertain origin. Ophitic orthopyroxene is also not uncommon. Oxide-orthopyroxene symplectite exists in most altered SKI, much as it does in the most altered BIF (Fig 5-20); however the percentage of oxide-orthopyroxene symplectite in the most altered SKI is greater than 5% compared to <5% for least altered SKI. Also common alteration of orthopyroxene to bastite exists in the most altered SKI.

Olivine: 11.2% (0-50%); (0.1-6.0 mm)

Anhedral, slightly pink to colorless pleochroic olivine shows common reaction rims of orthopyroxene or clinopyroxene. Olivine in the most altered SKI appears to be more forsteritic than the most altered BIF olivines according to 2V measurements (generally <100°), as would be expected for magmatic olivine. Other intergrowths of olivine include: alteration to iddingsite, especially along fractures; alteration of olivine to magnetite along the rims of olivine grains; alteration to acicular amphibole; and alteration throughout the olivine grain to chlorite and rare serpentine. Other than alteration, olivine also shows intergrowths with small inclusions of sulfide.

Ilmenite: 3.1% (1-7%); (<0.01-5.0 mm)

Hexagonal plates of subhedral ilmenite are commonly intergrown with magnetite. The ilmenite plates are observed grown into euhedral to subhedral magnetite grains, which in some cases appear to be replaced nearly to the grain boundaries, like pseudomorphs. Ilmenite lamellae in magnetite also commonly occur, possibly of exsolution/oxidation origin as discussed for ilmenite lamellae in magnetite from the most altered BIF (Fig 5-21). Ilmenite/orthopyroxene symplectite (Fig 5-20) is observed along with magnetite/orthopyroxene symplectite in some thin sections. A very common texture is titanium-rich biotite rimming ilmenite, which was also observed in the least altered SKI.

Magnetite: 1.5% (0-7%); (<0.01-2.5 mm)

Magnetite in the most altered SKI commonly occurs in the same textures as does ilmenite: symplectite with orthopyroxene (Fig 5-20), alteration products/inclusions in pyroxenes and olivine, intergrown with ilmenite as hosts for ilmenite lamellae (Fig 5-21) and rimming/being replaced by ilmenite.

Biotite: 2.2% (0-7%); (0.05-5.0 mm)

Subhedral to anhedral rims of biotite on ilmenite and sulfide is the most common occurrence of biotite, as in the

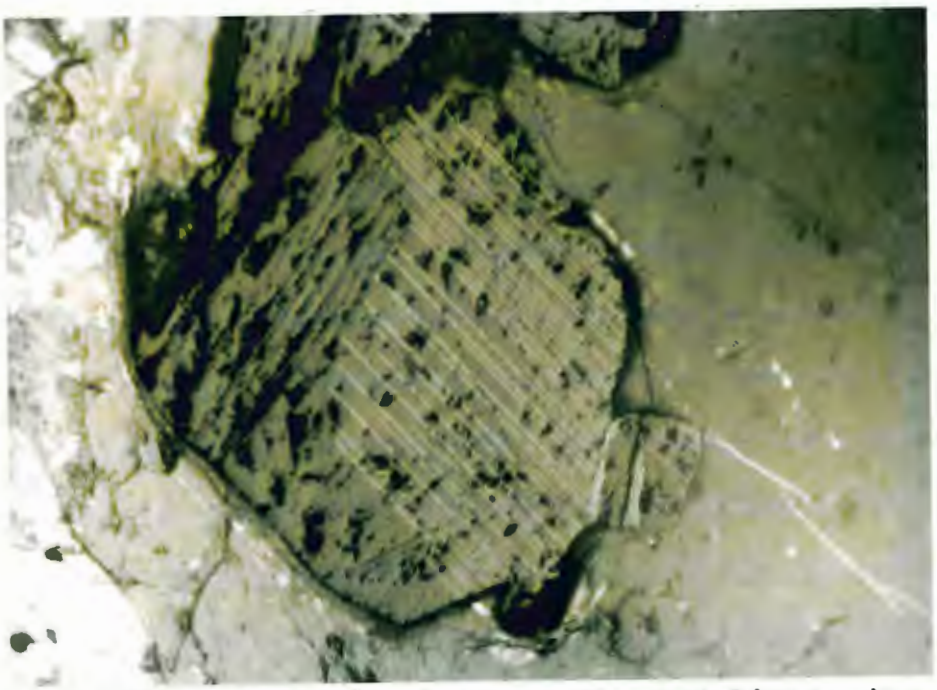

Fig 5-21 : (DP-7) Crossed polars, reflected light; ilmenite lamellae in magnetite in most altered SKI magnetite-ilmenite gabbro. Width of view is 1.3 mm.

least altered SKI. Less commonly biotite exists as distinct grains, and alteration of pyroxene.

Apatite: 0.5% (0-2%); (0.01-3.0 mm)

Subhedral to euhedral elongate prisms of apatite occur in much the same associations as in the least altered SKI, the most common being inclusions in biotite.

Amphibole:

Actinolite: 1.7% (0-8%); (<0.01-0.2 mm)

Acicular to shreddy aggregates of pale yellow-green pleochroic actinolite exist mainly as alteration of plagioclase and clinopyroxene. The main difference between actinolite in the least altered SKI and the most altered SKI is the greater abundance in the latter.

Hornblende: 0.3% (0-3%); (<0.01-2.0 mm)

Hornblende also exists in greater abundance in the most altered SKI, usually as alteration of clinopyroxene with abundant inclusions of apatite, biotite and opaques, or rarely as prismatic crystals.

Quartz: 0.2% (0-3%); (2.0-4.0 mm)

Anhedral quartz exists in most altered SKI often graphically intergrown with plagioclase, or interstitial to other minerals.

Sulfides(0-5%): **Pyrrhotite**(<0.01-1.5mm), **Chalcopyrite**(<0.01- 0.5mm), **Pentlandite**(<0.01-0.5mm), **Pyrite**(0.1-0.5 mm)

Sulfides occur mainly as anhedral blebs rimmed by biotite. Pyrrhotite hosts have exsolution blebs and zones of both chalcopyrite and pentlandite. Pyrite was observed in one thin section as rare isolated subhedral to anhedral equant crystals disseminated throughout the surrounding silicates.

SUMMARY OF PETROGRAPHY OF THE BASAL UNIT OF THE SOUTH KAWISHIWI INTRUSION

The main petrographic differences between the least altered and the most altered SKI are the changes in mineral abundances and the presence of several textural intergrowths in the most altered SKI which are absent from the least altered SKI. The changes in abundances of minerals (Table 5-2) include: (1) a decrease in the amount of plagioclase in the most altered SKI, (2) an increase in the amount of pyroxene in the most altered SKI, (3) an increase in the amount of amphibole as an alteration mineral in the most altered SKI, and (4) an increase in the amount of magnetite in the most altered SKI. The decrease in the amount of plagioclase in the most altered BIF may be accounted for by the heterogeneity of the SKI. An increase in the amount of pyroxene in the most altered SKI could possibly be related to

Table 5-2: Comparison of Average Modal Composition of Least/Most Altered SKI (standard deviation in [ ])

Mineral	Least Alt. SKI (n = 11)	Most Alt. SKI (n = 20)	Gain/Loss +/-
Plagioclase	59.0% [4.9]	56.2% [10.6]	- 2.8%
Clinopyroxene	14.0% [6.7]	17.2% [7.0]	+ 3.2%
Olivine	15.9% [5.4]	11.2% [12.7]	- 4.7%
Orthopyroxene	3.9% [2.6]	5.6% [5.0]	+ 1.7%
Ilmenite	3.1% [1.0]	3.1% [1.9]	even
Magnetite	0.5% [0.6]	1.5% [2.0]	+ 1.0%
Biotite	2.5% [1.6]	2.2% [1.7]	- 0.3%
Apatite	0.7% [0.5]	0.5% [0.5]	- 0.2%
Sulfides	0.7% [0.5]	0.7% [1.3]	even
Amphibole	0.7% [0.9]	2.0% [3.0]	+ 1.3%
Quartz	<0.1% [0.0]	0.2% [0.7]	+ 0.2%

an increase in the amount of total iron in the most altered SKI, or possibly may be related to a gain of silica to the most altered SKI. Olivine reacting with silica introduced from the BIF may have produced the increased amount of orthopyroxene in the most altered SKI. Increased amphibole content of the most altered SKI may be related to an increase in the amount of H_2O in the most altered SKI derived from H_2O driven off during the contact metamorphism of the BIF (Bonnichsen, 1968). Increased total iron in the most altered SKI may account for the increase in the modal abundance of magnetite in the most altered SKI.

Mineral intergrowths which are common in the most altered SKI but uncommon or absent in the least altered SKI include: (1) ilmenite crystals intergrown in magnetite crystals as partial pseudomorphs, (2) orthopyroxene-plagioclase symplectite, and (3) orthopyroxene-ilmenite or orthopyroxene-magnetite symplectite. Subhedral to euhedral magnetite crystals which have subhedral plates of ilmenite in their cores in the most altered SKI samples, appear to have been replaced by ilmenite much in the same manner as the magnetite being replaced by ilmenite in the most altered BIF. Magnetite may have been partially assimilated by the SKI and titanium from the magma subsequently diffused into the magnetite. This replacement of magnetite by ilmenite is not present at all in the least altered SKI, as magnetite is in very low abundance in the least altered SKI. This

magnetite in the most altered SKI may have then exsolved ulvöspinel which oxidized to ilmenite. Exsolution/oxidation in magnetites from the most altered SKI is also observed in ilmenite lamellae present in magnetite.

Symplectites of both orthopyroxene-plagioclase and orthopyroxene-Fe-Ti oxide occur in much greater abundance in the most altered SKI than in the least altered SKI. Similar symplectites have been described as having formed in subsolidus conditions via localized transfer of chemical components (Van Lamoen, 1979; Barton and van Gaas, 1988). Orthopyroxene-plagioclase symplectites occur along grain boundaries between plagioclase and pyroxene or olivine, and commonly protrude into plagioclase. If this orthopyroxene-plagioclase symplectite in the most altered SKI was formed by late-stage rapid simultaneous crystallization of the two phases, it would be unlikely that the symplectite would protrude into previously formed plagioclase. Rather, a metasomatic formation such as the local mass transfer of elements may be more likely, similar to that between olivine and plagioclase described by van Lamoen (1979). Symplectite of orthopyroxene and magnetite or ilmenite in the most altered SKI may be due to high grade retrogressive metamorphism, as suggested by Barton and van Gaas (1988) for the Bjerkreim-Sokndal Lopolith.

The differences in modal abundances and the textures present in the most altered SKI lead to the conclusion that

the most altered SKI was altered compositionally. This alteration was involved assimilation of some BIF minerals, and local redistribution of elements as suggested by the origin of the symplectites observed in the most altered SKI, and by the presence of ilmenite partial pseudomorphs after magnetite. This alteration is present in a zone within 25 feet of the BIF as defined in the introduction to the petrography section.

VI. OXIDE MINERAL CHEMISTRY

Chemistry of the oxides magnetite and ilmenite is of importance to this thesis for several reasons. The presence of TiO_2 in the structure of magnetite (titanomagnetite), along with TiO_2 in the form of ilmenite, is an impurity which is difficult to extract from the iron ore in the blast furnace using techniques designed for extracting only iron from relatively titanium-free ore (Ron Graber, personal communication). Titanium in the form of titanomagnetite in ore which elsewhere in the Biwabik Iron Formation would contain relatively titanium-free magnetite, implies that titanium must have been introduced to the iron formation from elsewhere. Also of interest are other cations substituting in the magnetite, which otherwise would be absent or in much lower quantities in the unaltered BIF. Compositions of the magnetite and ilmenite in the SKI are of interest for comparison with the equivalents in the BIF. Finally, the composition of coexisting magnetite and ilmenite is used as a geothermometer to predict both temperature of equilibration of Fe-Ti oxides in the basal unit of the South Kawishiwi Intrusion and in the Biwabik Iron Formation.

METHODS:

Mineral chemical compositions were obtained by electron microprobe analysis using MAC Electron Microprobe equipped with a Krisel Control computer and electronic package. Operating conditions were 15 KV with a sample current of ≈2

nAmperes. Corrections for the effects of absorption, fluorescence, and atomic number were made using an alpha matrix correction developed by Bence and Albee (1968). Chemical compositions of magnetite and ilmenite were obtained based on weight percents of the following constituent oxides: FeO, TiO_2, Al_2O_3, MgO, MnO, Cr_2O_3, and ZnO. Fe_2O_3 content was calculated by assuming stoichiometry using the basic computer programs Mag and Ilmen written by Michael Carr.

RESULTS:

Magnetite from the least altered upper slaty has a relatively low titania content, averaging 0.29 wt.% TiO_2 with a range of 0.00 to 0.72 wt.% TiO_2 (Table 6-1). Low titanium is to be expected in "normal" magnetites from the BIF (Table 6-3), as seen in the XRF analyses of magnetites from the Biwabik Iron Formation near Hoyt Lakes, Minnesota (unpublished Cleveland Cliffs XRF analyses, 1990-92). However, the amounts of aluminum are somewhat elevated in the least altered BIF (compare Tables 6-1 and 6-2 to Table 6-3). Values of weight percent Al_2O_3 of up to 2.68 were found, with an average of 1.59 wt.% Al_2O_3. At least two possible solutions exist for the presence of the elevated alumina values: either the magnetite gained Al_2O_3 released from the few surrounding aluminous minerals during metamorphism, or the elevated alumina values are due to metasomatism from the intrusion of the SKI. Aluminous minerals are not common in

Table 6-1: Selected Electron Microprobe Analyses of Magnetite from the Biwabik Iron Fromation at Dunka Pit (sample number locations on Figure 6-1, depth in drillcore in [ ] below sample number, AVERAGE is based on 14 analyses)

Least altered Upper Slaty BIF magnetite

	8427.3 [25']	8049.2 [18']	8053.2 [22']	8058.2 [26']	8183.2 [25']	AVERAGE
FeO	28.94	31.74	30.70	31.04	31.19	31.09
Fe_2O_3	66.61	65.76	67.24	66.84	67.41	66.67
TiO_2	0.23	0.36	0.18	0.32	0.32	0.29
Al_2O_3	1.34	2.68	0.92	1.14	1.21	1.59
MgO	1.18	0.03	0.15	0.06	0.04	0.13
MnO	0.10	0.23	0.04	0.13	0.41	0.17
Cr_2O_3	0.00	0.00	0.00	0.00	0.00	0.02
ZnO	0.14	0.04	0.18	0.13	0.03	0.11
TOTAL	98.54	100.84	99.41	99.66	100.61	100.07

Cation proportions, normalized to 4 oxygen atoms

Fe^{+2}	0.930	0.999	0.989	0.996	0.992	0.991
Fe^{+3}	1.927	1.862	1.949	1.931	1.928	1.912
Ti	0.007	0.010	0.005	0.009	0.009	0.008
Al	0.061	0.119	0.042	0.052	0.054	0.071
Mg	0.068	0.002	0.009	0.003	0.002	0.007
Mn	0.003	0.007	0.001	0.004	0.013	0.005
Cr	0.000	0.000	0.000	0.000	0.000	0.000
Zn	0.003	0.001	0.005	0.004	0.001	0.003
TOTAL	3.000	3.000	3.000	3.000	3.000	3.000

Table 6-2: Selected electron microprobe analyses of (**A**) magnetite and (**B**) ilmenite from the most altered Biwabik Iron Fromation at Dunka Pit (sample number locations on Figure 6-1, all samples are from the surface)

(A)	DP18C2	DP18C3	DP23A1	DP23A2	DP16A1	AVERAGE (n = 7)
FeO	31.86	33.68	36.23	31.34	35.11	33.25
Fe_2O_3	65.71	59.65	54.01	64.08	55.02	60.77
TiO_2	1.22	3.82	6.68	1.64	5.08	3.15
Al_2O_3	0.87	1.76	1.89	0.54	3.00	1.56
MgO	0.23	0.53	0.59	0.16	0.27	0.30
MnO	0.08	0.27	0.35	0.31	0.36	0.22
Cr_2O_3	0.08	0.00	0.08	0.84	0.00	0.15
ZnO	0.00	0.00	0.00	0.64	0.00	0.12
TOTAL	100.05	99.71	99.83	99.55	98.84	99.52
Cation proportions, normalized to 4 oxygen atoms						
Fe^{+2}	1.018	1.069	1.144	1.009	1.117	1.061
Fe^{+3}	1.889	1.704	1.535	1.856	1.575	1.746
Ti	0.035	0.109	0.190	0.047	0.145	0.090
Al	0.039	0.079	0.084	0.024	0.135	0.070
Mg	0.013	0.030	0.033	0.009	0.015	0.017
Mn	0.003	0.009	0.011	0.010	0.012	0.007
Cr	0.002	0.000	0.002	0.026	0.000	0.005
Zn	0.000	0.000	0.000	0.018	0.000	0.003
TOTAL	3.000	3.000	3.000	3.000	3.000	3.000

(B)	DP18C2	DP16A1	AVERAGE (n = 2)
FeO	40.19	35.78	37.99
Fe_2O_3	7.52	11.58	9.55
TiO_2	48.21	43.05	45.63
Al_2O_3	0.05	0.07	0.06
MgO	1.17	0.01	0.59
MnO	1.06	2.88	1.97
TOTAL	98.20	93.37	95.79
Cation proportions, normalized to 3 oxygen atoms			
Fe^{+2}	0.859	0.814	0.837
Fe^{+3}	0.145	0.237	0.189
Ti	0.927	0.880	0.904
Al	0.002	0.002	0.002
Mg	0.045	0.000	0.023
Mn	0.023	0.066	0.044
TOTAL	2.000	2.000	2.000

Table 6-3: Electron microprobe and XRF analyses of magnetite and ilmenite from unmetamorphosed BIF and various Duluth Complex intrusions for comparison

Unmetamorphosed BIF magnetite separates from XRF analyses (LTV Mining, R.Graber, unpublished)

Drillhole #	91964	8283	8400	8299	7286
Year Drilled	(1990)	(1991)	(1991)	(1992)	(1992)
SiO_2	0.39	1.84	1.85	1.88	1.92
FeO	28.84	29.91	29.88	29.79	28.97
Fe_2O_3 *	65.57	67.11	67.38	66.90	66.09
Al_2O_3	0.21	0.39	0.29	0.48	0.15
MgO	0.36	0.21	0.24	0.25	0.33
MnO	0.19	0.13	0.15	0.14	0.22
CaO	0.31	0.08	0.12	0.12	0.36
TOTAL	96.05	99.67	99.91	99.56	98.04

Note: all LTV samples from magnetic ore < -500 mesh except 91964 (-325 mesh) * = recalculated by stoichiometry

	Partridge River Intrusion (Mogessie, et al., 1991)		South Kawishiwi Intrusion (INCO) (Pasteris, 1985)	
	magnetite	ilmenite	magnetite	ilmenite
SiO_2	0.00	0.00	0.09	0.00
FeO	30.08	39.37	37.21	42.61
Fe_2O_3	68.48	2.36	56.45	8.02
TiO_2	0.00	52.41	6.03	49.00
Al_2O_3	0.09	0.01	1.78	0.00
MgO	0.00	4.04	0.16	0.44
MnO	0.04	0.55	0.20	0.65
Cr_2O_3	0.09	0.18	0.07	0.00
V_2O_5	0.00	0.62		
CaO			0.03	0.02
TOTAL	99.58	99.43	102.02	100.74
Cation proportions, normalized to 4(magnetite) or 3(ilmenite)				
Si	0.000	0.000	0.003	0.000
Fe^{+2}	0.999	0.810	1.155	0.894
Fe^{+3}	1.994	0.040	1.577	0.151
Ti	0.000	0.970	0.168	0.924
Al	0.004	0.000	0.078	0.000
Mg	0.000	0.150	0.009	0.016
Mn	0.001	0.001	0.006	0.014
Cr	0.003	0.000	0.002	0.000
V	0.000	0.010		
Ca			0.001	0.001
TOTAL	3.00	2.00	3.00	2.00

the iron formation (1.92 wt.% Al_2O_3 in the upper slaty BIF whole rock analyses, Morey, 1991), but enough Al_2O_3 may have been present in such premetamorphic minerals as stilpnomelane, minnesotaite and biotite to allow for the increase of Al in the magnetite. The extent of magnetite with 1.0 wt.% Al_2O_3 or greater covers the entire area of Biwabik Iron Formation sampled for this study (Fig 6-1). This area also coincides with the occurrence of magnetite with lamellae of hercynite along {111} crystallographic planes.

Comparatively, the most altered Upper Slaty BIF magnetites showed higher values of titania, averaging 3.15 wt.% TiO_2, with values ranging from 1.13 to 6.68 wt.% TiO_2 (Table 6-2). These values were produced from areas within the magnetite grain that contain no lamellae of ilmenite with a sharply focused beam, so that the TiO_2 present must be within the magnetite structurally as titanomagnetite, i.e. the solid solution of magnetite and ulvöspinel. The areal extent of magnetite with 1.0 wt.% TiO_2 or greater is smaller than that of the magnetite with elevated alumina values (Fig 6-1). The fact that the titania is in the form of titanomagnetite indicates that the titanium must have diffused into the magnetite from the SKI at high temperatures during metamorphism and stayed in solid solution. The amount of Al_2O_3 in the most altered BIF magnetite is very similar to the least altered BIF magnetite, averaging 1.56 wt.% with a

Figure 6-1: Extent of aluminous and titaniferous magnetite in the Biwabik Iron Formation

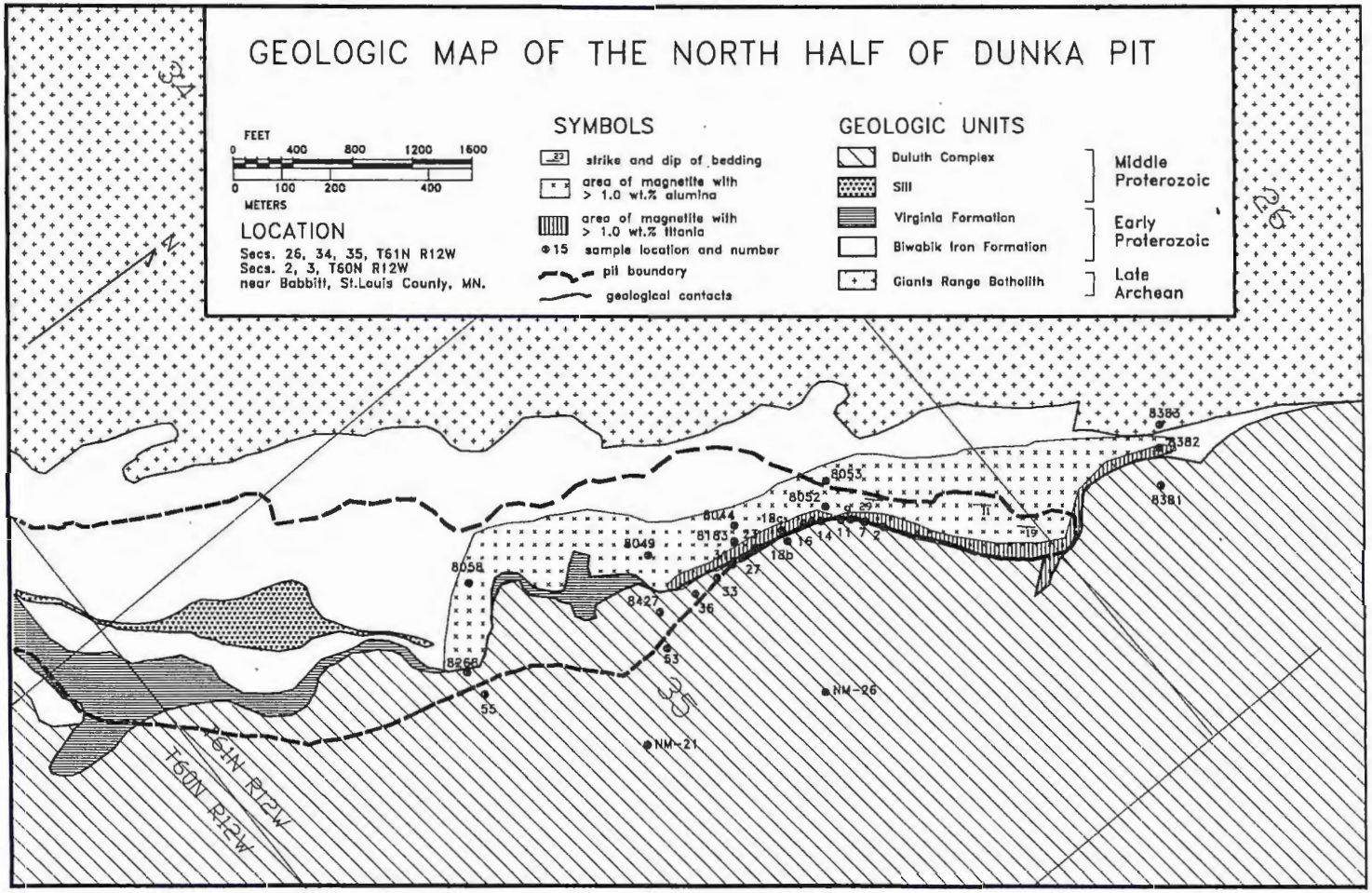

range from 0.54 to 3.00 wt.%.

A comparison of the compositions of magnetite from the most altered BIF with those from the least altered BIF is shown on the spinel prism (Fig 6-2) plotted using the program SPINEL (Williams, Rock, and Carroll, 1990). Two separate groups of spinels can be seen on the plot, which correspond directly to those more titaniferous magnetites near the contact and those less titaniferous magnetites further from the contact. Note that the magnetites plot both on the upper prism as solid circles and squares showing the magnetite component, and on the lower prism as open circles and squares showing the hercynite and ulvöspinel components. The difference in magnetite compositions between the most altered and least altered BIF can also be seen clearly on the plot of TiO_2 vs. Fe_2O_3 (Fig 6-3). Note that on Figure 6-3 magnetite analyses from the most altered SKI plot within the same range as the titaniferous magnetite of the most altered BIF.

Ilmenite in the most altered Upper Slaty BIF is present as lamellae and zones of exsolution/oxidation (previous section); it contains significant amounts of Fe_2O_3 as hematite in solid solution. Fe_2O_3 values varied from 7.52 to 11.58 wt.% from the two samples analyzed for ilmenite (Table 6-1). MgO (0.01-1.17 wt.%) and MnO (1.06-2.88 wt.%) show elevated amounts also.

Magnetite and ilmenite compositions from the most altered SKI (Table 6-4) are somewhat similar to the magnetite

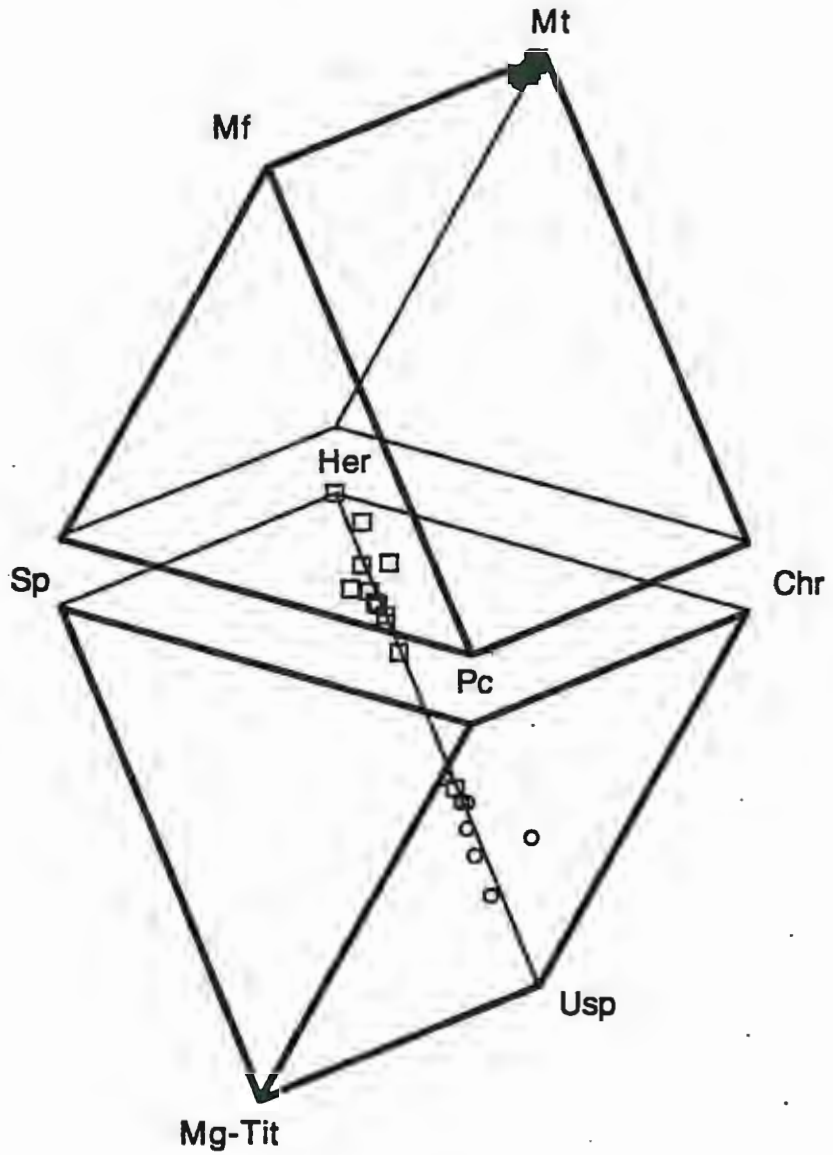

Figure 6-2: Compositions of magnetite from the Upper Slaty Biwabik Iron Formation plotted on the spinel prism; squares are magnetite from least altered BIF, circles are from most altered BIF. Mt=magnetite, Mf=magnesioferrite, Her=hercynite, Sp=spinel, Chr=chromite, Pc=picrochromite, Usp=ulvospinel, Mg-Tit=magnesiotitanite.

Fig 6-3:Titania vs. Fe(III) oxide

magnetite from Biwabik Iron Formation

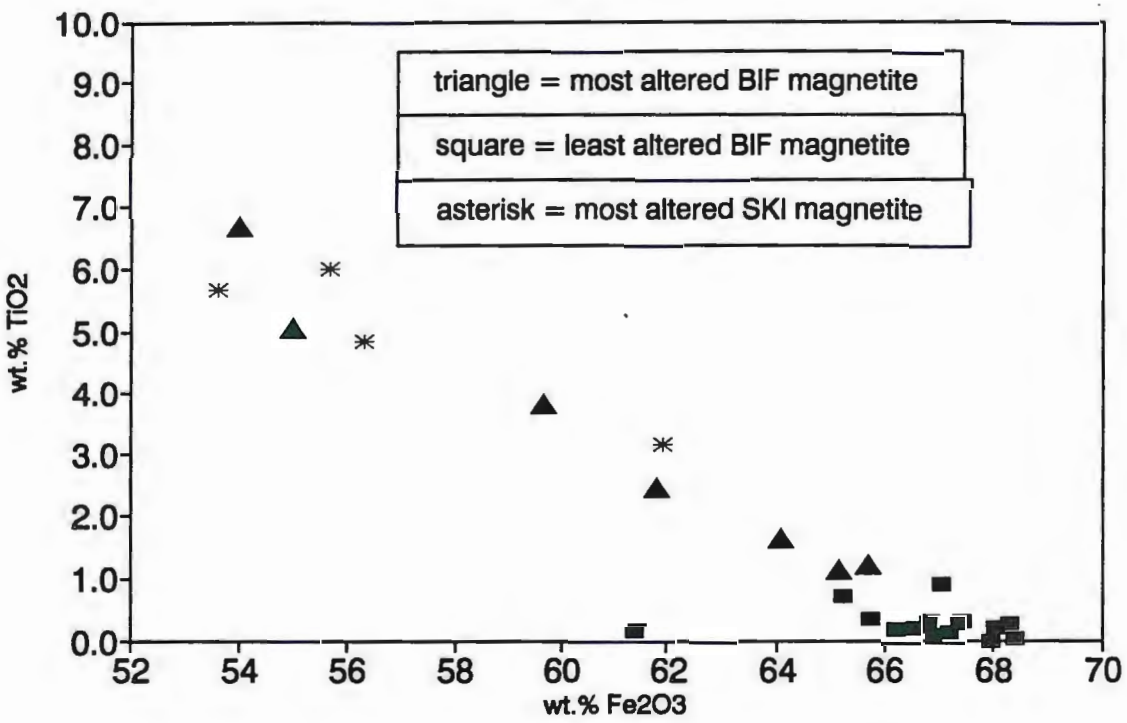

Table 6-4: Electron microprobe analyses of (A) magnetite and (B) ilmenite from the most altered South Kawishiwi Intrusion at Dunka Pit (sample number locations on Figure 6-1, all samples are from the surface)

(A)	DP18B1	DP14.1	DP14.2	DP14.4	AVERAGE (n = 4)
FeO	34.84	35.56	34.30	32.99	34.33
Fe_2O_3	53.62	55.67	56.33	61.88	56.88
TiO_2	5.68	5.99	4.84	3.16	4.92
Al_2O_3	2.54	1.62	1.88	0.60	1.66
MgO	0.62	0.42	0.13	0.27	0.36
MnO	0.32	0.46	0.32	0.32	0.36
Cr_2O_3	1.14	0.84	0.87	0.96	0.95
ZnO	0.81	0.60	0.99	0.62	0.76
TOTAL	99.21	101.16	99.66	100.80	100.21
Cation proportions, normalized to 4 oxygen atoms					
Fe^{+2}	1.093	1.113	1.092	1.046	1.086
Fe^{+3}	1.529	1.567	1.613	1.765	1.619
Ti	0.162	0.169	0.139	0.090	0.140
Al	0.113	0.071	0.084	0.027	0.074
Mg	0.035	0.023	0.007	0.015	0.020
Mn	0.010	0.015	0.010	0.010	0.011
Cr	0.034	0.025	0.026	0.029	0.028
Zn	0.023	0.017	0.028	0.017	0.021
TOTAL	3.000	3.000	3.000	3.000	3.000

(B)	DP18B1	DP14.1	DP14.2	DP14.4	AVERAGE (n = 4)
FeO	39.00	40.31	41.15	40.20	40.17
Fe_2O_3	7.05	9.77	9.00	10.40	9.06
TiO_2	47.98	46.92	48.31	48.01	47.81
Al_2O_3	1.81	0.00	0.00	0.00	0.45
MgO	1.46	0.09	0.43	0.75	0.68
MnO	1.16	1.26	1.02	0.95	1.10
Cr_2O_3	0.68	0.46	0.35	0.53	0.51
ZnO	0.44	0.50	0.55	0.76	0.56
TOTAL	99.56	99.31	100.81	101.60	100.33
Cation proportions, normalized to 3 oxygen atoms					
Fe^{+2}	0.814	0.861	0.863	0.836	0.843
Fe^{+3}	0.132	0.188	0.170	0.195	0.171
Ti	0.900	0.902	0.912	0.898	0.903
Al	0.053	0.000	0.000	0.000	0.013
Mg	0.054	0.003	0.016	0.028	0.026
Mn	0.025	0.027	0.022	0.020	0.023
Cr_2O_3	0.013	0.009	0.007	0.010	0.010
ZnO	0.008	0.009	0.010	0.014	0.010
TOTAL	2.000	2.000	2.000	2.000	2.000

and ilmenite compositions in the most altered BIF. The ilmenite composition shows considerable amounts of hematite in solid solution (averaging 9.06 wt.% Fe_2O_3), which is comparable to values from elsewhere in the SKI (Table 6-3). Magnetite from the most altered SKI contain similar amounts of titania, averaging 4.92 wt.% TiO_2. Magnetite and ilmenite microprobe analyses from elsewhere in the South Kiwishiwi Intrusion have similar compositions (Table 6-2) in their FeO, MgO, and TiO_2 contents. Least altered SKI magnetite and ilmenite are not included in this section because magnetite was not found in sufficient abundance to analyze, and data from other authors was available (Pasteris, 1985; Mogessie, Stumpfl, and Weiblen, 1991).

In summary, the magnetite from the most altered BIF contains considerable TiO_2 (1.13 to 6.68 wt.%), whereas the least altered BIF contains little TiO_2 (0 to 0.72 wt.%). Titanium in the most altered BIF magnetite is in solid solution as well as exsolved/oxidized to ilmenite. Titanium in the magnetite is believed to be derived from "fingers" of SKI magma adjacent to layers of magnetite in the most altered BIF. Least altered and most altered BIF both commonly contain magnetite grains with hercynite lamellae, and an aluminous component in solid solution (0.52 to 6.55 wt.% Al_2O_3). The aluminous component of magnetite in both the least and most altered BIF is believed to have originated during metamorphism from recrystallization of premetamorphic

aluminous minerals. Because the Upper Slaty BIF contains 1.92 wt.% Al_2O_3 (Morey, 1992) the aluminous content of the magnetite (1.59 wt.% Al_2O_3 on average) could be derived from other aluminous minerals in the Upper Slaty BIF. Magnetite makes up less than half of the Upper Slaty BIF, and the aluminous component of the magnetite would account for less than 0.80 wt.% Al_2O_3, which is less than half of the total alumina in the rock. Magnetite in the most altered SKI contains 3.16 to 5.99 wt.% TiO_2, and coexisting ilmenite has a significant ferric iron oxide component (7.05 to 10.40 wt.% Fe_2O_3), which is similar to values obtained elsewhere in the SKI (8.02 wt.% Fe_2O_3, Pasteris, 1985).

VII. GEOTHERMOMETRY

To establish a temperature of metamorphism for the altered Biwabik Iron Formation and a temperature of crystallization of the basal unit of the South Kawishiwi intrusion the geothermometer QUILF was utilized. QUILF is a PASCAL program to assess equilibria among Fe-Mg-Ti oxides, pyroxenes, olivine and quartz (Andersen, Lindsley and Davidson, 1992). Equilibrium temperatures and log fO_2 were calculated from compositions of coexisting ilmenite and magnetite for both the most altered Biwabik Iron Formation and the most altered South Kawishiwi Intrusion. Compositions of coexisting ilmenite and titanomagnetite were taken from electron microprobe analyses of ilmenite blebs, lamellae, and isolated grains coexisting with titanomagnetite. Titanomagnetite/ilmenite pairs were taken only from the most altered upper slaty iron formation and the basal unit of the most altered SKI. No calculations were conducted on compositions of oxides from the least altered upper slaty BIF because no ilmenite was present. Also, no calculations of least altered basal SKI were conducted because of lack of distinct magnetite grains, and the readily available data for comparison (Pasteris, 1985).

For each analysis of ilmenite, the mole fraction of $FeTiO_3$ (XIlm), Fe_2O_3 (XHem), $MgTiO_3$ (XGk), and $MnTiO_3$ (XPy) was calculated. These are used as the four components of an

asymmetric Margules solution model for ilmenite (Andersen and Lindsley, 1988; Andersen, et al., 1991). For each analysis of magnetite, the program calculates the number of Ti atoms in one four-oxygen formula unit (NTi), the number of Mg per formula unit (NMg), and the number of Mn per formula unit (NMn). These are used as a part of a modified Akimoto model (Andersen, et al., 1991) which assumes the following: spinels are perfectly inverse, Ti always replaces Fe^{+3} in the octahedral site, and Fe^{+3}, Mg, and Mn^{+2} are randomly distributed between octahedral and tetrahedral sites in the spinel. These assumptions result in the three independent compositional parameters NTi, NMg and NMn.

Temperatures obtained using this geothermometer for the most altered South Kawishiwi Intrusion range from 651°C to 689°C (Table 7-1), which are lower than expected for a magmatic crystallization temperature. These temperatures indicate that some subsolidus reequilibration must have occurred among the Fe-Ti oxides. The exsolution would take place as the intrusion cooled so that lower temperatures are expected. Temperatures in the same range (650 to 850°C) have been calculated on Fe-Ti oxides from the South Kawishiwi Intrusion from samples at the INCO Cu-Ni orebody to the north of Dunka Pit (Pasteris, 1985) and attributed to subsolidus reeqilibration. However, the reeqilibration was not indicated to be of metasomatic origin. In the analysis of the most altered South Kawishiwi, the change in oxide

Table 7-1:

GEOTHERMOMETRY DATA CALCULATED FROM COEXISTING Fe-Ti OXIDES
using QUILF (Andersen, et al., 1992)
using a constant pressure of 1500 bars (Pasteris, 1985)

MOST ALTERED SKI

SAMPLE #	ILMENITE				MAGNETITE			Temp(C)	Press.(b)	log fO2
	Xilm	XHem	XGk	XPy	NTi	NMg	NMn		constant	
DP141	0.879	0.090	0.004	0.028	0.171	0.023	0.015	689	1500	-15.55
DP142	0.881	0.081	0.016	0.022	0.141	0.007	0.011	679	1500	-16.179
DP144	0.860	0.091	0.028	0.020	0.092	0.015	0.010	651	1500	-16.229
DP18B1	0.857	0.063	0.055	0.025	0.165	0.034	0.011	662	1500	-17.38

MOST ALTERED BIF

SAMPLE #	ILMENITE				MAGNETITE			Temp(C)	Press.(b)	log fO2
	Xilm	XHem	XGk	XPy	NTi	NMg	NMn		constant	
DP16A1	0.815	0.119	0.000	0.066	0.145	0.014	0.012	655	1500	-15.236
DP18C2	0.860	0.072	0.045	0.023	0.035	0.013	0.003	550	1500	-18.815

DP141: small ilm next to mt
DP142: ilm rimming mt
DP144: distinct mt & ilm grains
DP18B1: large ilm bleb in mt
DP16A1: ilm lamellae in mt
DP18C2: distinct mt & ilm grains

composition could be caused by assimilation of magnetite. However, oxide textures of the basal unit of the South Kawishiwi Intrusion do not allow straightforward interpretation of the origins of Fe-Ti oxide. Magnetite irregularly intergrown with ilmenite and ilmenite rimming magnetite, both textures common to the most altered SKI, yield similar temperatures (Table 7-1).

Temperatures obtained for the most altered BIF included two analyses yielding temperatures of 550°C and 655°C (Table 7-1). The variance in temperatures from the two samples may be due to the fact that the higher of the two is from an ilmenite lamellae, as opposed to a larger distinct ilmenite grain coexisting with the larger magnetite. Thin ilmenite lamellae may represent a lesser degree of contamination of the magnetite with titanium and lesser oxidation, whereas coarser grains of ilmenite may represent more extensive Ti contamination or more exsolution and oxidation at lower temperatures. Also, the magnetite-ilmenite pair may not be in equilibrium, in which case the temperatures yielded by the geothermometer would not represent near peak contact metamorphic temperatures.

Neither of these temperatures are in agreement with those predicted by oxygen isotope studies on the unaltered BIF at Dunka Pit (Perry and Bonnichsen, 1966; Bonnichsen, 1968). Perry and Bonnichsen's oxygen isotope data indicated a peak metamorphic temperature at the contact with the Duluth

Complex of 700 to 750°C. This lack of agreement with previously established temperatures indicates that some sort of non-equilibrium exists in the compositions of the magnetite-ilmenite pairs, or the magnetite and ilmenite re-equilibrated at lower temperatures. However, the fact that ilmenite and titaniferous magnetite exist in the iron formation in itself is indicative of introduction of titanium. Geothermometry supports the explanation for metasomatic origin of coexisting titanomagnetite-ilmenite. A temperature lower than the peak of metamorphism would be expected for magnetite which was metasomatically enriched in titanium, then cooled, exsolving ulvöspinel which oxidized to ilmenite. This process (Andersen and Lindsley, 1988) would result in ilmenite which was a product of oxidation at much lower temperatures than peak metamorphism.

Along with temperature, oxygen fugacity is calculated using the QUILF program. Oxygen fugacities ranged from -15.55 log fO_2 to -17.38 log fO_2 for the most altered SKI, and -15.236 to -18.815 log fO_2 for the most altered BIF (Fig 7-1). These values, along with all of the temperature data above were calculated using a constant pressure of 1500 bars (Pasteris, 1985). To check the model for sensitivity to pressure, calculations were made using pressures of 2000 bars, also. The resulting temperatures were exactly the same, and the oxygen fugacities did not vary more than -0.011 log fO_2. Plotting -log fO_2 vs. temperature for the values

Fig 7-1: T-fO2 conditions from mt/ilm
from most altered BIF and SKI

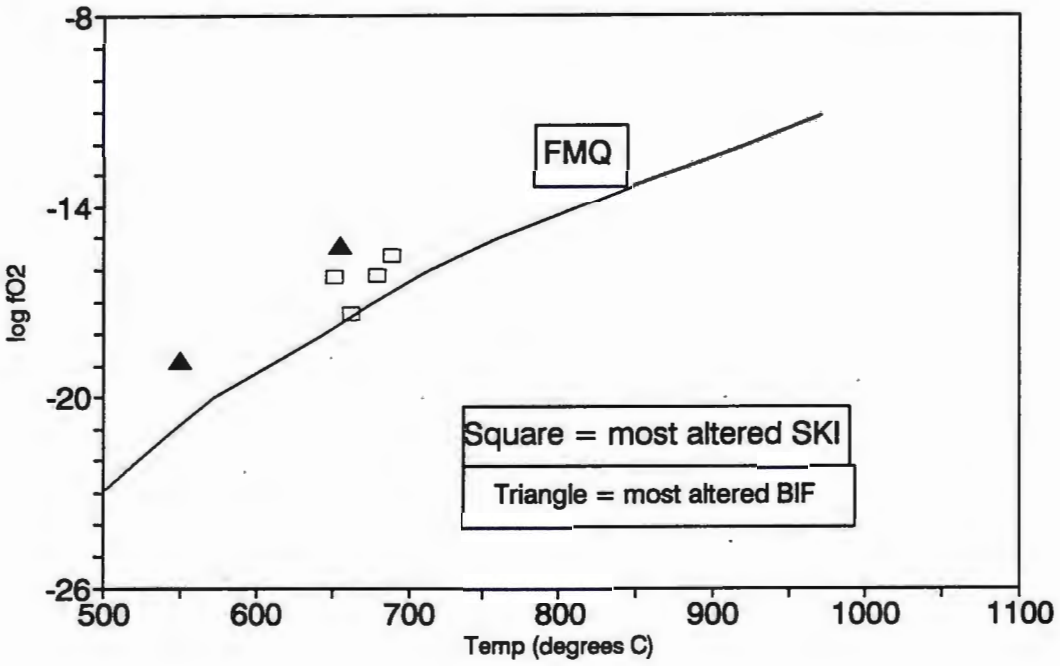

for both the altered BIF and SKI result in values lying slightly above the FMQ buffer curve (after Chou, 1978), indicating slightly more oxidizing environment than FMQ equilibrium conditions. This is in agreement with the introduction of titanium into the magnetite, which subsequently exsolved ulvöspinel and oxidized to ilmenite, according to the equation:

$$6Fe_2TiO_4 + O_2 \rightarrow 2FeFe_2O_4 + 6FeTiO_3$$

(Pasteris, 1985; Sassani, 1992).

In summary, temperatures of crystallization for the most altered SKI and of metamorphism of the most altered BIF have been calculated using coexisting ilmenite-magnetite pairs. These Fe-Ti oxide pairs yield lower temperatures than expected when compared to temperatures from their unaltered counterparts (Bonnichsen, 1968; Pasteris, 1985). Lower temperatures are explained by the introduction of Ti into the most altered BIF, and the assimilation of magnetite in the most altered SKI. These changes in composition for the most altered BIF and SKI cause non-equilibrium compositions, which either are the direct cause of the lower geothermometer temperatures, or they have actually re-equilibrated at lower temperatures. Oxidation of the ulvöspinel component of titanomagnetite to form ilmenite, in both the most altered BIF and SKI, is in agreement with the more oxidizing conditions indicated by points plotted above the FMQ buffer curve in similar areas on the log fO_2 - temperature diagram.

VIII. WHOLE ROCK GEOCHEMISTRY

To define the extent of the movement of titanium from the basal South Kawishiwi Intrusion (SKI) into the Biwabik Iron Formation (BIF), and all other concomitant chemical changes, it is necessary to examine the changes in whole rock geochemistry. 38 samples were analyzed for whole rock geochemistry: 4 least altered BIF, 11 most altered BIF, 5 least altered SKI, 18 most altered SKI (refer to Fig 8-3 for sample numbers and locations). SiO_2, Al_2O_3, CaO, MgO, Na_2O, K_2O, Fe_2O_3, TiO_2, and P_2O_5 content and LOI of both the samples taken from the BIF and the SKI were analyzed using x-ray fluorescence spectrometry (XRF) with the exceptions of FeO, which was analyzed by wet chemical titration and MnO, which was analyzed by XRF in the first round of samples and DCP plasma spectrometry in the second round of samples analyzed. Trace elements analyzed include: As, Ba, Co, Cr, Cu, La, Mo, Nb, Ni, Rb, S, Sb, Sc, Sn, Sr, V, Y, Zn, and Zr. However, due to the limitation of funding and time all of these elements were not analyzed for each sample. All whole rock samples have analyses for Cr, Cu, Ni, S, and with a few exceptions V. A list of trace elements and the means of analysis for each is listed in Appendix F. Results for least altered and most altered BIF and SKI are summarized in Appendices B - E.

In order to compare the compositions of the most altered

to those of the least altered for either the BIF or SKI, the isocon method is employed. This method involves simple solution of Gresens' equations, which were constructed to show the relative changes in concentration and volume during metasomatism (Gresens, 1967). The isocon method shows graphically the change in concentration of several chemical components relative to their concentration prior to alteration (Grant, 1986). Whole rock data from the least altered rock in wt.% oxides and ppm of trace elements are scaled to fit on the x axis, for values of x=0 to 30. These same scaling factors are then multiplied by the whole rock wt.% oxides and ppm trace elements of the most altered rock to find the values for the y axis. A plot of these scaled values, such as Fig 8-1, will show chemical components on an X-Y graph. The Y axis is the concentration in the most altered (C_a), whereas the X axis is the concentration in the least altered (C_o).

An isocon itself is a line connecting points of equal geochemical concentration, i.e. a line connecting points whose slopes (C_a/C_o) are equal. The isocon is simply a best fit straight line drawn on an isocon plot connecting the greatest number of unrelated chemical components. The greater the number of unrelated chemical components which the isocon intersects, the more likely the isocon. Chemical components with differing charge and ionic radii are less likely to behave similarly during alteration, and an isocon

which passes through such chemical components would be more believable. Any element that plots below the isocon is lost from the most altered; any above the isocon is gained to the most altered.

Averaged data for the BIF and SKI are shown in Table 8-1. Comparing the most altered BIF (II) to the least altered BIF (I) whole rock composition, a wide variation in the amount of change in concentration of the various chemical components is observed (Fig 8-1). Not all elements analyzed are included on the isocon plot, because of lack of space. The isocon used for this comparison is labeled Ca/Co = 1.0, which means that there was essentially little change in the mass of the rock due to alteration. The choice of this slope for the isocon was based on the fact that it passes through total Fe, MnO and Nb. Total Fe and MnO are related, however the presence of the unrelated component Nb increases the likelihood of the group of components chosen being relatively immobile. So total Fe, MnO, and Nb are assumed to have not been added to or depleted from the most altered BIF. Large amounts of enrichment of several elements occurred including: TiO_2 (2100%), V (850%), MgO (70%), Al_2O_3 (670%), CaO (35%), Ba (350%), K_2O (2900%), Na_2O (1675%), Rb (460%), Sr (890%), Cu (1440%), Ni (10,000%), S (975%), H_2O (240%), and Fe_2O_3 (15%). This enrichment is based on the displacement of the Ca/Co value of the component of interest from the Ca/Co value of the isocon (Ca/Co = 1.0). Loss of chemical components

Table 8-1: Average Whole Rock Composition of the Least Altered BIF (I), Most Altered BIF (II), Least Altered SKI (III), and Most Altered SKI (IV). Oxides and sulfur are in weight percent, trace elements are in parts per million.

	(I) (n=4)	(II) (n=11)	(III) (n=5)	(IV) (n=18)
SiO_2	48.53	32.24	46.56	44.64
Al_2O_3	0.82	6.34	16.58	13.70
CaO	3.18	4.32	9.67	7.35
MgO	4.01	6.68	7.10	8.02
Na_2O	0.04	0.71	2.49	1.84
K_2O	0.01	0.30	0.48	0.81
Fe_2O_3	17.23	19.57	1.58	4.04
FeO	24.18	20.88	11.48	13.04
MnO	0.40	0.39	0.17	0.20
Cr_2O_3	NA	NA	0.02	NA
TiO_2	0.19	4.15	2.41	2.80
P_2O_5	0.28	0.23	0.27	0.30
S	0.04	0.43	0.23	0.44
LOI	1.14	3.82	1.32	2.61
TOTAL	100.04	100.05	100.36	99.78
As	17	13	11	14
Ba	48	216	210	270
Co	12	97		84
Cu	80	1232	771	1251
La1(line 1)	6	9		14
La2(line 2)	3	5		11
Mo	NA	NA	NA	NA
Nb	68	54		45
Ni	5	506	262	408
Rb	5	28	20	40
Sb	2	1		1
Sc	2	19		16
Sn	1	2		3
Sr	10	99	220	231
V	50	473	218	259
Y	0	2	30	16
Zn	46	154		126
Zr	28	93	130	173

NOTE: NA means below detection limit; a blank means the element was not analyzed.

Fig 8-1: Isocon Plot:Whole Rock (BIF)

for averaged most alt./least alt. BIF

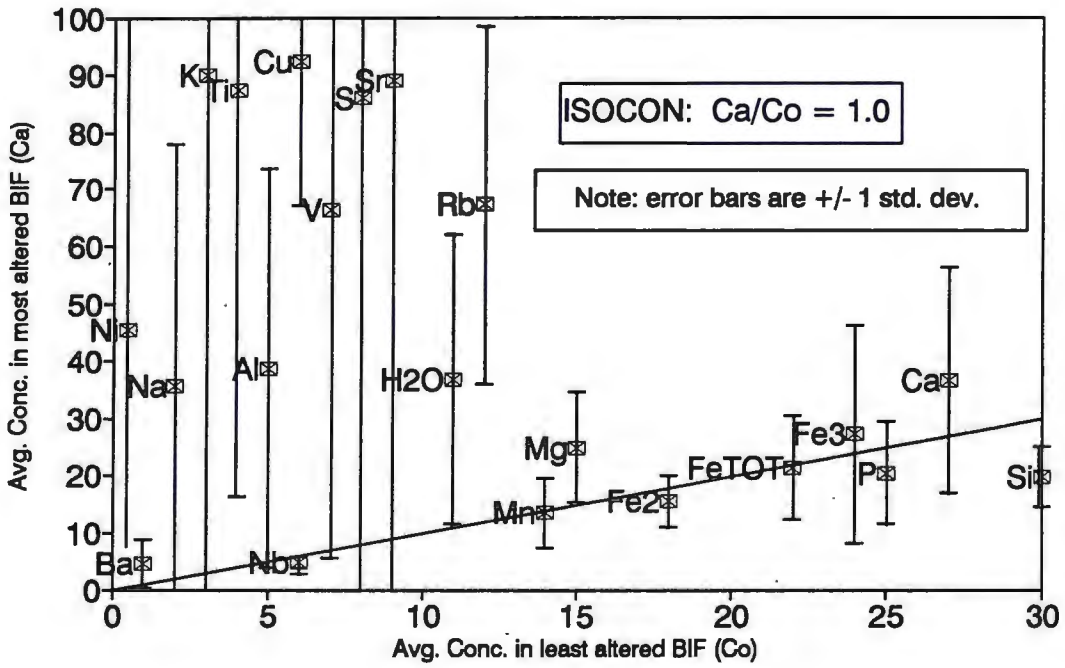

from the most altered BIF includes: SiO_2 (33%) and P_2O_5 (20%). It should be noted that these values are averaged and do not represent the composition of any one rock or pair of most altered/least altered rocks. Error bars on Figure 8-1 represent plus or minus one standard deviation from the average value.

A t-test was conducted for each of the chemical components of both the most altered BIF and SKI to discern whether apparent losses or gains relative to an isocon are statistically valid. The results of the t-test are shown in Table 8-2. All of the apparent gains and losses are substantiated, that is they are hypotheses which are accepted by the t-test, except for the elements sulfur (S) and niobium (Nb). Sulfur has a large standard deviation which causes rejection of the hypothesis that it is gained to the most altered BIF. Niobium is very near the isocon in Figure 8-1, but because its very small standard deviation does not include the isocon line, it is not accepted by the t-test.

Changes in whole rock composition for the average most altered SKI relative to the average least altered SKI are shown in Fig 8-3. Two possible isocons are shown on the isocon plot; the most likely of the two is the isocon which has a Ca/Co = 1.3 and passes through total Fe, Ba, and As. These chemical components are least like each other in ionic radii and charge, and are a likely choice as components which remained relatively immobile. Comparatively, many components

Table 8-2: Statistical analysis of gains and losses to most altered BIF and SKI (see APPENDIX G for means & standard deviations)

	Most altered BIF		Most altered SKI	
	Hypothesis	t-test	Hypothesis	t-test
SiO_2	lost	accepted	lost	accepted
Al_2O_3	gained	accepted	lost	accepted
CaO	gained	accepted	lost	accepted
MgO	gained	accepted	even	accepted
Na_2O	gained	accepted	lost	accepted
K_2O	gained	accepted	gained	accepted
Fe_2O_3	even	accepted	gained	accepted
FeO	even	accepted	even	accepted*
total Fe	even	accepted	even	accepted
MnO	even	accepted	even	accepted*
TiO_2	gained	accepted	even	accepted*
P_2O_5	lost	accepted	even	accepted*
S	gained	rejected	gained	accepted
H_2O	gained	accepted	gained	accepted
Ba	gained	accepted	even	accepted
Rb	gained	accepted	gained	accepted
Sr	gained	accepted	even	accepted*
V	gained	accepted	even	accepted
Nb	even	rejected		
Zr			even	accepted
Cu	gained	accepted	gained	accepted
Ni	gained	accepted	gained	accepted*

*Because two isocons are used for the most/least altered SKI isocon plot, two t-tests were required; one t-test accepted, but the other t-test rejected the hypothesis

Figure 8–2: Sample locations for whole rock analyses

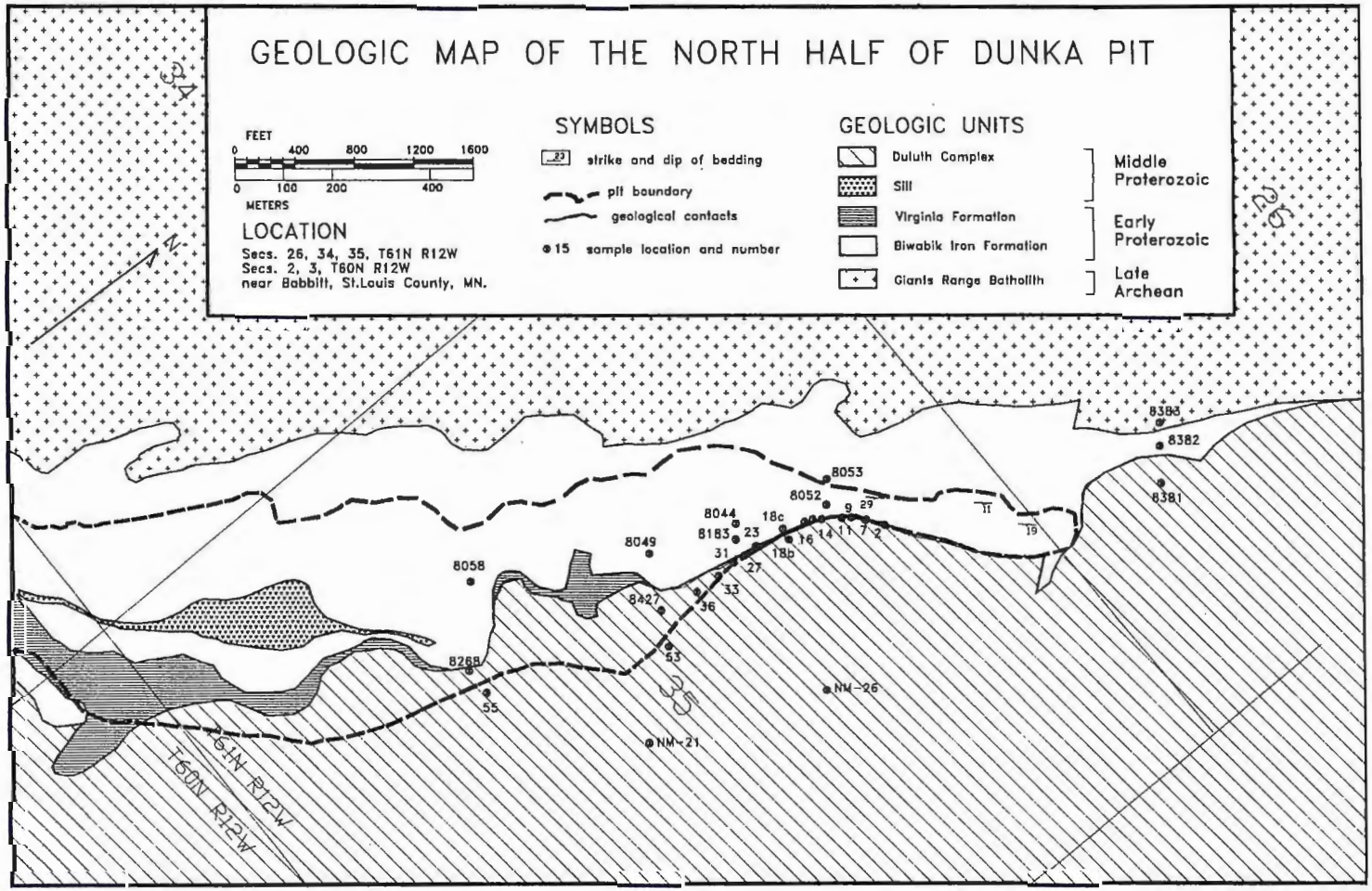

also fall on the Ca/Co = 1.2 isocon, although they are predominantly siderophile elements. Ti^{+4} and V^{+5} fit into tetrahedral sites in Fe-Ti oxides; Fe^{+3} and Mg^{+2} fit into octahedral sites in Fe-Ti oxides. Either the Ca/Co = 1.3 isocon or the Ca/Co = 1.2 isocon would be a likely choice, and both have similar slopes. Considering that the elements which lie on either of these isocons are relatively immobile, the elements which were gained to the average most altered SKI relative to the least altered SKI include: Cu (30%), Ni (25%), S (60%), K_2O (40%), Rb (70%), Fe_2O_3 (125%) and H_2O (70%). Those lost from the most altered SKI include: CaO (55%), Al_2O_3 (50%), Na_2O (55%), and SiO_2 (30%). Error bars again represent plus or minus one standard deviation from the average value.

Results of t-tests conducted on the most altered SKI data are shown in Table 8-2 to confirm initial gains and losses as being actual statistically significant gains or losses. All of the t-tests were conducted for both isocons shown on Figure 8-3, as both have similar slopes. Some chemical components which were close enough to one isocon to be considered "even", that is not lost from or gained to the most altered SKI, were accepted by the t-test involving the closer isocon but rejected by the t-test involving the more distant isocon. Chemical components which failed one t-test are noted by an asterisk on Table 8-2, and include: FeO, TiO_2, P_2O_5, and V.

Fig 8-3: Isocon Plot Whole Rock (SKI)

for averaged most alt./least alt. SKI

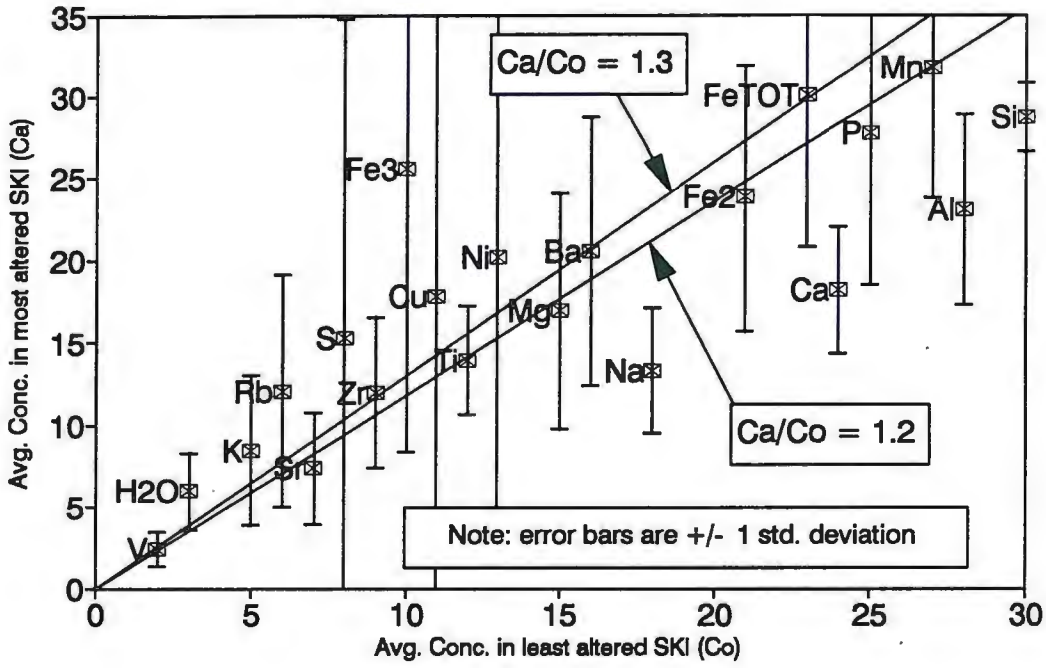

DISCUSSION

Of the gains and losses to the averaged data above, only those which are affirmed by the t-test will be considered to be real changes, with the rest being artifacts of averaging the data. All of the increases in chemical components which are statistically significant can be correlated to increases in the amounts of one mineral or another in the most altered BIF. The Fe-Ti oxides were, in the chapter on petrography, classified as minerals which showed definite replacement textures. This would mean that the chemical components which make up these minerals must have been transferred into the most altered BIF. The logical source of these components is the SKI, because it is relatively richer in these components than the BIF (Fig 8-1). A loss of 10 % of the TiO_2 (the maximum loss possible according to Figure 8-3) in the SKI would account for 0.24 wt. % TiO_2 lost from the SKI. The 2100% gain of TiO_2 to the most altered BIF amounts to a gain of 3.96 wt.% TiO_2 to the BIF. The only way all of the gain of titania to the BIF can be accounted for with the SKI as the source is if the titania was drawn from a volume of rock 16.5 times greater than the volume of BIF affected. Because the SKI has a much larger volume than the BIF, the possibility of movement of titania from a much larger volume of SKI into a much smaller volume of BIF is reasonable. Loss of 10% of the V from the most altered SKI (the maximum possible loss according to Figure 8-3) would account for the

loss of 26 ppm V. Gain of 850% V to the most altered BIF account for a gain of 425 ppm V. For the SKI to be the source of the vanadium, a volume of SKI rock affected must be 16.3 times as much as the volume of BIF rock affected. Metasomatic transfer of Ti from intrusions into wallrock in the presence of hydrothermal fluids has been documented (van Lamoen, 1979; Tarasenko, 1986; Force, 1991), and in laboratory experimentation Ti was proved to be mobile in hot slightly alkaline aqueous solutions (Agapova, 1989). Titanium has previously been thought to be immobile, but field evidence has indicated that the Gunflint Iron Formation also has gained Ti via transfer from the Duluth Complex (Broderick, 1917; Grout, 1933; Simmons, Lindsley and Papike, 1974).

Increases in the concentration of the other chemical components in the most altered BIF listed above to form plagioclase, sulfides and hydrous minerals, as well as the loss of quartz are not directly attributed to the replacement, as are the Fe-Ti oxides. Transfer of these components into the most altered BIF depends strictly on the origin of the minerals in which these components are found. The origin of plagioclase in the most altered BIF is attributed to infiltration of actual magma into the iron formation, and it is believed that sulfides also may have been introduced in such a manner. However, ilmenite in the most altered BIF is not attributed to direct crystallization

of magma due to the pseudomorphs of ilmenite after magnetite (Ch.5). A magmatic origin for the plagioclase is based on the similar magmatic textures which are also observed in the adjacent SKI (CH.5, Figs 5-10, 5-17). Introduction of "fingers" of magma into the iron formation thus accounts for the increase in CaO, Na_2O, Al_2O_3, Ba, Rb, Sr, Ni and Cu. Loss of SiO_2 is also attributed to the introduction of magma into the iron formation as quartz was melted and driven off by the high temperature gabbroic magma of the SKI. The gain of LOI to the most altered BIF, however, may be related to the proximity of the most altered BIF to fault B-29 (Fig 1-1). Movement of fluids along this fault may have caused the increase in hydrous minerals in the most altered BIF, and subsequently caused higher LOI values in whole rock analyses.

Changes in abundance of minerals in the most altered SKI relative to the least altered SKI explain the changes in chemical components. A gain in the concentration of K_2O would logically be explained by increased amounts of potassium feldspar, or biotite, however no such increase is observed in thin section (Table 5-2). Perhaps hornblende containing potassium is the product of the gain in K_2O. A possible source for the potassium is late stage granitic pegmatite sheets observed within the SKI near the contact with the BIF. These pegmatites are rich in orthoclase and hydrous minerals, such as biotite. Gain of potassium via transfer of potassium-rich fluids from these pegmatites into

the SKI may have occurred. The gain of ferric iron to the most altered SKI may reflect a change of the oxidation state of iron, but no overall gain of iron, as total Fe is very near the isocon line in all but one of the isocon plots. Increased LOI is reflected in greater amounts of amphibole in the most altered SKI, which may have a similar origin to those in the most altered BIF, i.e., movement of fluids along fault B-29.

Of the components lost from the average most altered SKI, Al_2O_3, CaO and Na_2O may be due to the loss of plagioclase. However, the loss of SiO_2 cannot be accounted for mineralogically. SiO_2 may have been removed from both the most altered BIF and SKI in a fluid. However, no evidence, such as veins of quartz in the SKI, exists to account for the loss of silica. Also the gain of TiO_2 and V to the most altered BIF are not accompanied by a loss of these components from the most altered SKI. It appears that the area defined as most altered SKI may have also been affected by loss of TiO_2 and V, as supported by the fact that a much larger volume of the SKI would be needed to produce the gains of titania and vanadium to the most altered BIF.

In summary, the whole rock data from the most altered BIF shows increases in the amounts of TiO_2, V, Al_2O_3, CaO, Na_2O, MgO, K_2O, Ba, Rb, Sr, H_2O, Cu and Ni and a decrease in the amount of SiO_2. Whole rock data from the most altered SKI shows increases in the amounts of K_2O, Fe_2O_3, S, H_2O, and

Rb and decreases in the amounts of Al_2O_3, CaO, Na_2O and SiO_2. Gain or loss of a particular component is based on consistent gain to or loss from the most altered samples from both average and specific data. Gain of TiO_2 and V to the most altered BIF is believed to be caused by the replacement of magnetite in the iron formation by ilmenite and titanomagnetite. Gain of Al_2O_3, CaO, Na_2O, K_2O, Ba, Rb, Sr, Cu and Ni to the most altered BIF is believed to be due to the infiltration of "fingers" of magma rich in these components into the iron formation. LOI increases in the most altered BIF is due to fluids moving along a fault in the are of the most altered BIF, converting anhydrous minerals to hydrous minerals.

An increased amount K_2O and Rb in the most altered SKI is attributed to the gain of potassium-bearing hornblende, which most probably was increased in amount due to introduction of potassium from granite pegmatites via a potassium-rich fluid. Another possibility for gain of K_2O is in the form of potassium dissolved in albitic plagioclase; however, the plagioclase from the most altered SKI has very similar albite content to that of the least altered SKI. A change in oxidation state of the iron in the most altered SKI is responsible for the increased amount of Fe_2O_3 in the most altered SKI. LOI increase in the most altered SKI is attributed to movement of fluids the same fault which produced hydrous minerals in the most altered BIF. Loss of

TiO_2 and MnO from the most altered SKI is due to transfer of these components into the most altered BIF. The extent of the transfer of titanium across the SKI-BIF contact is shown in the contour map of whole rock wt.% TiO_2 (Fig 8-4). If the area affected by the transfer of titanium is considered as that which has whole rock wt.% TiO_2 in excess of 1.0, then the maximum extent of transfer of Ti is 100 feet (30 meters) into the BIF.

Figure 8-4: Contour map of titania in whole rock samples

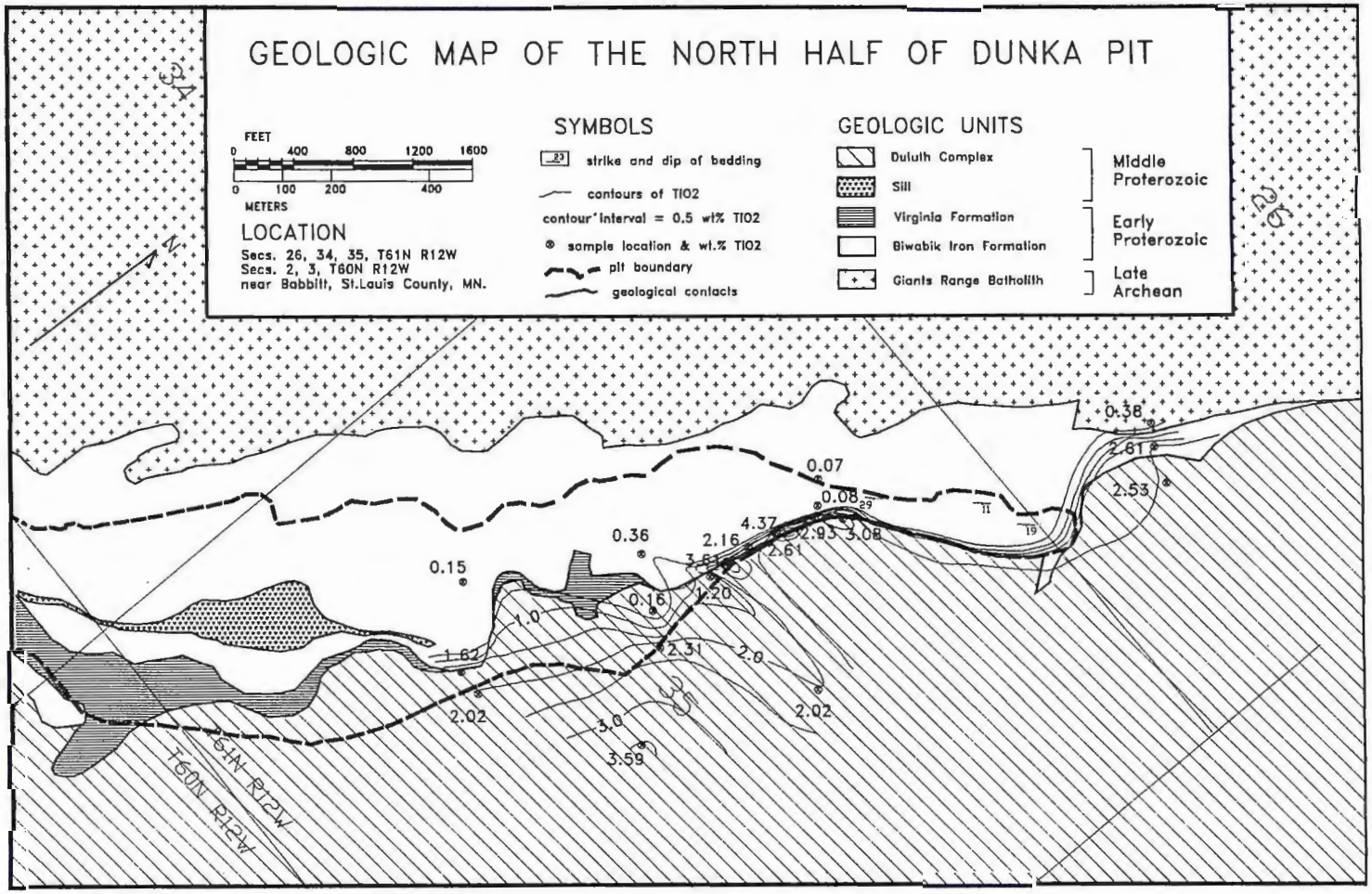

IX. OXYGEN ISOTOPE STUDIES

Fifteen whole rock samples and 1 set of mineral separate samples were analyzed for ^{18}O content relative to ^{16}O content at Indiana University by Dr. E. Ripley. Oxygen isotope analyses allow for assessment of content of ^{18}O in a given unaltered rock and also assessment of loss/gain of ^{18}O from/to a most altered rock. Oxygen isotopic compositions are measured by measuring the amount of the heavy isotope of oxygen, ^{18}O. The amount of ^{18}O in a rock is measured by standard mass spectrometry methods using BrF_5 in sample preparation (Clayton and Mayeda, 1963). This amount of the heavy oxygen isotope is then compared to the amount of the most abundant isotope of oxygen, ^{16}O, as a ratio. The ratio of $(^{18}O/^{16}O)$ in the sample is then compared to the ratio for Standard Mean Ocean Water (SMOW) in the following equation:

$$\delta^{18}O = \frac{(^{18}O/^{16}O)_{sample} - (^{18}O/^{16}O)_{SMOW}}{(^{18}O/^{16}O)_{SMOW}} \times 1000$$

Oxygen isotope compositions of both the Biwabik Iron Formation (BIF) and South Kawishiwi Intrusion (SKI) were studied in order to investigate any exchange of oxygen between the BIF and SKI. If the oxygen isotopic compositions of the most altered and least altered BIF are significantly different, then the isotopic composition of the most altered has been changed by interaction with the SKI. Changes in

isotopic compositions probably occur in the same manner and at the same time as changes of chemical components noted in Chapter VIII on whole rock geochemistry. Likewise, a change in composition of oxygen isotopes for the most altered SKI relative to the least altered SKI probably occurred with other geochemical changes, if the oxygen isotopic compositions of the least altered and most altered SKI are significantly different.

Results of this investigation are summarized in Table 9-1, which shows the $\delta^{18}O$ values in parts per thousand for whole rock samples of most altered BIF, least altered SKI, most altered SKI and mineral separates from the most altered BIF. Results from the most altered BIF for whole rock samples are shown to give an idea of the degree of mixing of isotopic compositions of the various minerals present in the most altered BIF. The values range from 7.60 to 9.00 parts per thousand.

In comparison the values from separated quartz and magnetite from the most altered BIF show very different values (Table 9-1). The value of $\delta^{18}O = 7.44$ for magnetite is considered "normal" relative to oxygen isotope values ($\delta^{18}O = 7.43$) from other magnetite separates sampled from near the contact with the SKI at Dunka Pit (Perry and Bonnichsen, 1966). Oxygen isotope values for quartz separates from the most altered BIF ($\delta^{18}O = 10.82$) show a greatly decreased value compared to "normal" values ($\delta^{18}O =$

Table 9-1: OXYGEN ISOTOPE VALUES FROM THE DUNKA PIT AREA
see Fig 8-4 for sample locations

SAMPLE #		ROCK TYPE	OXYGEN ISOTOPE VALUES delta O-18 per mil SMOW	DISTANCE FROM CONTACT feet [meters]
From whole rock data of most altered BIF				
DP9	*	Plag-Cpx-Mt BIF	7.80	5 [1.5]
DP15A	*	Plag-Cpx-Opx-Mt BIF	8.20	5 [1.5]
DP18B	*	Plag-Cpx-Mt BIF	7.60	10 [3.0]
DP23A	*	Plag-Actin-Mt BIF	9.00	5 [1.5]
DP27A	*	Opx-lim-Plag BIF	8.40	5 [1.5]
From Mineral Separates				
DP18C : QUARTZ		Mt-Amphibole BIF	10.82	5 [1.5]
DP18C : MAGNETITE		Mt-Amphibole BIF	7.44	5 [1.5]
From whole rock of most altered SKI				
DP11A		Aug Troctolite	7.60	5 [1.5]
DP14		Sauss. Gabbro	8.00	5 [1.5]
DP18A		Anorth Gabbro	9.40	5 [1.5]
DP21A		Aug Troctolite	8.80	5 [1.5]
DP23B		Gabbro	7.40	10 [3.0]
DP32A		Aug Troctolite	7.00	80 [24.4]
From whole rock of least altered SKI				
NM-21A		Gabbro	6.33	600 [183]
NM-21B		Gabbro	5.94	600 [183]
NM-26A		Troctolite	6.57	1050 [320]
NM-26B		Troctolite	6.28	1050 [320]

* = BIF which contains "fingers" of magmatic plag. & pyroxenes

analytical error = +/- .05 to .10 per mil
sampling error = up to .30 or .40 per mil

Data from mineral separates in Dunka Pit area (Perry and Bonnichsen, 1966)

M12056: QUARTZ	15.21	49 [15]
M12056: MAGNETITE	7.43	49 [15]
M12022: QUARTZ	12.91	171 [52]
M12022: MAGNETITE	4.69	171 [52]
M12133: QUARTZ	12.45	207 [63]
M12133: MAGNETITE	4.95	207 [63]

15.21) for quartz separates from "least altered" BIF near the contact with the SKI at Dunka Pit (Perry and Bonnichsen, 1966).

Quartz and magnetite show fractionation of oxygen isotopes during contact metamorphism due to heating and reequilibration. Values of $\delta^{18}O$ for quartz are normally higher in unmetamorphosed iron formation relative to metamorphosed iron formation quartz $\delta^{18}O$ values, which have given up some of their ^{18}O to surrounding magnetite. Likewise, magnetite oxygen isotope values are lower in unmetamorphosed iron formation than in metamorphosed iron formation in which the magnetite has gained ^{18}O from surrounding quartz (Perry, et al., 1973).

The magnetite oxygen isotope measurements for the most altered BIF have yielded values which agree with the fractionation of ^{18}O from quartz into magnetite. However, the quartz oxygen isotopic values are too low to be due to fractionation alone (Ripley, personal communication). Quartz normally reacts too slowly to produce such a low $\delta^{18}O$ value via fractionation with magnetite. The other possibility is nonequilibrium which could be the result of movement of ^{18}O in a metasomatic fluid.

In order to assess the possibility of gain of heavy oxygen isotopes to the SKI from the most altered BIF, the isotopic composition of the least altered and most altered SKI must be considered. Table 9-1 shows that the most

altered SKI has higher values of $\delta^{18}O$ relative to the least altered, as would be expected if ^{18}O were gained from the most altered BIF. The $\delta^{18}O$ values for the most altered SKI range from 7.00 to 9.40, whereas those for the least altered SKI range from 5.94 to 6.57. Values from typical basaltic magmas are for $\delta^{18}O$ range from 5.5 to 7.0 (Ripley and Al-Jassar, 1987), a range which includes the least altered SKI sample values but excludes those of the most altered SKI.

The most altered BIF has shown loss of ^{18}O (lower $\delta^{18}O$ values) from quartz relative to what would be expected via fractionation with magnetite during metamorphism. The most altered SKI has shown gain of ^{18}O (higher $\delta^{18}O$ values) relative to the least altered SKI. These two facts strongly suggest that the intrusion which has been shown to have lost Ti and other elements to the most altered BIF, also gained ^{18}O from the most altered BIF.

The heavy oxygen isotope which the most altered SKI has gained could have been gained through one of two mechanisms or a combination of the two. Either the fluids which were expelled from the BIF during metamorphism, enriched in ^{18}O, transferred the heavy oxygen isotope to the most altered SKI; or the most altered SKI gained ^{18}O through assimilation of the most altered BIF. Water and CO_2 which were lost from the iron formation during contact metamorphism have been proposed to have escaped into the overlying Virginia Formation and SKI via minute hairline fractures (Bonnichsen, 1968). Evidence

for infiltration of this fluid into the SKI includes the abundance of biotite in the basal unit of the SKI. Fluid derived from dewatering of the iron formation would have to be enriched in ^{18}O in order to increase the $\delta^{18}O$ in the most altered SKI. Calculation of the isotopic composition of such a fluid can be conducted using batch or Rayleigh volatilization methods (Valley, 1986).

However, textures in the most altered BIF indicate the likelihood of partial assimilation of quartz and other silicates by the SKI. Because quartz mineral separates from the least altered and most altered BIF contain higher values of $\delta^{18}O$ relative to the SKI, this method appears to be more likely. With $\delta^{18}O$ values of quartz from the least altered BIF ranging from 12.45 to 18.90 (Perry and Bonnichsen, 1966), and values of quartz from the most altered BIF of 10.82, the iron formation quartz is a strong possibility as the source of ^{18}O. Least altered SKI whole rock values of $\delta^{18}O$ from 5.94 to 6.57 are much lower than quartz mineral separate values from the BIF. Assimilation of BIF quartz layers by the SKI seem the most likely mechanism for enrichment of the most altered SKI in ^{18}O.

X. SUMMARY AND CONCLUSIONS ON THE TRANSFER OF TITANIUM

The purpose of this thesis is to give evidence for the transfer of titanium from the Duluth Complex (South Kawishiwi Intrusion) into the Biwabik Iron Formation, and to define the extent and changes involved in this transfer of titanium.

Evidence for the transfer of titanium from the South Kawishiwi Intrusion (SKI) into the Biwabik Iron Formation (BIF) exists in (1) ilmenite in layers of magnetite in BIF near the contact with the SKI, (2) elevated titanium content of magnetite near the contact with the SKI, and (3) high titanium content of whole rock analyses of magnetite near the contact with the SKI. Near the contact with the SKI, layers of magnetite within the BIF contain up to 5% ilmenite. Ilmenite in the magnetite layers occurs as lamellae and zones within magnetite grains. The author believes the textures indicate that ilmenite is replacing magnetite. One mechanism for the replacement of magnetite by ilmenite is diffusion of Ti into the magnetite with subsequent exsolution of ulvöspinel and oxidation of the ulvöspinel to ilmenite. Microprobe analyses of magnetite from BIF near the contact with the SKI show up to 6 wt.% TiO_2, indicating the magnetite has ulvöspinel in solid solution. Magnetite from BIF far from the contact averages <0.5 wt.% TiO_2.

Gain of titanium to the magnetite in the BIF is reflected in whole rock geochemistry of BIF. Samples of BIF

from 100 feet from the contact with the SKI contain 0.2 wt.% TiO_2, whereas samples of BIF within 25 feet of the contact with the SKI average over 4.0 wt.% TiO_2. Loss of titanium from the SKI is not apparent from whole rock data, but when analyzed using the isocon method the overall amount of titanium is observed to have been lost from SKI rocks near the contact with the BIF relative to other chemical components.

Extent of the transfer of titanium from the SKI into the BIF as observed in elevated TiO_2 in magnetite and whole rock values, and as observed in the presence of ilmenite in magnetite layers in the BIF is limited to a zone 5 to 25 feet wide paralleling the contact with the SKI. This zone of altered iron formation occurs in the north half of Dunka Pit only where there is a direct contact between the SKI and BIF. Where even a thin wedge of Virginia Formation exists between the BIF and SKI no increase in titanium is observed in whole rock chemistry, mineral chemistry, or in the presence of ilmenite. Direct contact of the SKI and BIF occurs also at depth underneath the SKI, however the BIF which exists beneath the SKI and other intrusions of the Duluth Complex are beyond the scope of this study. Rocks of the BIF near the contact with the SKI which exhibit significant change in mineralogy and chemical composition, especially those containing minerals not found in "normal" Biwabik Iron Formation, are labelled as most altered BIF. Rocks of the

SKI likewise are labelled most altered SKI on the basis of significant changes in mineralogy, chemical composition and proximity to the contact with the BIF.

Changes occurring with the transfer of titanium from the SKI into the BIF include: (1) changes in modal abundance of minerals in both the BIF and SKI, (2) changes in whole rock geochemistry of both the BIF and SKI, and (3) changes in the isotopic composition of the BIF and SKI. Modal abundance of several minerals show an increase in the most altered BIF relative to the least altered BIF, including: ilmenite, plagioclase, clinopyroxene, and hydrous minerals. Plagioclase and clinopyroxene are present in layers which formerly were comprised of quartz and iron silicate. Large crystals of (1.0 to 10.0 mm) plagioclase and clinopyroxene commonly poikilitically enclose layers of magnetite in the most altered BIF. Poikilitic and symplectic textures observed in the most altered BIF are believed to be magmatic textures. Ilmenite, as indicated above, is present within the magnetite layers of the most altered BIF. Loss of quartz, orthopyroxene, and fayalitic olivine from the most altered BIF occurs in the layers which now contain plagioclase, clinopyroxene and other minerals with magmatic textures. In the most altered SKI, loss of plagioclase and olivine is coupled by a gain of orthopyroxene, clinopyroxene and magnetite.

Changes in the whole rock geochemistry of the most

altered BIF include a gain of TiO_2, V, Al_2O_3, CaO, Na_2O, K_2O, Ba, Rb, Sr, MgO, Cu, Ni, and H_2O; and loss of SiO_2 and P_2O_5 relative to the least altered BIF. These changes are believed to reflect infiltration of magma which assimilated quartz and crystallized plagioclase, sulfides and amphiboles, and movement of Ti from the magma into the magnetite layers of the BIF. In the most altered SKI changes in whole rock geochemistry include gain of K_2O, Rb, Fe_2O_3, S and H_2O; and loss of Al_2O_3, CaO, Na_2O and SiO_2. These gains and losses are interpreted from isocon plots of most altered vs. least altered rocks.

Loss of ^{18}O from quartz in the most altered BIF is evident from one set of quartz-magnetite mineral separates ($\delta^{18}O$ = 10.82 for quartz) relative to other quartz values in least altered BIF ($\delta^{18}O$ = 15.21). Gain of ^{18}O has produced higher $\delta^{18}O$ values for the most altered SKI (7.00 to 9.40) compared to the least altered SKI (5.94 to 6.57).

Conclusions drawn from the evidence presented above are that (1) the South Kawishiwi Intrusion injected "fingers" of magma into the Biwabik Iron Formation in a zone 5 to 25 feet wide; (2) this magma assimilated the quartz, orthopyroxene and fayalite in the most altered BIF; (3) these fingers of magma crystallized to form plagioclase and clinopyroxene; (4) titanium from the SKI was transferred into layers of magnetite within the BIF, forming ilmenite via exsolution/oxidation of the titaniferous magnetite; (5) the

transfer of titanium into layers of magnetite in the BIF occurred via diffusion from surrounding magma or some mechanism other than crystallization of ilmenite directly from magma.

Presence of normally zoned, poikilitic plagioclase and poikilitic clinopyroxene, along with symplectic textures in the most altered BIF are evidence in favor of a magmatic origin for these minerals. Despite the fact that the plagioclase has a wider range of compositions in the most altered BIF (An_{39} to An_{59}) compared to plagioclase in the least altered SKI (An_{58} to An_{63}), the textural evidence strongly indicates a magmatic origin for the plagioclase. The amount of increase of Al_2O_3 in the most altered BIF supports the magmatic origin for plagioclase in these "fingers" of magma. Al_2O_3 values from whole rock analyses indicate an increase from 0.82 wt.% to 6.43 wt.% on average, an increase of 670% using the isocon method. Moving this much alumina (5.61 wt.%) by any method than injection of magma would be unlikely.

The conclusion that the magma assimilated quartz and iron silicates is supported by the fact that quartz is a low temperature mineral and the gabbroic magma would have been greater than the peak metamorphic temperature of 750°C at the time of intrusion (Ch.VII). Only isolated layers of quartz exist in the most altered BIF, so clearly most of the quartz was assimilated. Original quartz, orthopyroxene and

fayalitic olivine are now replaced by plagioclase and clinopyroxene, and abundant symplectite. Symplectite of orthopyroxene/plagioclase and orthopyroxene/magnetite is common to the most altered BIF in these fingers of magma. Re-equilibration of oxides and olivine or small scale transfer of chemical components are possible mechanisms of producing symplectites of Fe-Ti oxides and orthopyroxene (van Loeman, 1979; Garrison, et al., 1981).

A probable mechanism for enriching the magnetite of the most altered BIF in titanium is diffusion, due to the fact that some of the ilmenite observed intergrown with the magnetite is actually in the core of magnetite grains. In order to replace the core of a magnetite grain with ilmenite, the titanium must have diffused through the magnetite grain under high temperatures; the iron formation reached temperatures of near 750°C (Bonnichsen, 1968). Upon cooling the magnetite exsolved ulvöspinel which was oxidized to ilmenite.

Titanium which exists in magnetite of the most altered Biwabik Iron Formation is the reason for this thesis. Movement of titanium is believed to have occurred across the Duluth Complex - Biwabik Iron Formation contact, despite the fact that titanium is normally considered "immobile". It is now clear that the titanium in the most altered Biwabik Iron Formation was derived from the South Kawishiwi Intrusion of the Duluth Complex, creating a zone 5 to 25 feet wide in

which titaniferous magnetite and ilmenite have partially replaced layers of magnetite. The significance of this zone of titanium enrichment is that the iron ore derived from this zone cannot be separated using blast furnace techniques.

REFERENCES:

Abrajano, T.A., Holt, B.D., and Dyrkacz, G.R., 1991, Stable isotope geochemistry of organic matter alteration in Animikie Basin sediments within the thermal aureole of the Duluth Complex. Organic Geochemistry, V.17, N.4, P.477-482.

Agapova, G.F., Modnikov, I.S., and Shmariovich, Ye. M., 1989, Experimental study of the behavior of titanium in hot sulfide-carbonate solutions. Intl. Geology Rev., V.31, P.424-430.

Allison, I.S., 1925, The Giants Range Batholith of Minnesota. J. of Geology, V.33, P.488-508.

Andersen, D.J., and Lindsley, D.H., 1988, Internally consistent solution models for Fe-Mg-Mn-Ti oxides: Fe-Ti oxides. Am. Mineral., V.73, P.714-726.

Andersen, D.J., et al., 1991, Internally consistent solution models for Fe-Mg-Ti oxides and olivine. Am. Mineral., V.76, P.427-444.

Andersen, D.J., Lindsley, D.H., and Davidson, P.M., 1992, QUILF: A PASCAL program to assess equilibria among Fe-Mg-Ti oxides, pyroxenes, olivine and quartz. Computers & Geosciences, P.1-22.

Barton, M. and Van Gaas, C., 1988, Formation of orthopyroxene-Fe-Ti oxide symplectites in Precambrian intrusives, Rogaland, southwestern Norway. Am. Mineral., V.73, P.1046-1059.

Bence, A.E., and Albee, A.L., 1968, Empirical correction factors for the electron microanalysis of silicates and oxides. J. Geology, V.76, P.382-403.

Bonnichsen, B., 1968, General geology and petrology of the metamorphosed Biwabik Iron Formation, Dunka River area, Minnesota. Ph.D. thesis, University of Minnesota, 240 p.

Bonnichsen, B., 1969, Metamorphic pyroxenes and amphiboles in the Biwabik Iron Formation, Dunka River area, Minnesota. Mineral. Soc. Am. Spec. Paper 2, P.214-219.

Bonnichsen, B., 1972, Southern part of the Duluth Complex. in Geology of Minnesota: A Centennial Volume, Sims and Morey, eds., Minnesota Geol. Surv. Spec. Volume, Minneapolis, Minnesota, P.361-87.

Broderick, T.M., 1917, The relation of the titaniferous magnetites of northeastern Minnesota to the Duluth Gabbro. Econ. Geol., V.13, P.35-49.

Catanzaro, E.J. and Hanson, G.N., 1971, U-Pb ages for sphene from early Precambrian igneous rocks in northeastern Minnesota-northwestern Ontario. Canadian J. Earth Sci., V.8, P.1319-1324.

Chou, I., 1978, Calibration of oxygen buffers at elevated P and T using the hydrogen fugacity sensor. Am. Mineral., V.63, P.690-703.

Clayton, R.N., and Mayeda, T.K., 1963, The use of bromine pentafluoride in the extraction of oxygen from oxides and silicates for isotopic analysis. Geochim. et Cosmochim. Acta, V.27, P.43-52.

Foose, M.P., and Weiblen, P.W., 1986, The physical and petrologic setting and textural and compositional characteristics of sulfides from the South Kawishiwi intrusion, Duluth Complex, Minnesota, USA. Geology and Metallogeny of Copper Deposits, Friedreich, ed., Springer-Verlag, Berlin Heidelberg.

Force, E.R., 1991, Geology of Titanium-Mineral Deposits. Geol. Soc. Am. Spec. Paper 259.

French, B.M., 1964, Stability of siderite, $FeCO_3$, and progressive metamorphism of iron formations. Ph.D. thesis, Johns Hopkins University.

French, B.M., 1968, Progressive contact metamorphism of the Biwabik Iron Formation, Mesabi Range, Minnesota. Minn. Geol. Surv. Bull. 45.

Garrison, J.R., and Taylor, L.A., 1981, Petrogenesis of pyroxene- oxide intergrowths from kimberlite and cumulate rocks: co- precipitation or exsolution?. Am. Mineral., V.66, P.723-740.

Goldich, S.S., 1968, Geochronology in the Lake Superior region. Canadian J. Earth Sci., V.5, P.715-724.

Grant, J.A., 1986, The isocon diagram - a simple solution to Gresens' equation for metasomatic alteration. Econ. Geol., V.81, P.1976-1982.

Green, J.C., 1968, Chemical and physical characteristics of late Precambrian lavas of northern Minnesota. (abs.) Am. Geophys. Union Trans., V.49, P.363.

Green, J.C., 1971, The North Shore Volcanic Group. Ann. Inst. Lake Superior Geol., 17th, Proc., Duluth, Minnesota, P.74-85.

Green, J.C., 1993, Stratigraphy and Volcanology of the North Shore Volcanics in the Duluth Quadrangle, Ann. Inst. Lake Superior Geol., 39th, Proc., Eveleth, Minnesota, P.33-34.

Gresens, R.L., 1967, Composition - volume relationships of metasomatism. Chem. Geology, V.2, P.47-55.

Grout, F.F., 1933, Contact metamorphism of the slates of Minnesota by granite and by gabbro magmas. Bull. Geol. Soc. Am., V.44, P.989-1040.

Grout, F.F., and Broderick, T.M., 1919, The magnetite deposits of the eastern Mesabi range, Minnesota. Minn. Geol. Surv. Bull. 17, 58 p.

Gruner, J.W., 1924, Contributions to the geology of the Mesabi Iron Range with special reference to the magnetites of the iron- bearing formation west of Mesaba, Minnesota, Minn. Geol. Surv. Bull. 19, 71 p.

Gruner, J.W., 1946, Mineralogy and geology of the Mesabi Range. Office of the Commissioner, Iron Range Resouces and Rehabilitation, St.Paul, Minnesota, 127 p.

Gundersen, J.N., 1958, The stratigraphy and mineralogy of the metamorphosed Biwabik Iron-Formation, eastern Mesabi district. Ph.D. thesis, University of Minnesota, 180 p.

Gunderson, J.N. and Schwartz, G.M., 1962, The geology of the metamorphosed Biwabik Iron-Formation, eastern Mesabi district, Minnesota, Minn. Geol. Surv. Bull. 43, 139 p.

Holst, T.B., Mullenmeister, E.E., Chandler, V.W., Green, J.C., and Weiblen, P.W., 1986, Relationship of structural geology of the Duluth Complex to economic mineralization. Natural Resources Research Institute, Univ. Minnesota - Duluth Report 241-2.

Lepp, H., 1966, Chemical composition of the Biwabik Iron Formation, Minnesota. Econ. Geol., V.61, P.243-250.

Lepp, H., 1968, Trace elements in Minnesota iron-formations (abs.). Inst. Lake Superior Geol., 14th, Superior, Wisconsin (Proc.), P.9.

Lepp, H., 1972, Normative mineral composition of the Biwabik Formation: a first approach. in Studies in Mineralogy and Precambrian Geology, Doe and Smith, eds., Geol. Soc. Am. Memoir 135, P.265-278.

Listerud, W.H., and Meineke, D.G., 1977, Mineral resources of a portion of the Duluth Complex and adjacent rocks in St.Louis and Lake Counties, northeastern Minnesota: Minnesota Department of Natural Resources, Div. of Minerals, Hibbing, MN, Report 93, 49 p.

Mainwaring, P.R. and Naldrett, A.J., 1977, Country-rock assimilation and the genesis of Cu-Ni sulfides in the Water Hen intrusion, Duluth Complex, Minnesota. Econ. Geol., V.72, P.1269-1284.

Miller, J.D., 1993, Evidence of interruptions during fractional crystallization of the Duluth Complex layered series at Duluth (Abs). Ann. Inst. Lake Superior Geol., 39th, Proc., Eveleth, Minnesota, P.58-59.

Mogessie, A., Stumpfl, E.F., and Weiblen, P.W., 1991, The role of fluids in the formation of platinum-group minerals, Duluth complex, Minnesota: mineralogic, textural, and chemical evidence. Econ. Geol., V.86, P.1506-1518.

Morey, G.B., Papike, J.J., Smith, R.W., Weiblen, P.W., 1972, Observations on the contact metamorphism of the Biwabik Iron-Formation, east Mesabi district, Minnesota. in Studies in Mineralogy and Precambrian Geology, Doe and Smith, eds., Geol. Soc. Am. Memoir 135, P.225-264.

Morey, G.B., and Cooper, R.W., 1977, Bedrock geology of the Hoyt Lakes-Kawishiwi area,, St. Louis and Lake Counties, Northeastern Minnesota: Minnesota Geological Survey, open-file map, 1:48,000.

Morey, G.B., 1992, Chemical composition of the eastern Biwabik Iron Formation (early Proterozoic), Mesabi Iron Range, Minnesota. Econ. Geol., V.87, P.1649-1658.

Ojakangas, R.W., and Matsch, C.L., 1982, Minnesota's Geology, University of Minnesota Press, Minneapolis, Minnesota 255p.

Paces, J.B., and Miller, J.D., Jr., in press, Precise U-Pb ages of Duluth Complex and related mafic intrusions, northeastern Minnesota: New insights for physical, petrogenetic, paleomagnetic adn tectono-magmatic processes associated with 1.1 Ga Midcontinent rifting: Journal of Geophysical Research.

Pasteris, J.D., 1985, Relationship between temperature and oxygen fugacity among Fe-Ti oxides in two regions of the Duluth Complex. Canadian Mineral., V.23, P.111-127.

Perry, E.C., and Bonnichsen, B., 1966, Quartz and magnetite: oxygen-18-oxygen-16 fractionation in metamorphosed Biwabik Iron Formation. Science, V.153, P.528-529.

Perry, E.C., Tan, I.C., and Morey, G.B., 1973, Geology and stable isotope geochemistry of the Biwabik Iron Formation, northern Minnesota. Econ. Geol., V.68, P.1110-1125.

Prince, L.A., and Hanson, G.N., 1972, Rb-Sr isochron ages for the Giants Range Granite, northeastern Minnesota. in Studies in Mineralogy and Precambrian Geology, Doe and Smith, eds., Geol. Soc. Am. Memoir 135, P.217-224.

Ramdohr, P., 1980, The Ore Minerals and their Intergrowths. Int. Ser. in Earth Sci., V.35, Pergamon Press, Frankfurt.

Ripley, E.M., and Alawi, J.A., 1986, Sulfide mineralogy and chemical evolution of the Babbit Cu-Ni deposit, Duluth Complex, Minnesota. Canadian Mineral., V.24, P.347-368.

Ripley, E.M., and Al-Jassar, T.J., 1987, Sulfur and oxygen isotope studies of melt-country rock interaction, Babbit Cu-Ni deposit, Duluth Complex, Minnesota. Econ. Geol., V.82, P.87-107.

Sassani, D.C., 1992, Petrologic and thermodynamic investigation of the aqueous transport of platinum-group elements during alteration of mafic intrusive rocks. Ph.D. thesis, Washington University, St.Louis, Missouri.

Severson, M.J., in prep., Igneous stratigraphy of the South Kawishiwi intrusion, Duluth Complex, northeastern Minnesota, Nat. Res. Research Inst., Univ. Minnesota, Duluth, Technical Report.

Severson, M.J., and Hauck, S.A., 1990, Geology, geochemistry, and stratigraphy of a portion of the Partridge River intrusion. Nat. Res. Research Inst., Univ. Minnesota, Duluth, Technical Report, NRRI/TR-91-13a, 96 p.

Silver, L.T., and Green, J.C., 1963, Zircon ages for Middle Keweenawan rocks of Lake Superior region (abs.). Am. Geophys. Union Trans., V.44, P.107.

Simmons, E.C., Lindsley, D.H., and Papike, J.J., 1974, Phase relations and crystallization sequence in a contact-metamorphosed rock from the Gunflint Iron Formation, Minnesota. J. Petr., V.15, P.539-65.

Sims, P.K. and Viswanathan, S., 1972, Giants Range Batholith. in Geology of Minnesota: A Centennial Volume, Sims and Morey, eds., Minn. Geol. Surv. Spec. Vol., Minneapolis, Minnesota, P.120-139.

Tarasenko, V.S., 1986, Petrology and mineralization of the gabbro-anorthosite massifs of the Ukranian Shield. Intl. Geol. Rev., V.28, N.11, P.1278-1292.

Tyson, R.M., 1979, The mineralogy and petrology of the Partridge River troctolite in the Babbit - Hoyt Lakes region of the Duluth Complex, northeastern Minnesota. unpubl. Ph.D. thesis, Miami University, Oxford, Ohio, 179 p.

Valley, J.W., 1986, Stable isotope geochemistry of metamorphic rocks. in Stable Isotopes, Valley, Taylor and O'Neil, eds., Min. Soc. Am. Reviews in Mineralogy, V.16, 570 p.

Van Lamoen, H., 1979, Coronas in olivine gabbros and iron ores from Susimäki and Riuttamaa, Finland. Contr. Mineral. Petrol., V.68, P.259-268.

Watowich, S.N., Malcolm, J.B., and Parker, P.D., 1981, A review of the Duluth Gabbro Complex of Minnesota as a domestic source of critical and strategic metals: SME-AIME Fall Meeting, Denver, Colorado, 9 pp.

Weiblen, P.W., and Morey, G.B., 1976, Textural and compositional characteristics of sulfide ores from the basal contact of the South Kawishiwi intrusion, Duluth Complex, northeastern Minnesota. Ann. Mining Symposium, AIME, 37th, Minneapolis, 1976, Proc. (Minn. Geol. Survey Reprint Ser.32), 24 p.

Weiblen, P.W., and Morey, G.B., 1980, A summary of the stratigraphy, petrology, and structure of the Duluth Complex. Am. J. Sci., V.280, P.88-133.

White, D.A., 1954, The stratigraphy and structure of the Mesabi Range, Minnesota. Minn. Geol. Surv. Bull. 38, 92 p.

Williams, K.L., Rock, N.M.S., and Carrol, G.W., 1990, SPINEL and SPINELTAB: Macintosh programs to plot spinel analyses in the three-dimensional oxidized (magnetite) and reduced (ulvöspinel) prisms. Am. Mineral., V.75, P.1428-1430.

APPENDIX A:

Petrographic Modal Abundances for the Least Altered Biwabik Iron Formation

* = point count data, all others are visual estimates

Minerals	DP-46	DP-57 *	DP-8049 *	DP-8053 *	DP-8058 *	DP-8427
Magnetite	7	53	15	19	11	18
Orthopyroxene	0	0	45	33	29	24
Quartz	25	23	24	32	27	40
Cumm/Grun.	20	4	3	6	4	12
Olivine	46	16	2	5	10	2
Clinopyroxene	0	4	7	5	14	3
Biotite	<1	0	3	<1	3	1
Apatite	0	<1	0	<1	<1	0
Sulfide	0	0	<1	0	<1	0
Stilpnomelane	1	0	0	0	1	0
Chlorite	0	<1	1	<1	1	0
Hornblende	1	0	<1	<1	0	0
Ilmenite	0	0	0	0	0	0
Plagioclase	0	0	0	0	0	0
Actinolite	0	0	0	0	0	0

APPENDIX A cont'd.

Petrographic Modal Abundances for the Most Altered Biwabik Iron Formation

* = point count data, all others are visual estimates

	DP-15A *	DP-16A	DP-16B	DP-18C *	DP-23A	DP-24	DP-27A *	DP-27B	DP-31 *	DP-32B	DP-32C	DP-33
Magnetite	10	55	9	45	12	4	5	<1	45	45	25	70
Orthopyroxene	12	0	10	0	4	4	54	3	6	1	17	3
Quartz	0	1	1	12	0	0	0	0	0	0	50	10
Cumm/Grun.	0	0	0	24	0	1	4	19	0	11	0	8
Olivine	0	0	0	0	0	0	0	0	1	0	0	0
Clinopyroxene	26	19	10	0	8	15	0	50	12	0	5	0
Biotite	1	<1	1	0	1	1	<1	<1	2	2	1	1
Apatite	<1	1	<1	2	<1	3	0	0	1	0	0	1
Sulfides	0	0	0	<1	0	0	2	7	0	0	0	0
Stilpnomelane	0	0	0	<1	1	0	0	0	2	20	0	0
Chlorite	0	3	0	0	0	7	1	0	1	7	0	7
Hornblende	1	0	3	0	12	5	2	1	4	5	0	0
Ilmenite	3	5	4	5	2	5	21	20	1	0	<1	<1
Plagioclase	42	9	60	0	45	15	9	0	25	0	0	0
Actinolite	5	7	2	12	15	40	2	0	<1	9	2	0
TOTAL	100	100	100	100	100	100	100	100	100	100	100	100

APPENDIX A cont'd.

Petrographic Modal Abundances for the Least Altered South Kawishiwi Intrusion

* = point count data, all others are visual estimates

Minerals	NM-21A *	NM-21B	NM-26A	NM-26B *	DP-54A1 *	DP-54A2	DP-55 *	DP-60B	DP-61	DP-62	DP-63
Plagioclase	61	63	66	63	55	62	60	60	55	53	50
Clinopyroxene	17	15	5	12	28	5	7	14	15	18	17
Olivine	7	13	25	18	7	17	20	17	16	20	15
Orthopyroxene	4	3	2	3	tr	6	5	3	4	2	10
Ilmenite	3	4	1	2	4	4	2	3	4	3	3
Magnetite	2	<1	<1	tr	0	0	0	<1	<1	<1	<1
Biotite	2	2	<1	1	5	3	4	3	5	1	3
Apatite	1	<1	<1	tr	1	1	1	0	<1	1	<1
Sulfide	1	<1	1	1	tr	1	1	<1	<1	<1	<1
Amphibole	2	<1	0	tr	0	1	0	0	1	2	2
Quartz	tr	0	0	0	0	0	0	0	0	0	0
TOTAL	100	100	100	100	100	100	100	100	100	100	100

APPENDIX A cont'd.

Petrographic Modal Abundances for the Most Altered South Kiwishiwi Intrusion

* = point count data, all others are visual estimates

	DP-2	DP-5A	DP-5B	DP-7 *	DP-11A	DP-13	DP-14	DP-18A	DP-18B *	DP-19	DP-21A *
Plagioclase	60	67	62	65	55	60	44	65	58	50	60
Clinopyroxene	14	13	7	9	13	25	30	21	23	12	14
Olivine	0	7	24	0	18	8	4	1	1	28	20
Orthopyroxene	22	10	4	8	4	2	0	4	3	3	0
Ilmenite	2	1	1	6	3	4	3	2	3	4	2
Magnetite	<1	1	1	6	0	0	3	3	7	1	<1
Biotite	2	1	1	1	7	1	1	4	2	2	1
Apatite	<1	0	0	0	<1	<1	2	<1	<1	0	<1
Sulfide	0	<1	0	0	<1	<1	1	<1	0	0	<1
Amphibole	<1	<1	0	2	<1	<1	12	0	3	0	3
Quartz	0	0	0	3	0	0	0	0	0	0	0
TOTAL	100	100	100	100	100	100	100	100	100	100	100

APPENDIX A cont'd.

Petrographic Modal Abundances for the Most Altered South Kiwishiwi Intrusion

* = point count data, all others are visual estimates

	DP-21B	DP-23B	DP-23C	DP-32A	DP-35	DP-36	DP-42	DP-50	DP-53B *
Plagioclase	18	65	53	60	55	55	56	55	60
Clinopyroxene	14	21	30	13	22	22	8	13	24
Olivine	50	0	0	20	8	6	16	7	5
Orthopyroxene	8	4	10	3	3	3	4	12	5
Ilmenite	4	<1	5	1	2	4	6	7	2
Magnetite	0	1	0	1	0	1	2	2	0
Biotite	3	2	1	2	5	3	4	<1	1
Apatite	<1	<1	<1	0	<1	1	<1	1	0
Sulfide	3	1	0	0	5	<1	<1	0	0
Amphibole	0	6	1	0	0	5	4	3	3
Quartz	0	0	0	0	0	0	0	<1	0
TOTAL	100	100	100	100	100	100	100	100	100

APPENDIX B

Whole Rock Analyses of Least Altered Biwabik Iron Formation

	8049	8053	8058	8427	AVERAGE
OXIDES (%)					
SiO_2	46.40	47.20	48.60	51.90	48.53
Al_2O_3	0.97	0.27	1.43	0.60	0.82
CaO	5.23	0.58	4.43	2.49	3.18
MgO	5.42	3.11	4.82	2.69	4.01
Na_2O	0.07	NA	0.04	0.05	0.04
K_2O	0.02	NA	0.02	0.01	0.01
Fe_2O_3	12.84	17.55	11.61	26.93	17.23
FeO	26.60	30.10	25.90	14.10	24.18
MnO	0.53	0.44	0.44	0.20	0.40
Cr_2O_3	NA	NA	NA	NA	0.00
TiO_2	0.36	0.07	0.15	0.16	0.19
P_2O_5	0.54	0.06	0.44	0.06	0.28
S	0.05	0.02	0.08	0.02	0.04
LOI	1.21	0.85	1.53	0.97	1.14
SUM	100.24	100.25	99.49	100.18	100.04

NA = below detection limit; blank = not analyzed
Detection Limit = 0.01 wt.%, except FeO (0.1 wt.%)

APPENDIX B cont'd

Whole Rock Analyses of Least Altered Biwabik Iron Formation

	8049	8053	8058	8427	AVERAGE
TRACE ELEMENTS (PPM)					
As	12	14	15	26	17
Ba	40	70	40	40	48
Co	13	14	5	15	12
Cu	100	30	60	130	80
La1	9	4	7	2	6
La2	6	1	4	2	3
Mo	NA	NA	NA	NA	0
Nb	190	30	30	20	68
Ni	NA	NA	NA	20	5
Rb	20	NA	NA	NA	5
Sb	2	3	NA	3	2
Sc	4	NA	2	2	2
Sn	NA	NA	2	NA	1
Sr	10	NA	30	NA	10
V	60	35	80	26	50
Y	NA	NA	NA	NA	0
Zn	63	38	40	43	46
Zr	10	80	20	NA	28

NA = below detection limit; blank = not analyzed
Detection Limit = 10 ppm for Ba, Cu, Nb, Ni, Rb, Sr, Y, Zr
= 1 ppm for As, Co, La1, La2, Mo, Sb, Sc, Sn, V, Zn
La1 = line 1 of lanthanum on ICP
La2 = line 2 of lanthanum on ICP

APPENDIX C

Whole Rock Analyses of Most Altered Biwabik Iron Formation

	DP-15A	DP-16A	DP-16B	DP-18C	DP-23A
OXIDES (%)					
SiO_2	36.10	17.80	43.90	23.60	46.30
Al_2O_3	7.18	4.60	14.40	1.40	16.80
CaO	3.79	1.97	7.37	4.39	8.11
MgO	8.62	3.50	5.58	5.21	6.01
Na_2O	1.04	0.30	2.34	0.12	2.19
K_2O	0.22	0.23	0.73	0.02	1.04
Fe_2O_3	17.49	37.17	8.52	32.57	5.27
FeO	19.80	26.30	11.50	24.50	9.20
MnO	0.34	0.40	0.21	0.36	0.17
Cr_2O_3					
TiO_2	3.87	3.96	3.47	4.37	2.28
P_2O_5	0.20	0.18	0.30	0.24	0.30
S	0.05	0.04	0.06	0.09	0.09
LOI	1.30	3.93	1.43	2.68	1.62
SUM	100.00	100.38	99.81	99.55	99.38

NA = below detection limit; blank = not analyzed
Detection Limit = 0.01 wt. %, except for FeO (0.1 wt.%)

APPENDIX C cont'd.

Whole Rock Analyses of Most Altered Biwabik Iron Formation

	DP-24	DP-27A	DP-27B	DP-31	DP-32B
OXIDES (%)					
SiO_2	31.80	34.40	35.60	31.90	28.90
Al_2O_3	8.72	3.43	0.92	10.60	0.93
CaO	4.15	1.86	6.66	4.97	3.18
MgO	9.08	11.30	9.54	5.90	4.83
Na_2O	0.19	0.32	0.10	1.03	0.11
K_2O	0.36	0.09	NA	0.58	0.01
Fe_2O_3	9.90	3.24	8.79	20.35	31.86
FeO	22.40	26.60	27.00	16.60	20.10
MnO	0.44	0.27	0.33	0.34	0.75
Cr_2O_3					
TiO_2	4.17	13.20	5.48	3.61	0.04
P_2O_5	0.40	0.12	0.35	0.23	0.05
S	0.05	1.12	3.14	0.05	NA
LOI	8.54	3.36	4.41	3.70	8.79
SUM	100.20	99.31	102.32	99.86	99.55

NA = below detection limit; blank = not analyzed
Detection Limit = 0.01 wt. %, except for FeO (0.1 wt.%)

APPENDIX C cont'd.

Whole Rock Analyses of Most Altered Biwabik Iron Formation

	DP-33	AVERAGE
OXIDES (%)		
SiO_2	24.30	19.23
Al_2O_3	0.78	6.41
CaO	1.05	5.75
MgO	3.90	4.30
Na_2O	0.08	0.62
K_2O	0.03	6.84
Fe_2O_3	40.13	20.64
FeO	25.70	16.42
MnO	0.64	2.59
Cr_2O_3		
TiO_2	1.20	2.62
P_2O_5	0.17	0.63
S	NA	3.03
LOI	2.26	2.82
SUM	100.24	54.68

NA = below detection limit; blank = not analyzed
Detection Limit = 0.01 wt. %, except for FeO (0.1 wt.%)

APPENDIX C cont'd.

Whole Rock Analyses of Most Altered Biwabik Iron Formation

	DP-15A	DP-16A	DP-16B	DP-18C	DP-23A
TRACE ELEMENTS (PPM)					
As	22	10		7	23
Ba	136	157	268	79	771
Co	83	69		82	67
Cr	48	60	459	435	244
Cu	190	395	177	320	152
La1	8	12		10	11
La2	10	5		3	9
Mo	NA	NA		NA	NA
Nb	50	60	52	55	34
Ni	228	133	157	138	221
Rb	32	22	30	15	42
Sb	NA	3		2	NA
Sc	19	12		16	16
Sn	NA	NA		3	NA
Sr	60	15	314	149	346
V	485	393		403	239
Y	NA	NA	21	NA	NA
Zn	133	263		191	111
Zr	92	70	260	NA	156

NA = below detection limit; blank = not analyzed
Detection Limit = 10 ppm for Ba, Cr, Cu, Nb, Ni, Rb, Sr, Y, Zr; 1ppm for As, Co, La1, La2, Mo, Sb, Sc, Sn, V, Z

APPENDIX C cont'd.

Whole Rock Analyses of Most Altered Biwabik Iron Formation

	DP-24	DP-27A	DP-27B	DP-31	DP-32B
TRACE ELEMENTS (PPM)					
As		5	8		19
Ba	181	140	77	364	92
Co		228	191		12
Cr	1210	870	865	893	18
Cu	456	5030	6400	218	58
La1		9	10		4
La2		5	4		1
Mo		NA	1		NA
Nb	48	73	63	60	36
Ni	356	1440	2510	342	NA
Rb	50	25	NA	29	28
Sb		1	4		NA
Sc		57	29		NA
Sn		3	3		5
Sr	31	31	12	114	20
V		1458	657		23
Y	NA	NA	NA	NA	NA
Zn		206	185		43
Zr	109	101	48	133	11

NA = below detection limit; blank = not analyzed
Detection Limit = 10 ppm for Ba, Cr, Cu, Nb, Ni, Rb, Sr, Y, Zr; 1ppm for As, Co, La1, La2, Mo, Sb, Sc, Sn, V, Zn

APPENDIX C cont'd.

Whole Rock Analyses of Most Altered Biwabik Iron Formation

	DP-33	AVERAGE
TRACE ELEMENTS (PPM)		
As	12	6
Ba	115	88
Co	40	59
Cr	27	353
Cu	156	1120
La1	6	4
La2	2	2
Mo	NA	0
Nb	61	31
Ni	43	426
Rb	30	15
Sb	NA	1
Sc	4	11
Sn	2	2
Sr	NA	19
V	122	283
Y	NA	0
Zn	99	67
Zr	44	41

NA = below detection limit; blank = not analyzed
Detection Limit = 10 ppm for Ba, Cr, Cu, Nb, Ni, Rb, Sr, Y, Zr; 1ppm for As, Co, La1, La2, Mo, Sb, Sc, Sn, V, Zn

APPENDIX D

Whole Rock Analyses of Least Altered South Kiwishiwi Intrusion

	NM-21A	NM-21B	NM-26A	NM-26B	DP-55	AVERAGE
OXIDES (%)						
SiO_2	45.40	45.00	47.90	47.00	47.50	46.56
Al_2O_3	16.20	15.00	19.40	18.80	13.50	16.58
CaO	9.27	9.43	9.08	9.89	10.70	9.67
MgO	6.92	6.72	7.10	6.99	7.78	7.10
Na_2O	2.37	2.39	2.90	2.61	2.16	2.49
K_2O	0.42	0.43	0.39	0.44	0.70	0.48
Fe_2O_3	1.35	2.09	1.08	1.19	2.21	1.58
FeO	13.00	13.60	9.20	10.00	11.60	11.48
MnO	0.19	0.21	0.13	0.14	0.20	0.17
Cr_2O_3	0.01	0.01	NA	0.01	0.05	0.02
TiO_2	3.09	3.59	1.31	2.02	2.02	2.41
P_2O_5	0.39	0.48	0.10	0.12	0.28	0.27
S	0.09	0.11	0.11	0.15	0.68	0.23
LOI	1.45	1.51	1.02	1.11	1.49	1.32
SUM	100.15	100.57	99.72	100.47	100.87	100.36

NA = below detection limit; blank = not analyzed
Detection Limit = 0.01 wt.%, except for FeO (0.1 wt.%)

APPENDIX D cont'd

Whole Rock Analyses of Least Altered South Kiwishiwi Intrusion

	NM-21A	NM-21B	NM-26A	NM-26B	DP-55	AVERAGE
TRACE ELEMENTS (PPM)						
As					11	11
Ba					210	210
Co					59	59
Cu	222	267	844	713	1810	771
La1					15	15
La2					11	11
Mo					1	1
Nb					20	20
Ni	180	170	370	240	35	262
Rb					20	20
Sb					2	2
Sc					27	27
Sn					10	10
Sr					220	220
V	220	270	130	250	306	294
Y					30	30
Zn					98	98
Zr					130	130

NA = below detection limit; blank = not analyzed
Detection Limit = 10 ppm for Ba, Cu, Nb, Ni, Rb, Sr, Y, Zr
= 1 ppm for As, Co, La1, La2, Mo, Sb, Sc, Sn, V, Zn

APPENDIX E

Whole Rock Analyses of Most Altered South Kiwishiwi Intrusion

	DP-2	DP-5A	DP-5B	DP-7	DP-11A
OXIDES (%)					
SiO_2	49.80	45.40	44.80	41.00	45.60
Al_2O_3	14.00	14.10	15.40	12.40	14.10
CaO	10.10	7.40	7.84	6.37	7.63
MgO	9.03	5.53	8.13	5.35	9.45
Na_2O	1.91	2.03	2.03	2.02	1.86
K_2O	0.54	0.70	0.57	0.60	0.68
Fe_2O_3	1.36	2.47	4.30	11.41	2.18
FeO	10.20	14.60	11.70	13.40	13.60
MnO	0.20	0.19	0.18	0.21	0.18
Cr_2O_3					
TiO_2	1.54	3.08	2.37	4.34	1.93
P_2O_5	0.22	0.38	0.29	0.40	0.25
S	0.07	1.14	0.08	0.06	0.52
LOI	1.34	3.27	2.75	1.44	1.91
SUM	100.31	100.29	100.44	99.00	99.89

NA = below detection limit; blank = not analy
Detection Limit = 0.01 wt.%, except for FeO (

APPENDIX E cont'd.

Whole Rock Analyses of Most Altered South Kiwishiwi Intrusion

	DP-13	DP-14	DP-18A	DP-18B	DP-19
OXIDES (%)					
SiO_2	48.60	45.40	45.10	40.00	41.10
Al_2O_3	16.00	13.80	16.40	14.10	8.51
CaO	7.66	7.49	8.38	6.44	5.31
MgO	5.62	7.58	6.28	7.28	13.20
Na_2O	2.29	1.49	2.41	1.63	1.23
K_2O	1.75	0.73	0.89	0.63	0.59
Fe_2O_3	1.72	3.62	4.61	10.42	2.84
FeO	10.60	14.20	8.00	12.40	20.30
MnO	0.17	0.22	0.14	0.20	0.26
Cr_2O_3					
TiO_2	2.61	2.93	2.98	2.61	3.41
P_2O_5	0.31	0.34	0.39	0.25	0.24
S	0.10	0.49	0.03	0.13	0.64
LOI	1.43	2.13	4.14	2.48	2.11
SUM	98.86	100.42	99.75	98.57	99.74

NA = below detection limit; blank = not analyzed
Detection Limit = 0.01 wt.%, except for FeO (0.1 wt.%)

APPENDIX E cont'd.

Whole Rock Analyses of Most Altered South Kiwishiwi Intrusion

	DP-21A	DP-21B	DP-23B	DP-23C	DP-32A
OXIDES (%)					
SiO_2	48.60	36.80	42.80	47.00	44.90
Al_2O_3	12.60	3.21	11.90	14.80	15.40
CaO	7.87	2.82	6.25	8.35	8.49
MgO	6.55	19.20	8.34	8.09	6.95
Na_2O	1.90	0.36	1.36	1.75	1.64
K_2O	2.05	0.23	0.82	0.70	0.48
Fe_2O_3	2.26	3.84	4.17	2.81	5.19
FeO	11.10	25.70	17.30	10.70	11.80
MnO	0.18	0.31	0.24	0.19	0.22
Cr_2O_3					
TiO_2	3.70	3.34	2.16	2.16	2.99
P_2O_5	0.55	0.13	0.26	0.26	0.30
S	0.09	0.76	2.16	0.09	0.11
LOI	2.24	2.36	4.38	2.59	1.41
SUM	99.69	99.06	102.14	99.49	99.88

NA = below detection limit; blank = not analyzed
Detection Limit = 0.01 wt.%, except for FeO (0.1 wt.%)

APPENDIX E cont'd.

Whole Rock Analyses of Most Altered South Kiwishiwi Intrusion

	DP-35	DP-36	DP-53B	AVERAGE
OXIDES (%)				
SiO_2	44.90	45.50	46.30	44.64
Al_2O_3	15.30	15.20	19.30	13.70
CaO	8.11	7.98	7.72	7.35
MgO	5.56	6.61	5.59	8.02
Na_2O	2.35	2.14	2.70	1.84
K_2O	1.02	0.92	0.67	0.81
Fe_2O_3	2.05	4.09	3.42	4.04
FeO	12.10	10.00	7.00	13.04
MnO	0.16	0.18	0.09	0.20
Cr_2O_3			0.02	0.00
TiO_2	2.99	2.95	2.31	2.80
P_2O_5	0.39	0.30	0.15	0.30
S	1.14	0.22	0.06	0.44
LOI	2.85	3.41	4.73	2.61
SUM	98.92	99.50	100.06	99.78

NA = below detection limit; blank = not analyzed
Detection Limit = 0.01 wt.%, except for FeO (0.1 wt.%)

APPENDIX E cont'd

Whole Rock Analyses of Most Altered South Kiwishiwi Intrusion

	DP-2	DP-5A	DP-5B	DP-7	DP-11A
TRACE ELEMENTS (PPM)					
As	23	18	22		4
Ba	182	228	188	220	204
Co	55	103	72		84
Cu	142	1760	167	211	1270
Cr	635	112	267	1020	206
La1	9	20	16		12
La2	8	16	12		10
Mo	NA	NA	NA		NA
Nb	22	40	31	55	50
Ni	124	542	317	231	488
Rb	25	25	35	26	21
Sb	NA	NA	NA		NA
Sc	15	17	15		15
Sn	NA	12	NA		NA
Sr	221	173	200	158	184
V	264	277	240		201
Y	20	20	NA	28	NA
Zn	115	162	101		121
Zr	136	216	179	272	135

NA = below detection limit; blank = not analyzed
Detection Limit = 10 ppm for Ba, Cr, Cu, Nb, Ni, Rb
Sr, Y, Zr; 1 ppm for As, Co, La1, La2, Mo, Sb, Sc, Sn, V, Zn

APPENDIX E cont'd

Whole Rock Analyses of Most Altered South Kiwishiwi Intrusion

	DP-13	DP-14	DP-18A	DP-18B	DP-19
TRACE ELEMENTS (PPM)					
As		8	20	11	
Ba	492	310	308	185	208
Co		88	64	85	
Cu	147	1320	236	549	2530
Cr	166	134	109	649	378
La1		11	20	12	
La2		9	16	9	
Mo		NA	NA	NA	
Nb	52	45	49	41	53
Ni	65	388	176	461	925
Rb	96	43	35	50	36
Sb		2	NA	2	
Sc		14	20	15	
Sn		NA	NA	NA	
Sr	523	283	329	200	100
V		261	284	285	
Y	14	17	16	NA	10
Zn		131	112	136	
Zr	142	155	229	146	149

NA = below detection limit; blank = not analyzed
Detection Limit = 10 ppm for Ba, Cr, Cu, Nb, Ni, Rb, Sr, Y, Zr; 1 ppm for As, Co, La1, La2, Mo, Sb, Sc, Sn, V, Zn

APPENDIX E cont'd

Whole Rock Analyses of Most Altered South Kiwishiwi Intrusion

	DP-21A	DP-21B	DP-23B	DP-23C	DP-32A
TRACE ELEMENTS (PPM)					
As	25	19	12	11	9
Ba	434	157	439	390	144
Co	73	174	148	63	74
Cu	333	1860	3630	351	229
Cr	143	365	175	277	134
La1	31	8	12	11	11
La2	26	4	11	9	9
Mo	NA	NA	NA	NA	NA
Nb	63	53	52	24	61
Ni	119	947	913	175	134
Rb	105	23	39	36	23
Sb	1	2	3	NA	2
Sc	22	17	16	19	19
Sn	34	NA	1	NA	NA
Sr	172	16	200	289	332
V	374	340	212	228	316
Y	46	14	21	27	NA
Zn	114	201	150	109	137
Zr	362	89	131	138	129

NA = below detection limit; blank = not analyzed
Detection Limit = 10 ppm for Ba, Cr, Cu, Nb, Ni, Rb, Sr, Y, Zr; 1 ppm for As, Co, La1, La2, Mo, Sb, Sc, Sn, V, Zn

APPENDIX E cont'd

Whole Rock Analyses of Most Altered South Kiwishiwi Intrusion

	DP-35	DP-36	DP-53B	AVERAGE
TRACE ELEMENTS (PPM)				
As	12	10	4	14
Ba	333	192	240	270
Co	40	80	60	84
Cu	7160	258	370	1251
Cr	139	109		295
La1	6	17	8	14
La2	2	12	7	11
Mo	NA	NA	NA	0
Nb	39	46	30	45
Ni	917	157	260	408
Rb	39	47	20	40
Sb	NA	1	NA	1
Sc	4	20	10	16
Sn	2	NA	2	3
Sr	230	265	280	231
V	122	281	199	259
Y	32	27	NA	16
Zn	99	122	73	126
Zr	219	172	110	173

NA = below detection limit; blank = not analyzed
Detection Limit = 10 ppm for Ba, Cr, Cu, Nb, Ni, Rb, Sr, Y, Zr; 1 ppm for As, Co, La1, La2, Mo, Sb, Sc, Sn, V, Zn

APPENDIX F

LIST OF TRACE ELEMENTS ANALYZED AND MEANS OF ANALYSIS

Element	Analytical Technique
As	ICP
Ba	XRF
Co	ICP
Cr	XRF
Cu	XRF
La	ICP
Mo	ICP
Nb	XRF
Ni	XRF
Rb	XRF
S	XRF
Sb	ICP
Sc	ICP
Sn	ICP
Sr	XRF
V	ICP,DCP
Y	XRF
Zn	ICP
Zr	XRF

APPENDIX G: Means and standard deviations for whole rock isocon data used for standard t-test in wt.% (major and minor elements) and ppm (trace elements).

	Most altered BIF		Most altered SKI	
	Mean	Std.dev.	Mean	Std.dev.
SiO_2	32.24	8.50	44.64	3.27
Al_2O_3	6.34	5.70	13.70	3.43
CaO	4.32	2.31	7.35	1.54
MgO	6.68	2.54	8.02	3.39
Na_2O	0.71	0.84	1.84	0.53
K_2O	0.30	0.35	0.81	0.44
Fe_2O_3	19.57	13.64	4.04	2.72
FeO	20.88	6.19	13.04	4.43
total Fe	40.45	17.02	17.08	5.25
MnO	0.39	0.17	0.20	0.05
TiO_2	4.15	3.37	2.80	0.67
P_2O_5	0.23	0.10	0.30	0.10
S	0.43	0.96	0.44	0.57
H_2O	3.82	2.61	2.61	1.03
Ba	216	203	270	107
Rb	28	13	40	24
Sr	99	123	231	107
V	473	434	259	114
Nb	54	12		
Zr			173	66
Cu	1232	2240	1251	1775
Ni	506	772	408	315